SSD 102.3

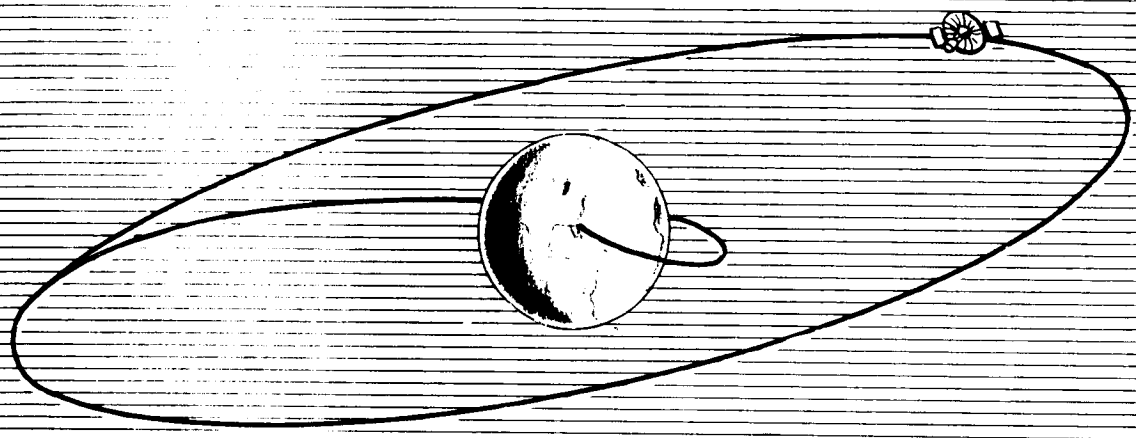

VOLUME 5 OF 8

Final Report

ATS-4

PREPARED BY

FAIRCHILD HILLER
SPACE SYSTEMS DIVISION

FOR

NASA
Goddard Space Flight Center

DECEMBER 1966

SSD 102.3

ATS-4 STUDY PROGRAM
FINAL REPORT

(Contract NASW-1411)

VOLUME FIVE OF EIGHT

prepared by

FAIRCHILD HILLER SPACE SYSTEMS DIVISION

Sherman Fairchild Technology Center

Germantown, Maryland

for

GODDARD SPACE FLIGHT CENTER

NATIONAL AERONAUTICS AND SPACE ADMINISTRATION

December 1966

TABLE OF CONTENTS

VOLUME ONE

TABLE OF CONTENTS

VOLUME TWO

TABLE OF CONTENTS

VOLUME THREE

TABLE OF CONTENTS

VOLUME THREE (Continued)

TABLE OF CONTENTS

VOLUME FOUR

TABLE OF CONTENTS

VOLUME FOUR (Continued)

TABLE OF CONTENTS

VOLUME FIVE

TABLE OF CONTENTS

VOLUME SIX

TABLE OF CONTENTS

VOLUME SEVEN

TABLE OF CONTENTS

VOLUME SEVEN (Continued)

LIST OF ILLUSTRATIONS

VOLUME ONE

LIST OF ILLUSTRATIONS

VOLUME TWO

LIST OF ILLUSTRATIONS

VOLUME THREE

LIST OF ILLUSTRATIONS

VOLUME THREE (Continued)

LIST OF ILLUSTRATIONS

VOLUME THREE (Continued)

LIST OF ILLUSTRATIONS

VOLUME THREE (Continued)

LIST OF ILLUSTRATIONS

VOLUME FOUR

LIST OF ILLUSTRATIONS

VOLUME FOUR (Continued)

LIST OF ILLUSTRATIONS

VOLUME FIVE

LIST OF ILLUSTRATIONS

VOLUME FIVE (Continued)

LIST OF ILLUSTRATIONS

VOLUME SIX

LIST OF ILLUSTRATIONS

VOLUME SIX (Continued)

LIST OF ILLUSTRATIONS

VOLUME SIX (Continued)

LIST OF ILLUSTRATIONS

VOLUME SEVEN

LIST OF ILLUSTRATIONS

VOLUME SEVEN (Continued)

LIST OF ILLUSTRATIONS

VOLUME SEVEN (Continued)

PREFACE

This report covers the efforts of Fairchild Hiller Corporation and its team of subcontractors on NASA Contract (NAS-W-1411). The team organization and responsibilities during the study effort are shown on the accompanying chart. The report is divided into eight volumes, as follows:

Volume 1	Summary
Volume 2	Systems Analysis
Volume 3	Vehicle Engineering
Volume 4	Power System
	Orbital Analyses, Propulsion and Guidance
Volume 5	Stabilization and Control
Volume 6	Communication Experiments
Volume 7	Radio Interferometer Experiment
	Telemetry and Command Systems
Volume 8	Program Budgetary Costs and Schedules

ATS-4 TEAM ORGANIZATION

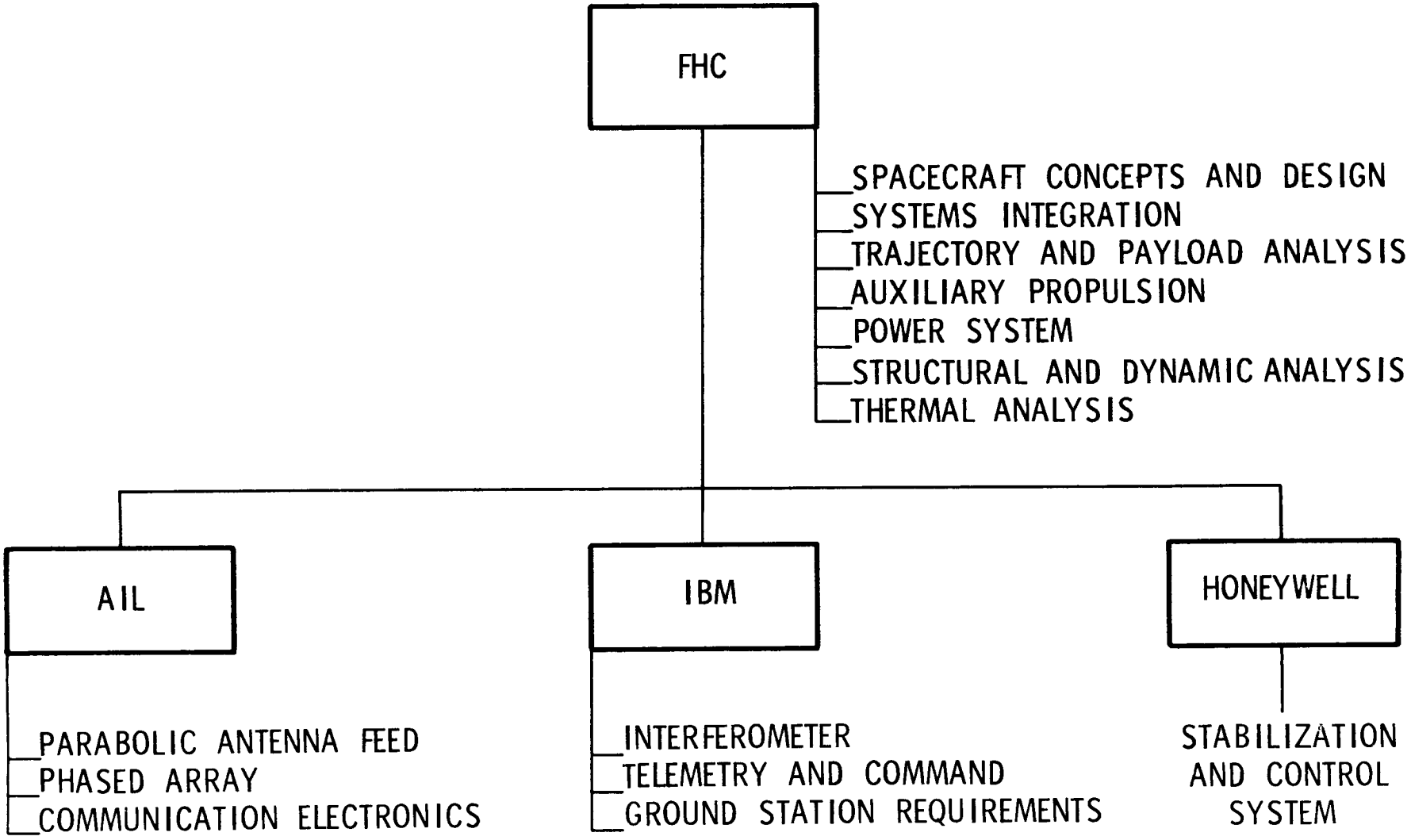

SECTION 6.0
ATTITUDE STABILIZATION AND CONTROL SYSTEM

6.1 ATTITUDE STABILIZATION AND CONTROL REQUIREMENTS

6.1.1 Mission Requirements

The requirements for the ATS-4 mission, as imposed on the Attitude Stabilization and Control System (SCS), are to establish a desired vehicle orientation, control the commanded offset pointing direction of the spacecraft-antenna, execute commanded tracking maneuvers, monitor system performance, and perform certain control system experiments. This is to be accomplished throughout a two year mission with a complete SCS reliability goal of 0.9.

6.1.2 Control Accuracy

Upon command, the SCS is required to offset point (from the nominal direction) the spacecraft-antenna to any point on the Earth disc within a 3-sigma accuracy of ± 0.1 degree in pitch and roll, and ± 0.2 degree in yaw. The time to change from an offset pointing direction on one edge of the Earth disc to a direction on the opposite edge, and again achieve the specified pointing accuracy, shall be no more than 30 minutes. While performing commanded tracking maneuvers (e.g., using low-Earth satellites) the accuracy requirement is ± 0.5 degree (3-sigma), up to a maximum tracking rate of 10 milliradians per minute.

6.1.3 Control Modes

Throughout the mission, numerous control modes are employed with specific control requirements. These control modes are listed below, with their detailed requirements and operational characteristics given in the subsequent section of this report.

- Ascent and orbit injection
- Initial rate arrest
- Acquisition
- Offset pointing
- Satellite tracking

6.2 ATTITUDE REFERENCE SUBSYSTEM

6.2.1 Alternate Approaches

Various Attitude Reference Sub-system (ARS) configurations have been considered for the ATS-4 vehicle. They have been examined relative to acquisition, attitude hold and maneuvering requirements. They include:

- Horizon Sensor/ Polaris Star Tracker ARS
- Multiple Star Tracker ARS
- ESG/Star Tracker ARS
- Horizon Sensor/Monopulse/Polaris Star Tracker ARS
- Gyro Attitude Reference ARS

These configurations are discussed below with their advantages and disadvantages in the various modes. A diagram showing the nominal Earth-orbit reference coordinate system is shown in Figure 6-1.

Horizon Sensor

Because the ATS is kept earth-oriented, the most direct method for determining local vertical (pitch and roll) is by use of a horizon sensor. The yaw sensing could be obtained by gyro compassing techniques using rate integrating gyros which are stabilized on the long term basis by the horizon sensor. A Polaris star tracker could be used to provide yaw attitude error in lieu of the gyro compassing technique. Sun sensors are required for initial acquisition.

The yaw accuracy in a gyro compassing configuration is dependent upon the drift of the roll gyro. At synchronous orbit altitude the orbital rate is small; thus, the rate component sensed by the roll gyro to give the yaw information will be very small. To achieve 0.2 degree accuracy in yaw will require a

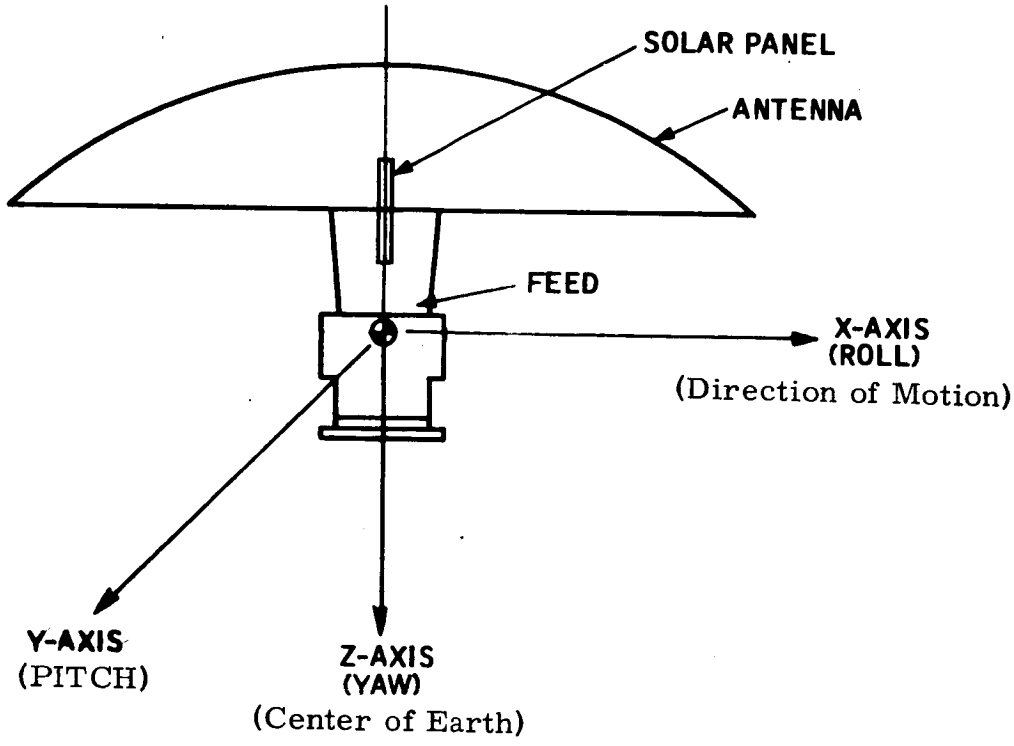

Figure 6-1. Reference Coordinate Frame (Nominal)

roll gyro with a total drift of less than 0.04 degree/hr. Drift trimming during the mission will be required to maintain this drift rate. Offsets of the roll torquer and torquer amplifier will also contribute to the yaw error. To provide drift trim, the drift rate of the gyro must be determined. Because of the roll-yaw coupling in an earth-oriented mode, this will be difficult to measure. For example, the yaw error is a function of the roll gyro drift, but there is no means to provide roll drift directly. Both the roll and yaw errors are functions of the yaw gyro drift. Roll error could be determined from the horizon sensor; however, the portion that is due to yaw gyro drift must be separated from the other error components. To remove the effects of the roll-yaw coupling the vehicle would have to be controlled to an inertially fixed reference (i.e., sun or star) for a period of time. With vehicle fixed, the gyro outputs then could be monitored for an indication of drift.

Additional errors result in both roll and yaw during the time that roll offset angles are being held. Because of the offset condition, the yaw gyro will sense a component of the orbital rate even though there is no yaw error. This results in an additional hangoff error for both the roll and yaw axes. If the gains can be made high enough in the gyro loops these errors should be small.

The required yaw accuracy is easily achieved by using a star tracker to track Polaris. Small diurnal corrections must be provided since Polaris is not exactly perpendicular to the orbit plane. Table 6-1 lists the characteristic of a horizon sensor ARS using a Polaris star tracker as the yaw reference. The physical characteristics for the rest of the SCS are also included in Table 6-1 for reference purposes; these will be substantiated in later portions of this section.

Multiple Star Tracker ARS -- The desired attitude reference could also be obtained by employing two or more star trackers to derive pitch and roll information. These additional star trackers would require large excursion

Table 6-1. SCS Characteristics - Horizon Scanner/Polaris Star Tracker ARS

Components	Volume (cu. inch)	Weight (lbs)	Power (watts)	
			Peak	Average
Polaris Star Tracker	1000	20	20	4
2-Axis Horizon Scanner	500	18	6	3
Acquisition Sun Sensor	28	3	--	--
3-Axis Gyro Unit	300	10	30	20
Wheel Drive Electronics	140	5	12	4.5
Inertia Wheels	1060	34.2	60	21
Reaction Jet Subsystem	2800	54	20	0.5
SCS Controller	860	30	30	30
Power Inverter	520	18.6	20	5
TOTAL	7208	192.8	198	88.0

gimbals and a significant increase in computation complexity over the approach described previously. Depending upon the gimbal travel and field of view, at least three additional star trackers would be required to alternately track different stars in the vicinity of the earth's equatorial plane. The increased computation, increased cost, and decreased reliability of this approach are its undesirable features.

Because ATS-4 is earth oriented, the star references appear to be varying constantly in body coordinates. Thus, in determining the attitude errors, an orbital ephemeris must be included in the computations. Because the stars do not have an orthogonal relationship, the attitude error computations are more complex than for the gyro or horizon sensor configuration.

If one star tracker were to provide the pitch control for the entire orbit, it would have to be gimballed to provide 360 degrees of freedom about the pitch axis. This also means that the star tracker will have to be mounted on the vehicle such that no part of the vehicle obstructs the line of sight to the star at any time during the orbit. This does not appear to be a practical mechanization either from the design of the star tracker or the mounting of the tracker on the vehicle. In addition, no existing star trackers have this capability.

If it were desired to use the same star as reference throughout the orbit with limited field-of-view trackers, several trackers could be mounted about the vehicle as on the OAO satellite. Switching of control could be made directly from one tracker to the next. The same orbital ephemeris could be used if the star tracker readouts were properly synchronized. Present OAO trackers have a gimbal freedom of ±60 degrees, therefore a minimum of three trackers are required. Although 360 degrees of freedom is not required on the star tracker itself, a free composite field of view of 360 degrees is still required on the vehicle.

With a limited field of view, several different stars can be used by one star tracker to provide pitch control. A pitch gyro would stabilize the vehicle while the tracker is being moved to another reference star. When switching to a new star the orbital ephemeris must also be modified. With a gyro in the loop it can be torqued by the star tracker whenever a star is being tracked. Thus, it will always be in the proper orientation when necessary to switch to another star. Also, the control loop is not affected by the changes in gain due to tracking different magnitude stars.

The star tracker can provide the desired sensing accuracy. The gimbal readout will have to be capable of reading angles of less than 0.01 degree. For 360 degrees this is 36,000 readout increments, thus a digital position encoder of 16 bits is required. The OAO tracker developed by Bendix uses a 16 bit optical encoder with a gimbal freedom of ±60 degrees in two axes.

It appears that the most likely configuration involves the use of one star tracker on Polaris to provide yaw and roll information and additional trackers tracking a selected star to provide pitch information. Use of a pitch gyro permits transfer from one star tracker to another without losing control. During the tracking period the pitch star tracker supplies the necessary error signals to hold the gyro at the desired reference.

In this configuration, the acquisition sequence would be sun-Polaris-equatorial star. The sun line would be established using sun sensors as for the previous case. Then, by rolling about the sun line with the Polaris tracker field-of-view fixed at an angle established by the ephemeris, Polaris will be observed. With the sun and Polaris acquired, any of several other stars could be found using the ephemeris.

The characteristics of complete SCS with a multiple star tracker ARS using three equatorial star trackers to track one reference star are shown in Table 6.2.

Table 6-2. SCS Characteristics - Multiple Star Tracker ARS

Components	Volume (cu. inches)	Weight (lbs)	Power (watts)	
			Peak	Average
Polaris Star Tracker	1000	20	20	4
Gimballed Equatorial Star Tracker (3)	1800	56	40	20
Acquisition Sun Sensor	28	3	--	--
3-Axis Gyro Unit	300	10	30	20
Wheel Drive Electronics	140	5	12	4.5
Inertia Wheels	1060	34.2	60	21
Reaction Jet Subsystem	2800	54	20	0.5
Controller	1030	36	60	60
Power Inverter	520	18.6	20	5
TOTAL	8678	236.8	262	135.0

ESG/Polaris Star Tracker ARS

An ESG system could be used as an alternate to using multiple star trackers for pitch attitude control. In this case, only one equatorial star tracker could be used for gyro up-date. The sun sensor and Polaris star tracker would continue to be required and the sequence of acquisition would be the same as for the multiple star tracker configuration. The ESG system, used to provide pitch information would require updating at a frequency of less than once per three days.

There are several possible concepts for an ESG attitude reference system. The most appropriate one for the ATS-4 vehicle would determine vehicle attitude by calculating the direction cosines of the vehicle reference axes from the ESG and star tracker outputs. Commands to this system for changes in vehicle attitude would be the direction cosines of the desired positions of the two vehicle reference axes.

Although an ESG system would require considerably more computation than the horizon scanner system, preliminary analysis indicates that it can provide the pointing accuracy required. An additional star tracker for pitch control update would be required. The system, therefore, represents a potentially feasible back-up approach to the primary horizon scanner system.

The characteristics of SCS using an ESG/Polaris star tracker ARS are listed in Table 6.3

Horizon Sensor/Monopulse/Polaris Star Tracker ARS

This configuration is the same as the horizon sensor/Polaris star tracker ARS, with the exception that provision is made for an attitude error signal from the monopulse system. This signal would be used for pitch and roll control whenever pointing at a ground station. The physical characteristics are the same as the horizon sensor/Polaris star tracker ARS as shown in Table 6-1.

Table 6-3. SCS Characteristics - ESG /Polaris Star Tracker ARS

Components	Volume (cu. inches)	Weight (lbs)	Power (watts)	
			Peak	Average
Polaris Star Tracker	1000	20	20	4
Equatorial Star Tracker	1200	18	20	20
Acquisition Sun Sensor	28	3	--	--
Electrically Suspended Gyro Unit	160	14	80	20
3-Axis Gyro Unit	300	10	30	20
Wheel Drive Electronics	140	5	12	4.5
Inertia Wheels	1060	34.2	60	21
Reaction Jet Subsystem	2800	54	20	0.5
Controller	975	34	34	34
Power Inverter	520	18.6	20	5
TOTAL	8183	210.8	296	129.0

3-Axis Gyro ARS

If short term reference is required, a system worthy of possible consideration is a three axis gyro reference system, consisting of three rate integrating gyros operating in a digital pulse torqued or caged mode. In this configuration, the sum of the pulses represent attitude and the frequency of the pulses represent rate. Since this information already may be required for certain maneuvers and autopilot damping, a gyro reference system also could be used for short term attitude reference with frequent updating from external sources.

Updating the gyro reference to remove errors caused by drift could be accomplished by sun sensors and/or star trackers. The period of time between updating is dependent upon the magnitude of the gyro drift. Drift trim circuitry with sufficient resolution will have to be provided along with gyros having low random drifts so they can be used for long periods without updating. Some method of measuring the drift at the beginning of an update period is required, so that proper drift trim may be inserted.

Additional compensation must be provided in the pitch axis to torque the pitch gyro at orbital rate. The orbital rate torquing signal must be altered slightly when offset pointing in roll is required. During roll offset pointing, the yaw gyro will sense a component of the orbital rate. This component is equivalent to 2.35°/hr at an offset attitude of nine degrees. Because this component is a function of the magnitude of offset angle, the compensation to the yaw gyro must be varied accordingly.

As noted previously, periodic correction of gyro drift is necessary. The frequency of correction depends upon the gyro drift. It is also obvious that the sensor used to provide the correction signals must have an accuracy much better than the required accuracy. The sources for references are a sun sensor and/or star trackers. Both of these units can provide the desired accuracy; however, because of the non-orthogonal relationship of the space referenced coordinates, computation must be provided to determine the proper correction signals. Two sensors are required to provide the correction signals for all three gyros. The orbital ephemeris of these references must also be provided.

The other alternative is to use the AOSO type sun sensor or gimbals and readout attitude information from the gimbal positions.

Errors which will contribute to the gyro reference system errors include

1) Ability to match the orbital rate components,
2) Resolution in trimming non-g sensitive drift,
3) Random drift of gyros during periods between correction,
4) Errors of reference sensors used for drift correction.

One advantage of an integrating gyro is that null errors of electronics downstream of the gyro will not appear as attitude hang-off errors, when the gyros are referenced to a long-term stellar reference. The physical characteristics of this system will be similar to the horizon sensor system.

Some gain in reliability could result by use of gyros -- if the sensors could be de-energized between updating periods. Due to the required accuracy, gyros with extremely low drift rates must be obtained to avoid updating by the sensors frequently. Obtaining rate integrating gyros with a low enough drift rate is doubtful; thus, the sensors probably must remain energized at all times -- because frequent switching on and off will reduce the reliability of the unit.

6.2.2 Candidate Reference Sensors

Sun Sensor

The basic requirement for the sun sensor on ATS-4 is to provide a sun-line reference for initial acquisition of earth and Polaris. The sun sensor requirements for ATS-4 can be accomplished with one having a 4π steradian field of view. The 4π steradian sun sensor for acquisition provides pitch-yaw attitude control signals for the spacecraft. The accuracy of this sensor need only be sufficient to allow acquisition of the sun within the ±10 degree field of view of the fine sun sensor.

Basically the concept involves the use of flat silicon photo-voltaic detectors and requires no additional optics. The silicon detector is used because of its high source impedance and its high order of stability with time and temperature.

The general concept employed in the 4π steradian sensor utilizing the flat detectors is illustrated in Figures 6-2a, b, and c. Figure 6-2a illustrates the arrangement of cells about one sensitive axis (into the page) where the cell normals are oriented at 90 degrees to one another for simplicity of illustration and analysis. The output (V_c) of each cell is proportional to the projected area (A) and the responsivity (R). The projected area and responsivity in turn are proportional to the solar energy incident angle (ϕ). Therefore,

$$V_c = K \cos^2 \phi \tag{1}$$

where the constant (K) includes the normal cell responsivity and area as well as incident flux.

Selecting the null direction as shown in Figure 6-2a, the cell outputs are as follows:

$$V_{c1} = k_1 \cos^2(\theta - 45°) \text{ for } -135° \leq \theta \leq 45° \tag{2}$$

$$V_{c2} = k_2 \sin^2(\theta - 45°) \text{ for } -45° \leq \theta \leq 135° \tag{3}$$

$$V_{c3} = k_3 \sin^2(\theta + 45°) \text{ for } 45° \leq \theta \leq 225° \tag{4}$$

$$V_{c4} = k_4 \cos^2(\theta + 45°) \text{ for } 135° \leq \theta \leq 315° \tag{5}$$

where θ is the angle between the sun and the spacecraft null axis. These functions are illustrated in Figure 6-2b. Assuming

$$k_1 = k_2 = k_3 = k_4 = K \tag{6}$$

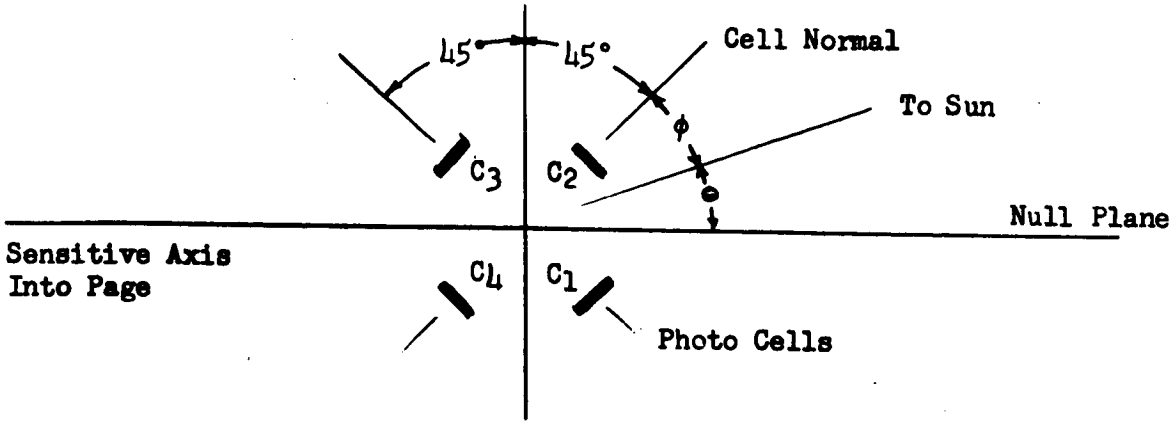

Figure 6-2a. Cell Orientation

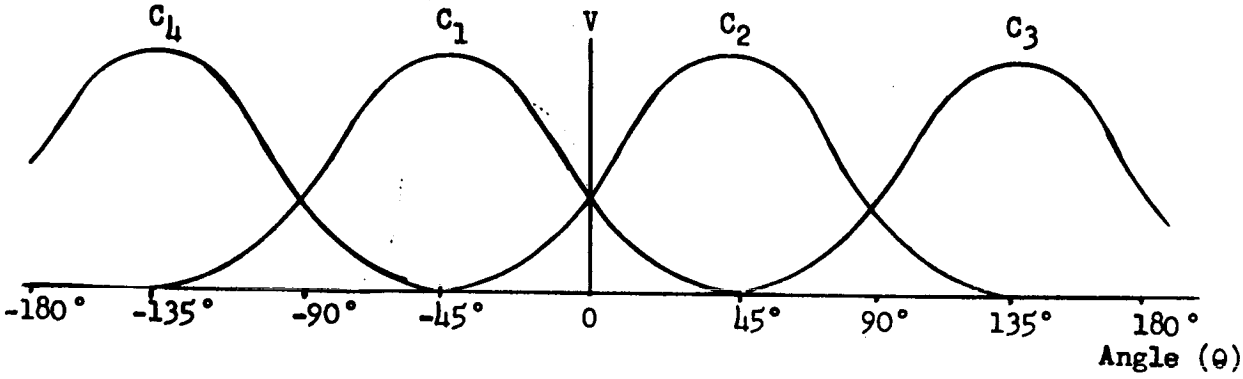

Figure 6-2b. Cell Outputs

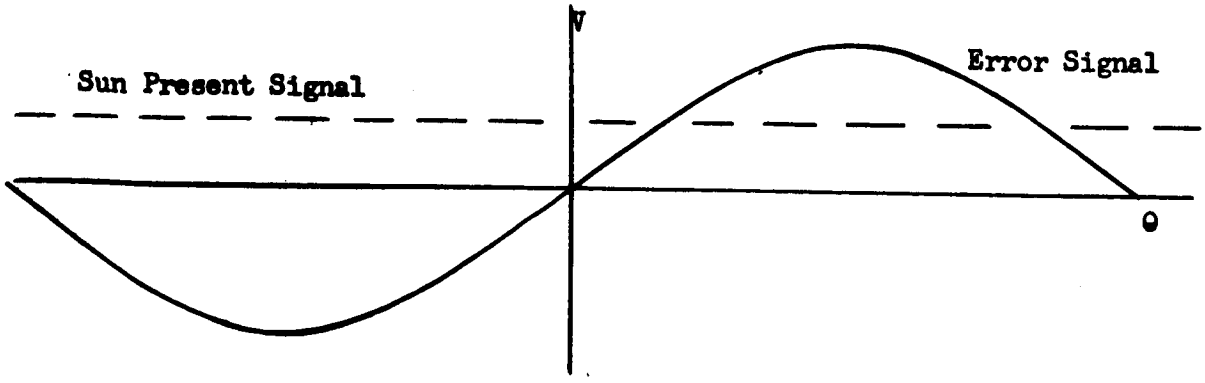

Figure 6-2c. Sun Sensor Signals

The outputs can be summed and differenced so that

$$V_{c1} + V_{c2} + V_{c3} + V_{c4} \geq K \text{ (Sun Present signal)} \quad (7)$$

and

$$(V_{c1} + V_{c4}) - (V_{c2} + V_{c3}) = K\left[2\cos^2(\theta - 45^\circ) - 1\right] \text{ (error signal)} \quad (8)$$

These functions are shown in Figure 6-2c. Automatic gain control can be incorporated to increase the overall performance.

The summed output (Equation 7) is also used to signal sun occult by planets or planetary satellites. The example used (90 degrees between detector normals) is a unique configuration when considering AGC in that the sun remains constant over 4π steradians (assuming the ideal case of infinite AGC gain) thus making the transfer function only dependent on the differential output. However, other configurations may be used satisfactorily to provide the desired functional output. Additional optics and electronic signal conditioning may be used to enhance the characteristics and convert the output to a digital signal if desired.

The fine sensor consists of two cells in each axis which are differentially summed to obtain the error signal. The physical orientation of the cells will be arranged to give the required field of view.

Horizon Sensor

A two-axis horizon sensor is required for acquisition of the earth and control of the vehicle at local vertical during the mission. In addition, it must be programmable for offset pointing with respect to local vertical.

There are basically two concepts presently used in earth horizon sensors. They are:

1) Horizon Scanning - where a sensor instantaneous field of view is caused to scan via a mechanical-optical modulator and the center of the earth is detected by bisecting the points at which "opposite horizons" are crossed.

2) Radiometric Balance Sensing - where two sensor instantaneous fields of view are aligned to view "opposite horizons" and the center of the earth is defined when the outputs from these sensors are equal.

The first approach lends itself to high accuracy, both in earth centered pointing or offset pointing via gimballing or electrically biasing the system reference. The second approach, although simpler and more reliable, is less accurate because of its susceptability to differential drift in critical components. The first concept is therefore required to achieve the pitch and roll accuracy budgeted for attitude control on ATS-4.

Performing offset pointing places the following requirements on the sensors, reference system, and control system:

- The horizon scanner must be capable of providing orientation sensing in pitch and roll while the spacecraft is pointed to any desired location on the visible hemisphere. This may be accomplished either by gimballing the scanning dither in each axis or by biasing the earth center pulse in the scanner output signal. Gimballing the scanning dither allows the horizon scanner optical reference to remain on the earth's center while the antenna is pointed

to any location on the earth's visible hemisphere. However, biasing the earth center pulse results in offsetting the scan plane from the earth center. Although this configuration is basically more reliable than the gimballed approach, the scanner must retain a visible portion of the earth disk at all times causing blindspots approximately one half degree from the horizon in both pitch and roll. This is shown in the diagram below:

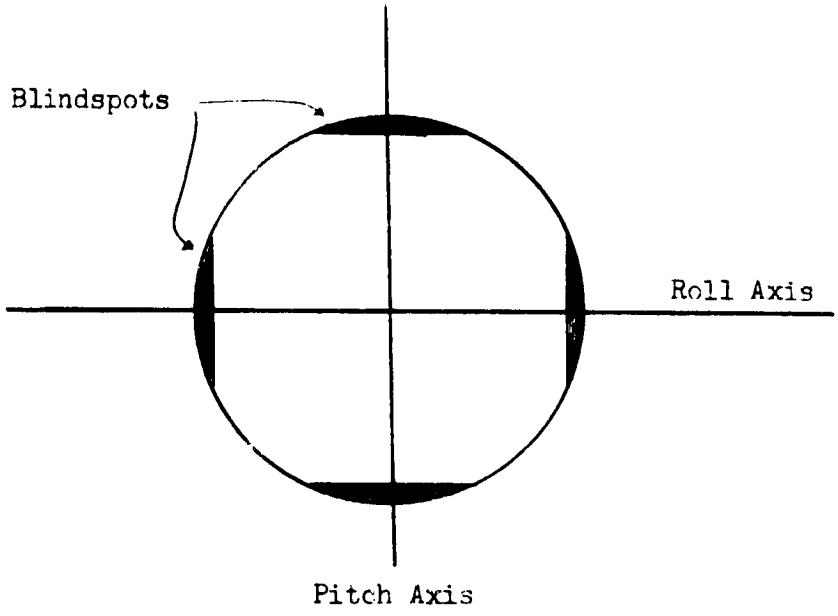

Blindspots in these remote locations may be completely acceptable; however, they may be prohibitive in other maneuver modes.

A concept which avoids this limitation is a two mirror configuration designed by ATD. One mirror provides the dither motion which provides the error signal. The other mirror compensates for large vehicle tilts by displacing the line of sight so that the scan plane coincides with the center of the earth. Thus, accuracy is not degraded due to scanning small chords on

the earth while at offset points. It is also possible to point off of the earth's disc. This may be desirable for earlier interception for low-earth satellites which are to be tracked, and for large antenna pattern measurement maneuvers.

A breadboard model of this double mirror concept has been built and tested by ATD. Modification of this design would be required to achieve the desired field of view and accuracy for synchronous altitude.

The horizon scanner which best meets the ATS-4 requirements is a combination of the Apollo and MOGO designs with the incorporation of the double positor and mirror concept. This configuration uses the optics from the MOGO system and the digital electronics from the Apollo system. However, to protect the proprietary rights of the Advanced Technology Division (ATD) of American Standard, a detailed description of these concepts cannot be included in this final report. References 10 and 11 should be consulted for a technical description of these concepts.

Star Tracker

The Polaris star tracker is required to provide an accurate yaw reference for the ATS-4 control system. Although offset pointing does not require a yaw maneuver, the star tracker must be provided with a means of maintaining stellar reference during offset maneuvers. Offset pointing about the pitch axis imposes no restriction on the star tracker; however, offset pointing in roll would cause loss of Polaris unless a gimballing technique is included.

The star tracker field of view (FOV) requirements are dictated primarily by the acquisition and offset pointing requirements. Since the acquisition sequence has been established as sun-earth-Polaris, the line of sight (LOS) to Polaris will lie normal to the yaw axis within the accuracy of the Horizon Sensor and the roll component of the angle between Polaris and the earth's axis. Therefore, the minimum allowable instantaneous field of view on the star tracker is approximately 2.0 degrees for acquisition without the use of gimbals. Gimballing the telescope for offset pointing via the horizon sensor would allow some reduction in the instantaneous FOV. Additional requirements in the roll FOV are imposed by the vehicle offset pointing requirements.

The initial offset pointing requirement is ±9 degrees and requires that the star tracker field of view be equivalent to this angle in the roll axis. This may be accomplished by extending the star tracker instantaneous FOV or by gimballing the minimum field of view discussed above. Thus, the minimum FOV requirements for the star tracker are ±1.0 degree in yaw and ±10.0 degrees in roll.

It is desired that antenna study maneuvers be made which require driving the vehicle through an angle of 15 degrees in roll and pitch. If star reference is not to be lost, the roll gimbal capability must exceed 15 degrees.

Since the basic requirement of the Polaris star tracker is for yaw reference, roll accuracy (and in turn sensitivity) may not be required. However, if accuracy in roll were provided, the star tracker could be used to calibrate the horizon sensor. This could be accomplished by providing one specific calibration point (e.g., roll gimbal zero) or by making the roll accuracy equivalent to that of the yaw axis throughout the ±9 degrees range, in which case the star tracker could be used as a backup for pointing in roll. The latter approach is more complex in that an accurate gimbal readout would be required and in either case the design is complicated by the specific requirement of roll sensitivity and accuracy.

The star acquisition sequence is initiated from an earth-sun stabilized attitude. Therefore, with knowledge of the ephemeris, the angle to Polaris and the stars between the spacecraft and Polaris are known. Thus, star acquisition may be accomplished by yawing through the proper angle via gyro reference control -- or until the proper stars have been passed through, then the switching yaw control to the star tracker when Polaris is reached. In either case the star tracker must sense the magnitude of Polaris which is approximately +2.1. The nearest bright star to Polaris is Kochab which lies about 12 degrees away in the constellation of Ursa Minor. Other bright stars lie outside the maximum

angle of 23.5 degrees from which star acquisition is initiated. It is conceivable therefore that acquisition can be easily accomplished with only a lower limit on the star presence sensor. However, other modes of operation may require both an upper and lower threshold. Therefore, the requirement on this parameter is tentatively set at ±1.0 degrees magnitude from Polaris. Thus the basic Polaris Star Tracker requirements are as follows:

- Roll FOV - ±15.0 degrees
- Yaw FOV - ±1.0 degree
- Yaw Accuracy - ±1.0 arc minute
- Star Recognition - +2.1 ±1.0 magnitude

Other requirements for the Polaris star tracker which may be desirable are:

- The addition of correction for the diurnal angle between Polaris and the earth's axis
- The addition of a calibrated position in roll which would give approximately the same accuracy as that required in yaw

The diurnal motion of Polaris about the pole can only be corrected with the star tracker. This may be accomplished by gimballing the optical axis of the tracker or by summing a bias with the output to offset the electrical null. In either case an additional requirement is placed on the tracker design; that of the gimbal or the increased gain linearity and stability respectively.

At the present time, there appears to be no tracker designed specifically for tracking Polaris. The OAO tracker is designed to track stars as faint as +2.5 magnitude. The OAO tracker consists of a telescope supported by precision pitch and roll gimbals, each having ±60 degrees of freedom. The tracker weighs 14.5 pounds and requires considerable computation to obtain the attitude error output.

Another tracker which is more suited to the accuracy and functional requirements of the ATS-4 vehicle; is the JPL designed tracker used on the Mariner vehicle. This tracker is presently being modified for the Mariner 69 flight. It will have an instantaneous field-of-view of 0.85 degrees by 9.5 degrees. The electronically gimballed field of view in the non sensitive axis is 34 degrees. This will allow antenna pattern studies to ±17 degrees. The tracker's accuracy is better than 0.1 degree.

To adapt this tracker for ATS-4 and Polaris tracking would require modification of the optics and electronics to increase the sensitivity required for tracking Polaris. The roll gimballing is performed by voltages applied to the image dissector tube deflection plates. Scanning to develop the error signal is also performed by voltage applied to the deflection plates. Correction for the duirnal motion may be made by introducing a bias voltage to the deflection plates.

Gyros

Although the gyros probably will be deenergized for the major part of the mission, they will be used during despin and acquisition, alternate modes of maneuvering and for monitoring functions. An important requirement is that the gyro have a drift rate less than of 0.1 degree/hr.

The Honeywell GG334 strapdown Gas Bearing Gyro can meet this and other requirements. This is a high performance, single-degree-of-freedom floated device designed primarily to meet advanced strapped-down system requirements for attitude reference space system applications. This reliable, precision, inertial-grade gyro offers long life, high-g capability, low-order stable-drift rates, and high-torquing capability.

Principal features of the GG334 for the ATS-4 application are:

- Low power hydrodynamic gas-bearing spin motor with maximum bearing life and reliability. The gyro has a start-stop capability of over 10,000 cycles.
- High rate permanent magnet torquer capable of continuous torquing rates of 15 deg/sec.
- Low torquer time constant suitable for pulse rebalance as well as analog rebalance systems.
- Random drift rates of less than 0.1°/hr.
- Floated gimbal with pivot and jewel output axis bearing.
- Microvernier balance pan.
- Spin motor running detector.

The gyros will be used in a three-axis reference package which incorporates the necessary electronics for caging and torquing the gyros and for generating the rate and attitude information. An example of this package is the DAR (Digital Attitude Reference) which Honeywell has designed specifically for application in a broad variety of space missions. The DAR has the following characteristics:

1) The DAR provides complete three axis attitude information with the output in digital format which makes it compatible with advanced digital control systems.

2) The DAR is completely self contained, relying only on external 28 vdc power and generating internally all other necessary voltages and frequencies.

3) The DAR utilizes passive temperature control via a variable thermal impedance mechanism. This provides a reduced power requirement for inertial sensor temperature control.

4) The DAR is mechanized using the latest advances in electronics circuitry and packaging technology for a minimum size and weight package.

6.2.3 Selected Configuration

The selected configuration for the reference subsystem is summarized below:

Sun Sensors

To provide a full 4π steradian 12 individual sensors are mounted on the vehicle with a null along the x-axis of the vehicle (plus x-axis for a sunrise injection into the final synchronous orbit and minus x-axis for a sunset injection, depending on the launch time of year). Eight cells would normally be sufficient; however, the large antenna causes some obstruction and the additional sensors are required. The fine sun sensor consists of four cells with a narrow field of view for accurate pitch and yaw control to the vehicle-sun line during the acquisition phase.

Horizon Sensor

The most desirable configuration for the horizon sensor appears to be the ATD concept where the scan plane remains through the center of the earth as the vehicle is commanded to offset points or even off of the earth disc. This avoids use of any mechanical gimbal

Star Tracker

Because of offset pointing and antenna maneuvers, gimballing to keep the star in the field-of-view is required. Electronic gimballing is desirable and is used in the JPL Canopus Tracker. Modification of the tracker will be required to increase its sensitivity and to provide electronic gimballing in yaw to account for the diurnal motion of Polaris.

Gyros

The gyros are to be used for both rate and/or attitude information. The gyros selected should be capable of being pulse-torqued in a reference package such as, the DAR. The digital outputs of the DAR are compatible with the controller.

6.2.4 Sensor Performance

A summary of the basic parameters of the sensors is detailed below:

Sun Sensors

- Coarse Acquisition
  - 4π Steradian field-of-view
  - Accuracy ±3 degrees
- Fine Acquisition
  - ±10 degrees field of view
  - Accuracy ±0.25 degrees

Horizon Sensor

- Field of view - ±20 degrees
- Accuracy - ±0.067 degrees (on earth disc)
- Output - Digital, 0.01 degree resolution
- Gimbal capability - ±15 degree

Star Tracker

- Field of view - ±1 degree (sensitive axis)
  - ±9 degree (non-sensitive axis)
- Accuracy - ±0.18 degrees
- Gimbal capability - ±17 degrees (non-sensitive axis)

Gyro Reference Package

- Drift - 0.1 degree/hr
- Output - Rate and attitude (digital)

6.3 DISTURBANCE TORQUES

6.3.1 Meteoroid Impact

Initially, it is worthwhile to distinguish the word meteoroid from meteor or meteorite. Meteoroids are restricted to particles or debris travelling in space. Meteors designate the luminous phenomena associated with meteoroids as they enter the earth's atmosphere. A meteorite denotes a meteoroid which has been found on the earth's surface. The scientific investigation of meteoroids is confined to masses ranging from perhaps 10^{-13}gm to about 100 gms. In size, they vary down to perhaps 1-2μ in diameter. When the dimensions of meteorids reach this limiting order, the large increase in the ratio of area of particle to its mass results in the dominance of solar light pressure effect over solar gravitational force. These tiny particles are driven away from the sun by the radiation pressure, and little or no data is available concerning them.

Origin and Composition of Meteoroids

Meteoroids are generally classified into two groups which are defined by their origin; asteroidal or cometary. A third possible existing group, constituting a very small per cent of the meteoroid distribution, is that of interstellar debris.

The asteroidal particles represent less than ten per cent of the total influx of particles entering the earth's atmosphere. They originate in the asteroidal belt which astronomers believe to have resulted from the fragmentation of a planet into smaller bodies, the asteroids. Iron, nickel, and various stony materials in varying amounts make up the composition of these bodies. The particle densities are of the order of 3.5 gms/cm^3.

The cometary particles represent some ninety per cent or greater of the total influx of particles. Their porous nature, low density (0.03 to 0.05 gms/cm^3), and frangible characteristics, favor the production of a flaring meteor. (See Reference 1)

Meteoroid Streams

Nearly 70 percent of all incoming meteors were earlier classified as belonging to streams in some conic path about the sun. These streams are either narrow with closely packed particles, or very broad in extent with widely separated particles. Of the total incoming flux, about 30 per cent is associated with particular streams, e.g., the Leonids; the remainder is referred to as sporadic. Present day classification describes all meteoroids as belonging to streams; however, the streams are classed as periodic or sporadic. (See Reference 2)

Tables and graphs describing meteoroid flux per square unit per unit time represent statistical averages over long periods. The meteoroid flux rate is never constant - even after correction for the observed effects of large-particle showers. The variation in flux rate is one or two orders of magnitude, with periods of low or high flux measurements of a few days duration. Certain of these variations are due to known meteor showers, and cause annual variations. Random variations also exist with periods of a few days, and can be dealt with only on a statistical basis. Hence, shortlived satellites or rockets may give meteoroid flux measurements very different from the average. Therefore, meteoroid interception by impact sensors is dependent upon both the probability of intercepting a meteoroid stream of known average density, and the probability of encountering a given flux intensity during the sampling period.

Meteor data is made up of two components, the sporadic meteors and the shower meteors belonging essentially to the well-defined short-period

comets and meteor streams. The shower meteors are distinguished by their common radiants and make up about 20 to 30 percent of the meteors sighted. The peak activity during these showers may be four to five times the sporadic meteor rate, but on extremely rare occasions much greater. For example, a rate increase of 5000 was reported on 9-10 October 1946, when the Giacobinid-Zinner comet orbit was crossed by Earth. One of the most spectacular visual displays was that of the Leonids shower in 1833 in which a rate increase estimated to be 20,000 times the normal rate was observed.

Meteoroid Velocity

Meteoroids encountered by the earth will have velocities relative to the earth ranging from 11 km/sec to 72 km/sec. This is based on the fact that for a particle following a parabolic path about the sun the maximum velocity it could have at the distance of Earth from the sun is approximately 42 kilometers per second. If such a particle meets Earth head on, as it orbits the sun at a velocity of approximately 30 kilometers per second, a combined velocity (neglecting Earth's gravitational attraction) or approximately 72 kilometers per second is obtained. To achieve higher velocities would require the particles to be following hyperbolic paths and thus be of interstellar origin. The lower limit occurs when the particles obtain their velocity relative to Earth by Earth gravitational attraction alone. For space vehicles encountering these particles the range of relative velocities could be somewhat greater. This is due to the velocity of the space vehicle.

The brighter meteors have higher velocities and the fainter meteors are slower. In reference 4, a total of 2529 photographs of meteors were evaluated to determine a mean meteoroid velocity of 28 km per second. It is pointed out, however, that many meteoroids are much slower and that they enter the earth's atmosphere unobserved. Hence, the mean meteoroid velocity should be reduced to about 22 km per second on this basis.

A second argument shown in reference 4 indicates that the determination of the meteor ionizing efficiency is proportional to its velocity to the fourth power. This would result in a mean meteoroid velocity calculation of greater than 30 km per second.

Since the mean velocity is not well defined, a conservative value of 30 km per second is generally accepted by most authors.

Meteoroid Flux Density

The meteoroid flux density could have a day-to-day variation of several orders of magnitude due to encountering the orbits of known meteoroid streams. There may be as many meteoroids striking a spacecraft in one day due to a meteoroid stream as there are in a whole year due to sporadic meteoroids. Also, the meteoroids in a particular stream are all travelling in the same orbit with the same relative velocity. For example, the Geminid stream has a mean velocity of 36.2 km per second and the Orionid stream has a mean velocity of 67.7 km per second (reference 1). Sporadic meteoroids, however, are omni-directional, vary in velocity from 11 to 72 km per second, and have a very low flux density.

Numerous attempts have been made to determine an average value of the meteoroid flux environment in the vicinity of the earth. Due to assumptions and different methods, these calculations have resulted in flux density values which are several orders of magnitude apart. Reference 3 cites several flux equations which result in widely varying densities. Two values are given (3.4×10^{-8} gm/meter^2-sec, and 1.96×10^{-10} gm/meter^2-sec) using two different approximations to the density curve shown in Figure 6-3. Both of these calculations, however, are biased toward the smaller, more dense particles and highly susceptible to the assumed particle size cut-off point. It is assumed that particles smaller than a certain magnitude are all swept away by solar radiation pressure. Additionally, two other quantities

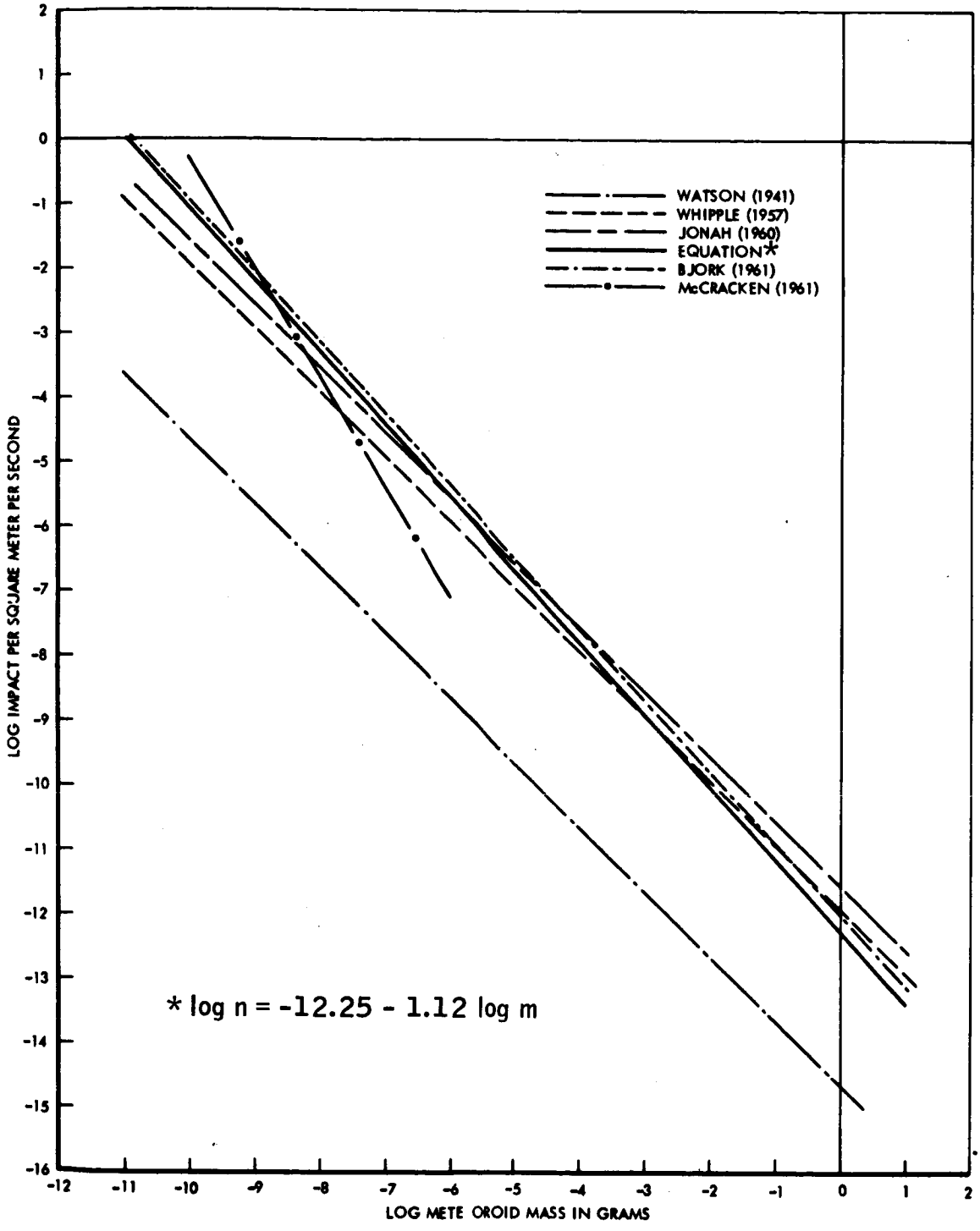

Figure 6-3. Meteoroid Extrapolations

are given (3.62×10^{-11} gm/meter^2-sec) and (3.0×10^{-11} gm/meter^2-sec) which are biased toward the larger particles and are somewhat insensitive to the smaller particles. In this case, the assumed cut-off point on the large particle end of the scale strongly influences the calculation. Since the larger particles occur more rarely, a cutoff point of one impact per square meter per year could be made, which would result in reducing the flux calculation by more than an order of magnitude (2.5×10^{-12} gm/meter^2-sec).

Since wide disagreement exists in the literature concerning the development of an averaged flux density equation, another approach is to determine the momentum of each meteoroid of each size and examine its probability of occurrence. The control system, then, would be sized to balance the disturbance induced by each meteoroid impact separately. Meteors may be classed accordingly to their visual magnitude. Magnitudes fainter than +5, which cannot be observed visually, are detected by radar observations of ion trails. The data show in Figure 6-3, then corresponds to the mass and particle frequency versus visual magnitude shown in Table 6-4. Using this data, the momentum of each meteoroid of each size together with its frequency of occurrence is used to determine the total control impulse required to balance the disturbance. All of these calculations assume that all meteoroids impinge on the surface, and there is a pure momentum transfer to the impacted surface. Modification to this momentum transfer assumption is discussed in the next section of this report.

In Table 6-4, Column 1 shows the visual meter magnitude as a function of meteoroid mass (Column 2) assuming an average relative velocity of 30 km per second. Column 3 shows the accumulated flux density of meteoroid mass, m, and larger which corresponds to the curves shown in Figure 6-3, (reference 5). The meteoroid flux density within each visual magnitude is then shown in Column 4. Using a calculated vehicle surface area of 25.5 square meters and a two-year mission time, the probability of encountering a meteoroid of mass, m, is shown in Column 5. The momentum of a meteoroid of each size, shown in Columns 6 and 7 is multiplied by the probability of

Table 6-4. Meteroid Momentum Data

1 Meteor Visual Magnitude	2 Mass, m (grams)	3 Flux Density, N ($lb/meter^2$-sec) accumulative	4 N_M (Flux Density in Each Magnitude	5 N'_M Impacts in Two Years in Each Mag.	6 MV, $(\frac{gm\text{-}cm}{sec})$ Momentum of Each Meteoroid Size	7 MV, (lb_f-sec)	8 MV N'_M (lb_f-sec)
5	.250	1.82×10^{-11}	1.82×10^{-11}	2.91×10^{-2}	7.50×10^{5}	1.69	4.92×10^{-2}
6	9.95×10^{-2}	5.30×10^{-11}	3.48×10^{-11}	5.56×10^{-2}	2.98×10^{5}	6.70×10^{-1}	3.73×10^{-2}
7	3.96×10^{-2}	1.34×10^{-10}	8.10×10^{-11}	1.30×10^{-1}	1.19×10^{5}	2.67×10^{-1}	3.47×10^{-2}
8	1.58×10^{-2}	3.35×10^{-10}	2.01×10^{-10}	3.22×10^{-1}	4.74×10^{4}	1.07×10^{-1}	3.44×10^{-2}
9	6.28×10^{-3}	8.41×10^{-10}	5.06×10^{-10}	8.10×10^{-1}	1.88×10^{4}	4.23×10^{-2}	3.43×10^{-2}
10	2.50×10^{-3}	2.12×10^{-9}	1.28×10^{-9}	2.05	7.50×10^{3}	1.69×10^{-2}	3.46×10^{-2}
11	9.95×10^{-4}	5.30×10^{-9}	3.18×10^{-9}	5.09	2.98×10^{3}	6.70×10^{-3}	3.41×10^{-2}
12	3.96×10^{-4}	1.34×10^{-8}	8.10×10^{-9}	1.30×10^{1}	1.19×10^{3}	2.67×10^{-3}	3.47×10^{-2}
13	1.58×10^{-4}	3.35×10^{-8}	2.01×10^{-8}	3.22×10^{1}	4.74×10^{2}	1.07×10^{-3}	3.45×10^{-2}
14	6.28×10^{-5}	8.41×10^{-7}	5.06×10^{-8}	8.10×10^{1}	1.88×10^{2}	4.23×10^{-4}	3.43×10^{-2}
15	2.50×10^{-5}	2.12×10^{-7}	1.28×10^{-7}	2.05×10^{2}	7.50×10^{1}	1.69×10^{-4}	3.46×10^{-2}
16	9.95×10^{-6}	5.30×10^{-7}	3.18×10^{-7}	5.09×10^{2}	2.98×10^{1}	6.70×10^{-5}	3.41×10^{-2}
17	3.96×10^{-6}	1.34×10^{-6}	8.10×10^{-7}	1.30×10^{3}	1.19×10^{1}	2.67×10^{-5}	3.47×10^{-2}
18	1.58×10^{-6}	3.35×10^{-6}	2.01×10^{-6}	3.22×10^{3}	4.74	1.07×10^{-5}	3.45×10^{-2}
19	6.28×10^{-7}	8.41×10^{-6}	5.06×10^{-6}	8.10×10^{3}	1.88	4.23×10^{-6}	3.43×10^{-2}
20	2.50×10^{-7}	2.12×10^{-5}	1.28×10^{-5}	2.05×10^{4}	7.50×10^{-1}	1.69×10^{-6}	3.46×10^{-2}
21	9.95×10^{-8}	5.30×10^{-5}	3.18×10^{-5}	5.09×10^{4}	2.98×10^{-1}	6.70×10^{-7}	3.41×10^{-1}
22	3.96×10^{-8}	1.34×10^{-4}	8.10×10^{-5}	1.30×10^{5}	1.19×10^{-1}	2.67×10^{-7}	3.47×10^{-1}
23	1.58×10^{-8}	3.35×10^{-4}	2.01×10^{-4}	3.22×10^{5}	4.74×10^{-2}	1.07×10^{-7}	3.45×10^{-2}
24	6.28×10^{-9}	8.41×10^{-4}	5.06×10^{-4}	8.10×10^{5}	1.88×10^{-2}	4.23×10^{-8}	3.43×10^{-2}
25	2.50×10^{-9}	2.12×10^{-3}	1.28×10^{-3}	2.05×10^{6}	7.50×10^{-3}	1.69×10^{-8}	3.46×10^{-2}
26	9.25×10^{-10}	5.30×10^{-3}	3.18×10^{-3}	5.09×10^{6}	2.98×10^{-3}	6.70×10^{-9}	3.41×10^{-2}
27	3.96×10^{-10}	1.34×10^{-2}	8.10×10^{-3}	1.30×10^{7}	1.19×10^{-3}	2.67×10^{-9}	3.47×10^{-2}
28	1.58×10^{-10}	3.35×10^{-2}	2.01×10^{-2}	3.22×10^{7}	4.74×10^{-4}	1.07×10^{-9}	3.45×10^{-2}
29	6.28×10^{-11}	8.41×10^{-2}	5.06×10^{-2}	8.10×10^{7}	1.88×10^{-4}	4.23×10^{-10}	3.43×10^{-2}
30	2.50×10^{-11}	2.12×10^{-1}	1.28×10^{-1}	2.05×10^{8}	7.50×10^{-5}	1.69×10^{-10}	3.46×10^{-2}
31	9.95×10^{-12}	5.30×10^{-1}	3.18×10^{-1}	5.09×10^{8}	2.98×10^{-5}	6.70×10^{-11}	3.41×10^{-2}

occurrence to determine the expected impulse exerted against the vehicle (Column 8). The sum of Column 8 results in a total of 0.947 lb-sec. Assuming that a meteoroid may strike anywhere on the vehicle, and estimating an average distance of impact from the center of gravity of 12 feet with a control moment arm of 4 feet, 2.841 lb-sec of control impulse is required to balance the meteoroid disturbance torque. Since the control system will be required to compensate for the individual impacts of the larger more sparse meteoroids, the impulse required to balance a magnitude 5 meteoroid impacting on the solar panel (18 feet from the c.g.) and traveling at 72 km per second could be as high as 24 lb-sec. However, the probability of encountering a meteoroid of magnitude 5 traveling at 72 km per second is less than once in 150 years. Further, an impact of this nature would penetrate several inches of material, causing most of the meteoroid to continue through the spacecraft resulting in lower momentum exchange and possible damage to the spacecraft.

For comparison, 0.947 lb-sec of total impulse converts to 9.41×10^{-10} gm/meter^2-sec average flux density as follows:

$$\left(\frac{\text{sec}}{30 \times 10^5 \text{cm}}\right)\left(\frac{0.947 \text{ lb ft-sec}}{63 \times 10^6 \text{sec}}\right)\left(\frac{1}{25.5 \text{ ft}^2}\right)\left(\frac{4.448 \text{ newtons}}{\text{lb}_f}\right)\left(\frac{1 \times 10^5 \text{dynes}}{\text{newton}}\right)\left(\frac{\text{ft}^2}{0.0929 \text{ m}^2}\right)\left(\frac{\frac{\text{gm-cm}}{\text{sec}^2}}{\text{dyne}}\right)$$

This compares favorably to the mean of the previously stated average flux density calculations. Since this results in a pressure force of 5.89×10^{-10} lbs/ft^2 it may be concluded that meteoroid impact provides a disturbance torque which is a factor of 170 below solar radiation pressure (1×10^{-7} lb/ft^2). It is restated, however, that this assumes a one to one momentum exchange from the meteoroid to the spacecraft.

Momentum Amplification

Several theoretical calculations have been proposed concerning a momentum amplification due to hypervelocity meteoroid impact. Since a meteoroid can

displace or expell more material mass from a surface than its own, several authors (reference 3) have advanced the theory of momentum amplification ranging from a factor of 2 to a factor of as high as 36. A factor of 2 is conceivable for the smaller particles which may strike a surface and "bounce back" at nearly the same velocity. Larger or faster meteoroids, however, will cause craters resulting in expelling material (ejecta) from the surface. This phenomenon gives rise to the momentum amplification theory. Still other particles will completely penetrate the surface and continue through the spacecraft carrying some material with it; this could result in a slightly less than one momentum exchange factor.

The material erosion on satellites necessary to substantiate a high momentum amplification factor has not been observed. Therefore, it is assumed that through the spectrum of meteoroids, there could be momentum amplification factors ranging from slightly less than one to possibly greater than 2 or 3. Using an average momentum amplification factor of 2, the impulse becomes 1.894 lb/sec which converts to 1.882×10^{-9} gm/meter^{2}sec, or 1.178×10^{-9} lb_f/ft^2, which is a factor of 85 below solar radiation pressure.

Although the study of the meteoroid environment is not sufficient to permit the formation of an accurate meteoroid disturbance model, the above calculations indicate that the average meteoroid disturbance torque is nearly two orders of magnitude below that of solar radiation pressure. Except for high flux densities during possible meteoroid streams or in the improbable event that a large, high velocity meteoroid is encountered, the disturbance torque due to meteoroid impact may be neglected.

6.3.2 Gravity Gradient

The effect of gravity gradient torques for the ATS-4 configuration will be small because of the synchronous altitude and the near local vertical orientation. Expressions used to evaluate the gravity gradient torques are:

$$T_X = -4\omega_o^2 (I_Y - I_Z)\phi \quad \text{(roll axis)}$$

$$T_Y = -3\omega_o^2 (I_X - I_Z)\theta \quad \text{(pitch axis)}$$

$$T_Z = -\omega_o^2 (I_Y - I_X)\psi \quad \text{(yaw axis)}$$

where

T_X, T_Y, T_Z = Torques (ft lbs)

I_X, I_Y, I_Z = Principal axis inertias (slug-ft^2)

ω_o = Orbital rate (radians per sec)

ϕ = Roll angle (radians)

θ = Pitch angle (radians)

ψ = Yaw angle (radians)

These equivalent torque expressions include the dynamic phenomena associated with the rotating (local vertical) coordinate frame and the tendency of a rotating, freely-suspended body to rotate about its maximum axis of inertia. These equations were used in determining impulse requirements for the reaction jet system. The torque at offset points of 0.1 radians are as follows:

$$(72.9 \times 10^{-6})^2 \ (1226 - 167)(0.1) = 93.7 \times 10^{-8} \text{ roll}$$

$$(72.9 \times 10^{-6})^2 \ (2150 - 1677)\ (0.1) = 77.5 \times 10^{-8} \text{ pitch}$$

These torques are a factor of 200 less than peak solar radiation torques and a factor of 40 less than the average roll solar radiation torque.

6.3.3 Magnetic Disturbance

The torques due to the magnetic moment of the vehicle interacting with the earth's magnetic field are small compared to the solar radiation torques. Assuming that the ATS-4 spacecraft has a magnetic moment equal to 4000 dyne-cm per gauss (AOSO requirements), the torque in a field of 200 gamma (synchronous altitude) is 60×10^{-8} ft. lb. This is small compared to the solar radiation pressure torque.

6.3.4 Internal Rotating Equipment

Momentary torque disturbances will occur due to starting and stopping of tape recorders, gyros etc. The momentum contributed by these sources will be stored by the reaction wheels.

6.3.5 Solar Pressure

Theory

Interplanetary radiation originates primarily from our own solar system. Galactic radiation, compared to solar radiation contributes little to the total radiation pressure exerted on a unit area of a spacecraft.

Solar radiation is further divided into electromagnetic radiation and particle radiation. Electromagnetic radiation consists of quanta called photons which propagate in wave forms having wavelengths in the continuous spectrum. Photons have zero rest mass, no electrical charge, and no magnetic moment, but they do posses energy resulting in a force producing a pressure termed "Light

Pressure." Particle radiation, however, consists of electrons, protons, neutrons, alpha and beta particle plasma and many other sub particles. These particles, which have a rest mass, are expelled from the sun at velocities of from 400 to 1500 km per second. This particle radiation which sweeps throughout interplanetary space is termed "Solar Wind".

Electromagnetic Radiation -- The intensity of electromagnetic radiation is inversely proportional to the square of the distance to the sun. About 99 per cent of this solar energy is concentrated in the narrow range from 3000 to 4000 Angstroms (Reference 6), with the remaining 1 per cent distributed in the ultraviolet, infrared and radio frequencies. The rate at which solar electromagnetic radiation is received outside the earth's atmosphere on a unit surface normal to the incident radiation and at a distance of one astronomical unit from the sun is called the solar constant. This quantity which produces "light pressure" is virtually unchanged with high solar activity. The solar constant has the value of

$$1396 \text{ watts/meter}^2$$

being accurate to ±1 per cent due to gradual long term variations and instrument measurement error. Dividing the solar constant by the speed of light and converting the units produces the quantity of solar light pressure exerted on a unit area.

$$P = \frac{\left(\frac{1394 \text{ watts}}{\text{meter}^2}\right)\left(\frac{\text{hp}}{746 \text{ watts}}\right)\left(\frac{550 \text{ ft-lb-sec}^{-1}}{\text{hp}}\right)\left(\frac{10^{-4} \text{ meter}^2}{\text{cm}^2}\right)\left(\frac{2.54^2 \text{ cm}^2}{\text{in}^2}\right)\left(\frac{144 \text{ in}^2}{\text{ft}^2}\right)}{9.83514 \times 10^8 \ \frac{\text{ft}}{\text{sec}}}$$

$$P = 0.970814 \times 10^{-7} \text{ lb/ft}^2$$

Partical Radiation -- The solar atmosphere is composed primarily of ionized particles that flow continuously outward from the sun. This flow which represents an expansion of the solar corona is called the "Solar Wind". The corona is composed primarily of hydrogen; hence, the solar wind consists primarily of highly ionized hydrogen particles (electrons and protons). Since the mass of the proton is 1837 times the mass of the electron, the energy of the solar wind can be determined from the particle energy of the proton alone, which is about one Kev during quiet sun periods. The mass of a proton (Reference 7) is given as:

$$M = 1.67 \times 10^{-24} \text{gm}$$

During quiet sun periods, the solar wind particles at one astronomical unit are traveling at a velocity of about 400 kilometers per second with a density of about 10 particles per cubic centimeter (Reference 6).

$$P = M N V^2 \cos \theta$$

where

M = particle mass
N = particle density
V = particle velocity
θ = particle incident angle

A surface exposed 90° to the solar wind will have a zero incident angle. In this case,

$$P = M N V^2$$

$$P = (1.67 \times 10^{-24} \text{ gm}) \left(\frac{10}{\text{cm}^3}\right) \left(4 \times 10^7 \ \frac{\text{cm}}{\text{sec}}\right)^2$$

$$P = 267.2 \times 10^{-10} \frac{gm}{cm\text{-}sec^2}$$

Converting the units,

$$P = \left(267.2 \times 10^{-10} \frac{gm}{cm\text{-}sec^2}\right)\left(\frac{dynes}{\frac{gm\text{-}cm}{sec^2}}\right)\left(\frac{1 \times 10^{-5} \text{ newton}}{\text{dyne}}\right)\left(\frac{lb_f}{4.448222 \text{ newton}}\right)\left(\frac{929.03 \text{ cm}^2}{ft^2}\right)$$

$$P = 5.581 \times 10^{-11} \frac{lb}{ft^2} \qquad \text{(Quiet Sun Particle pressure)}$$

During active sun periods, however, the solar pressure due to particle radiation is greatly magnified. Solar flares cause a rapid expansion of the corona producing an increase in the velocity and density of the solar plasma.

Solar flares vary in magnitude and brightness and are classified according to their area (per cent of solar disk involved). Observations have shown that the frequency and duration of solar flares vary as a function of their class (Reference 8). Small flares (class 1) occur every few hours and have durations of about 10 to 40 minutes.

Conversely, the large flares (class 3 and class 3+) occur more rarely but have longer durations. As many as six or seven class 3+ flares with mean durations of about three hours may be expected in one year during the active portion of the eleven year solar cycle.

As a result of a class 3+ flare, the solar plasma velocity may increase to about 1500 kilometers per second with particle density increasing to as high as 100 particles per cubic centimeters (References 6 and 9). During this brief period, the solar particle radiation pressure increases as follows:

$$P = M N V^2$$

$$P = 1.67 \times 10^{-24} \text{ gm}) \left(\frac{100}{\text{cm}^2}\right)\left(15 \times 10^7 \quad \frac{\text{cm}}{\text{sec}}^2\right)$$

$$P = 37575.0 \times 10^{-10} \frac{\text{gm}}{\text{cm-sec}^2}$$

Converting the units

$$P = 7.848 \times 10^{-9} \frac{\text{lb}_f}{\text{ft}^2}$$ (Particle radiation pressure during a class 3+ flare)

Conclusion

Based upon the foregoing analysis, the particle radiation pressure, even during a large flare, is several orders of magnitude less than the electromagnetic radiation pressure. Therefore, particle radiation pressure may be neglected.

In developing the solar pressure disturbance torque model, a constant pressure of 1×10^{-7} lb_f/ft^2 may be used for a surface normal to the sun-line with no variation due to solar activity.

This analysis has been directed only toward determining the magnitude of the solar radiation pressure and as such, particle radiation is insignificant. However, particle radiation may impose severe material degradation particularily during high solar flare activity. Radiation damage to materials has not been considered in this analysis.

6.3.6 Disturbance Torque Model

An analysis of the ATS-4 vehicle configuration indicates that the only significant external disturbance torque is due to solar radiation pressure. Meteoroid impact and gravity gradient disturbance torques are both several orders of magnitude below solar pressure, although the rare occurrence of a relatively large meteoroid could result in an individual impact disturbance torque sufficiently large to require control system correction. Therefore, this disturbance torque model considers solar radiation pressure only.

The magnitude of the solar pressure coefficient is approximately 1×10^{-7} lb_f/ft^2. This quantity is derived from the solar constant (photon radiation) which does not vary with high solar flare activity. Solar flares produce an increase in the solar wind (particle radiation) resulting in a force which is two to four orders of magnitude below photon radiation. This coefficient is the force exerted on one square foot of totally absorbing surface in a plane perpendicular to the sun-line.

Antenna Projected Surface Area --The antenna consists of a petal structure covered with a wire mesh. The mesh is made of one mil wire with 80 thousandths spacing. A segment of this wire mesh which is in a plane perpendicular to the sun-line results in a 20.8 per cent shaded surface area or 79.2 per cent open area. As the solar incident angle decreases, the per cent of projected surface area in each mesh segment increases. One hundred percent surface area per mesh segment is achieved between 86° and 90° solar incident angle. This is shown in Figure 6-4.

Since the antenna is not a flat surface, the amount of open area in each mesh segment varies over the paraboloidal surface. To determine the effective projected surface area of the paraboloidal antenna over a 24-hour period, a series of representative cross-sectional segments of the antenna were examined

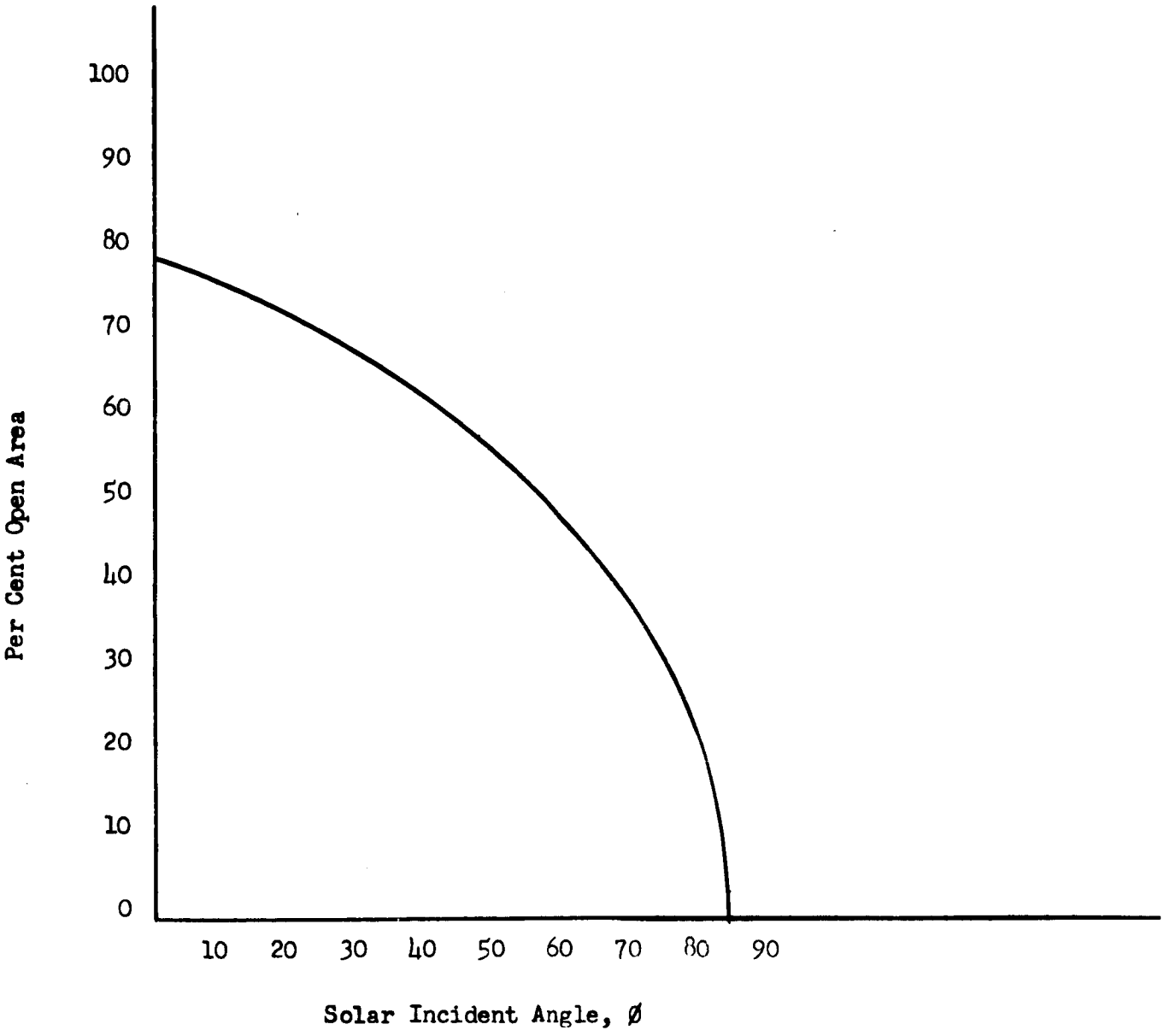

Figure 6-4. Percent Open Area in Each Mesh Segment As a Function of Solar Incident Angle

at several points in the orbit. When the solar incident angle is zero (sun-line perpendicular to the plane of the antenna, xy plane) the antenna presents a symmetrical surface to the sun line, and the disturbance torque is zero in all three axes. However, as the vehicle pitches through 360° and the sun-line changes from an equinox to a solstice orientation, a continuously varying projected surface results. A series of five cross-sectional slices of the antenna mesh and petal structure were examined to form a representative definition of the projected area and center-of-pressure. Along the projection of each cross-sectional slice, a total of 14 station locations were selected for analysis. By geometrically determining the solar angle of incidence at each of the 14 stations on each of the five cross-sectional slices, a projected surface density map was generated. This process is illustrated in Figure 6-5. At each intersecting point on the projected surface, a ratio of shaded to total area was determined as a function of vehicle orientation. With this information, the total projected area was summed and a weighted center of pressure was determined by the mean of the integrated area under each curve. The projected area is graphically illustrated in Figure 6-6. The disturbance torque in each axis is determined from the projected area and center-of-pressure moment arms of each of the three major vehicle parts; panels, antenna, and spacecraft module. This analysis considers the amount of sunlight passing through the antenna onto the module. Similarily, the module shading against the antenna in the opposing orientation is considered. The calculated moment arms in each axis, for both an equinox and a solstice condition and for a full 360° vehicle orientation, are shown in Table 6-5.

In this analysis, it is assumed that the solar radiation striking each surface is perfectly absorbed. If a perfectly reflecting body is assumed, photons striking a flat surface at a zero incident angle would produce a momentum amplification factor of 2. For cylinderical surfaces (such as wire mesh) and a zero incident angle, a momentum amplification factor of 1.27 would

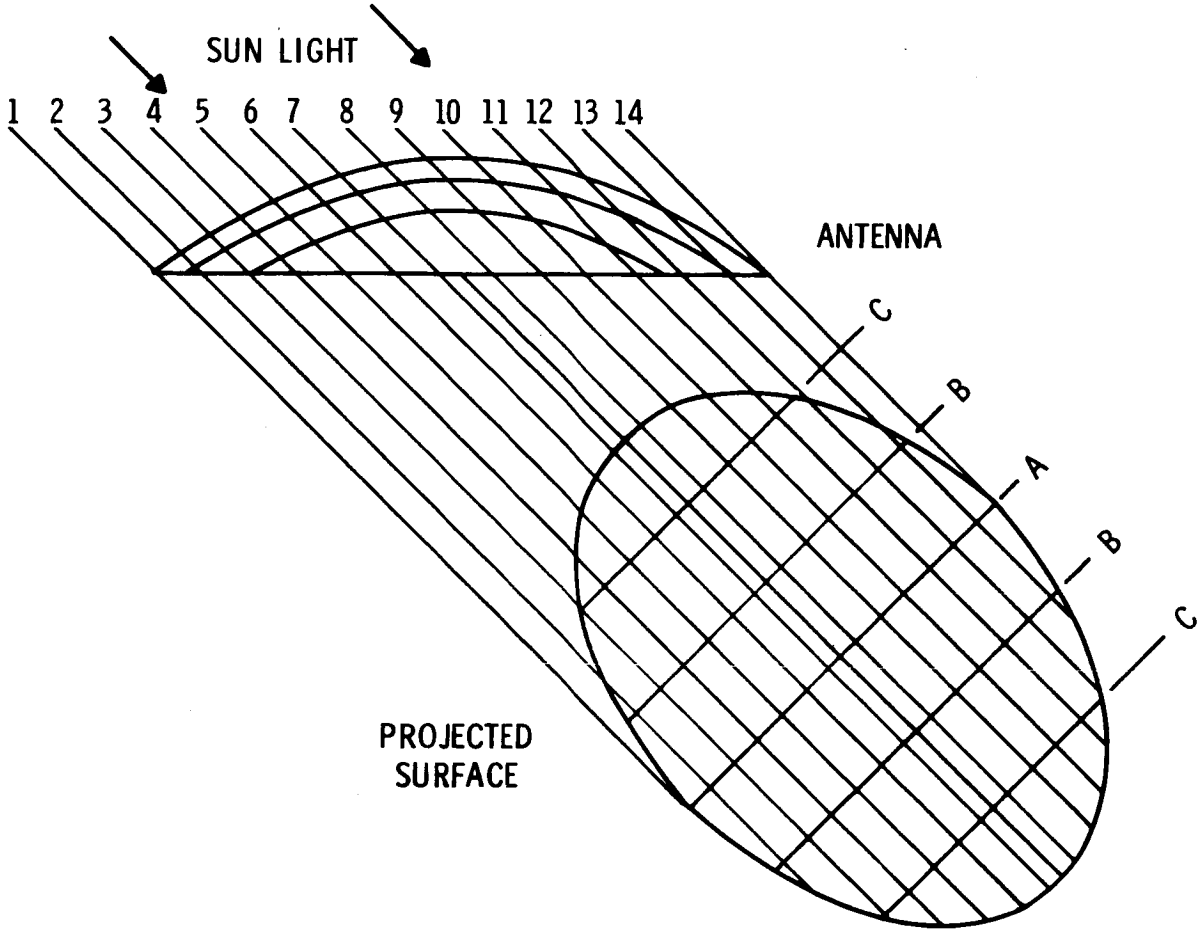

Figure 6-5. Antenna Projected Surface Map

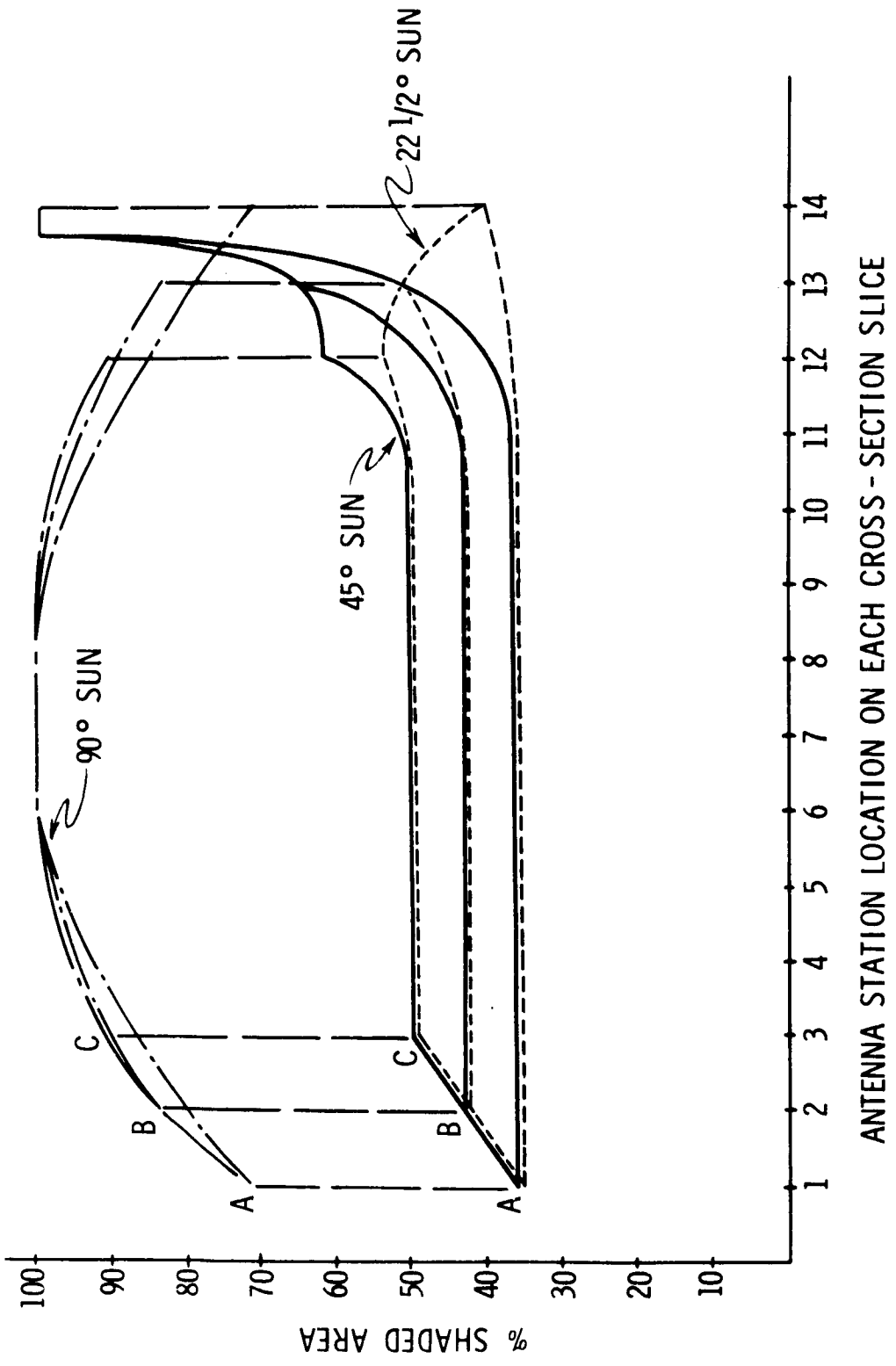

Figure 6-6. Projected Antenna Shaded Area Profile

Table 6-5. Solar Pressure Moment Arms, Feet

Orientation θ	PITCH						ROLL						YAW	
	PANELS		ANTENNA		MODULE		PANELS		ANTENNA		MODULE		PANELS	
	EQU	SOL	EQU	SOL	EQU	SOL	EQU	SOL	EQU	SOL	EQU	SOL	EQU	SOL
0°	-	-	0	0	0	0	19.2	15.6	0	3.1	0	.75	0	0
45°	3.5	3.5	4.6	4.6	1.25	1.25	-	2.3	0	2.1	0	.5	-	2.3
90°	5.0	5.0	7.0	7.0	1.7	1.7	0	0	0	0	0	0	19.2	15.6
135°	3.5	3.5	4.75	4.75	1.25	1.25	-	2.3	0	2.1	0	.5	-	2.3
180°	-	-	0	0	0	0	19.2	17.9	0	3.3	0	.75	0	0
225°	3.5	3.5	4.75	4.75	1.25	1.25	-	2.3	0	2.1	0	.5	-	2.3
270°	5.0	5.0	7.0	7.0	1.7	1.7	0	0	0	0	0	0	19.2	17.9
315°	3.5	3.5	4.6	4.6	1.25	1.25	-	2.3	0	2.1	0	.5	-	2.3
360°	-	-	0	0	0	0	19.2	15.6	0	3.1	0	.75	0	0

result. However, the solar panels, which are the only flat surfaces of any significance, may be considered absorbing bodies. Further, a zero incident angle on the cylindrical wire in the antenna mesh is seldom encountered. An indicdnt angle relative to the normal to the axis of a cylinder, results in a decreased momentum amplification factor. As the incident angle goes from o° to 36°, the amplification factor goes from 1.27 to 1.0. For angles greater than 36°, the amplification factor is less than one. Since all solar incident angles from 0° to 90° are present during peak torque periods, the average incident angle is greater than 36°, and a reflecting body momentum amplification factor of less than one may be considered. Therefore, the assumption that the antenna is a perfectly absorbing body, having a 1:1 momentum exchange, may be considered slightly conservative.

The resulting solar pressure disturbance torques in each of the three axes is shown in Figures 6-7 to 6-11. Figure 6-7 shows the pitch torque for both an equinox and a solstice condition due to all three spacecraft parts. In roll, there is no resultant torque on the antenna and module during an equinox condition. However, at all other solar positions an offset sine wave results as shown in Figure 6-8. The roll torque due to the fixed solar panels is shown in Figure 6-9. A composite torque model for the roll axis including the antenna, module, and panels for the equinox and both solstice conditions is shown in Figure 6-10. The yaw torque, shown in Figure 6-11, is due to the fixed solar panels alone. This is the same as the roll torque due to the panels but displaced 90 degrees.

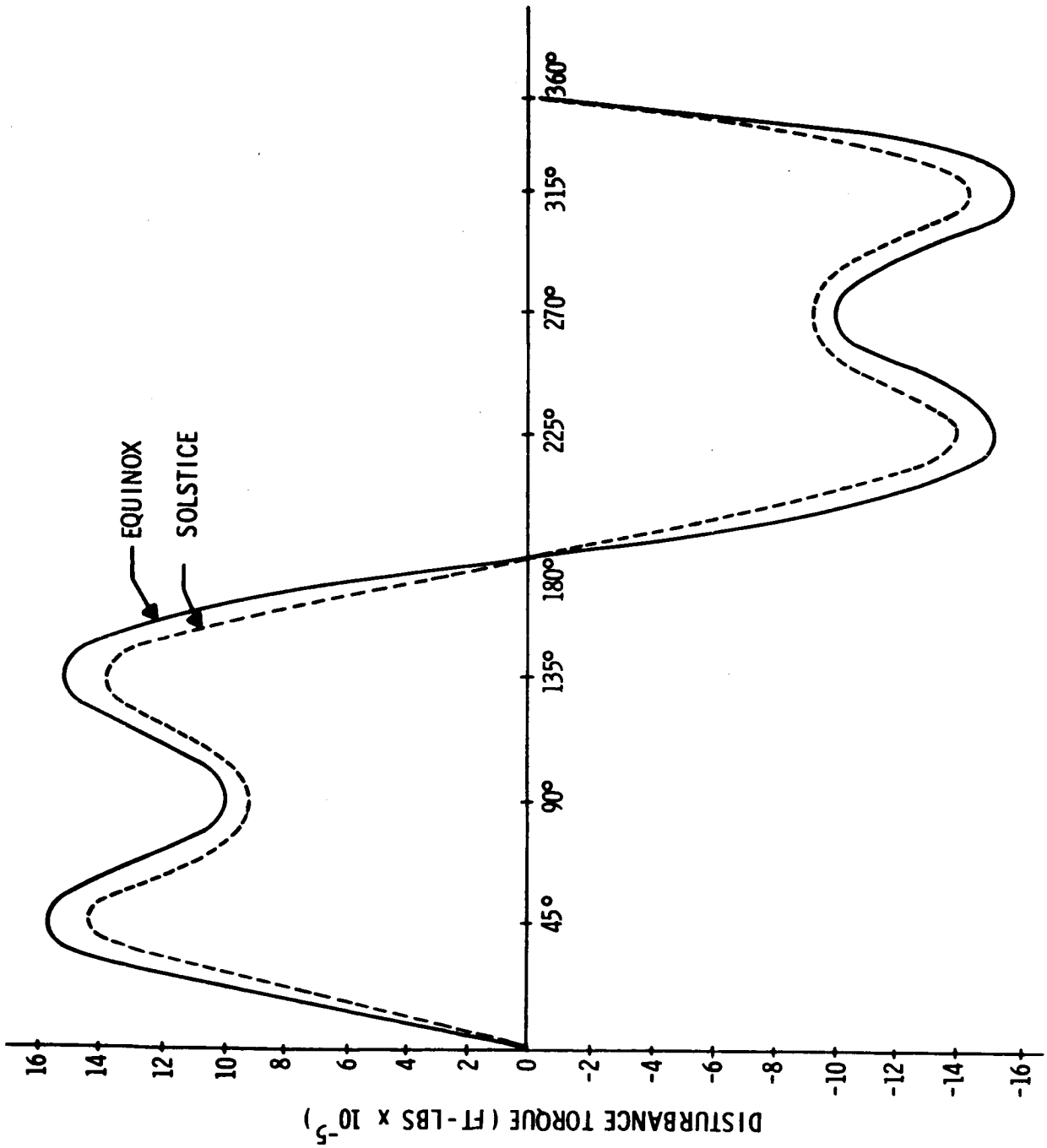

Figure 6-7. Pitch Axis Solar Pressure Disturbance Torque

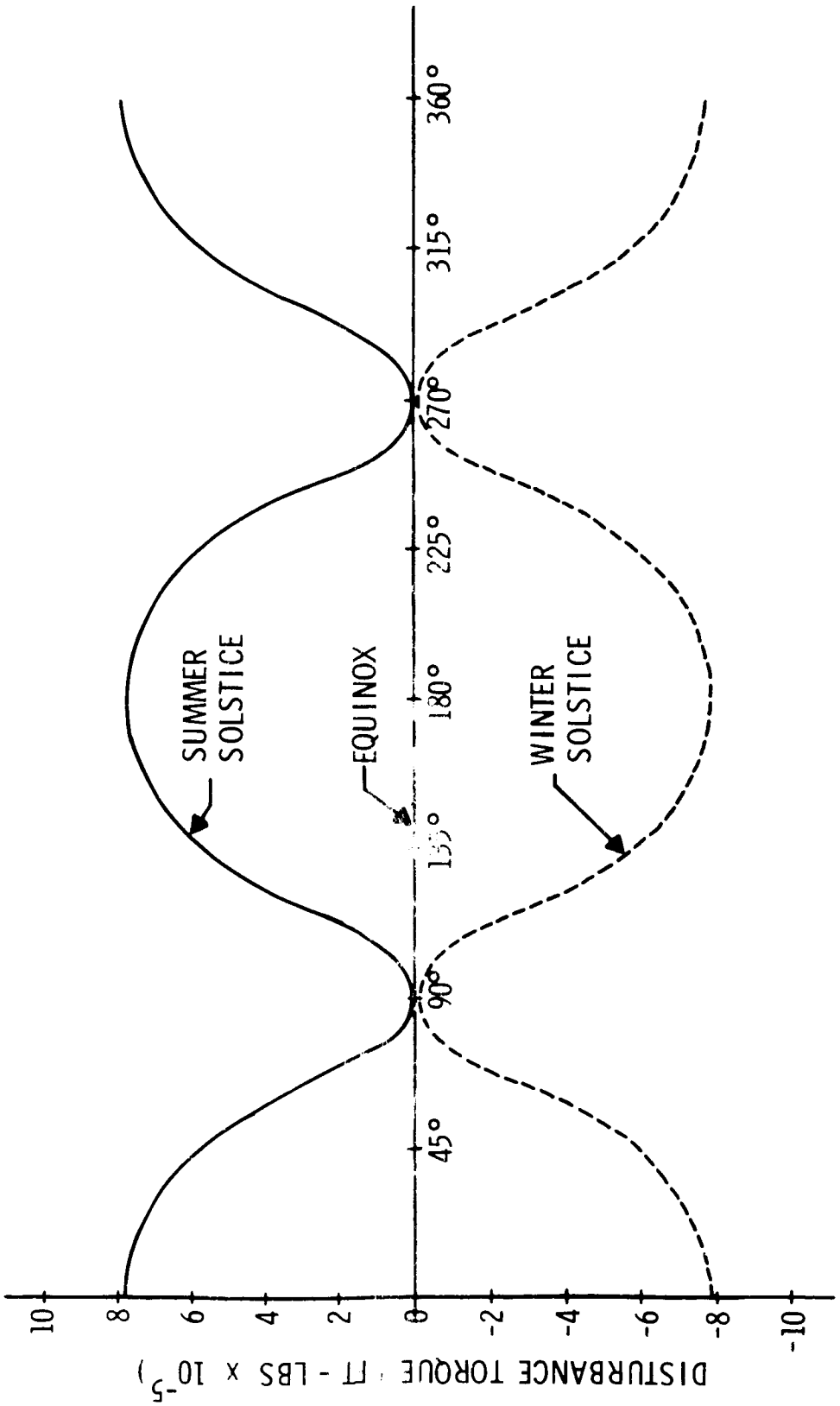

Figure 6-8. Roll Axis Solar Pressure Disturbance Torque Due to Antenna and Feed System

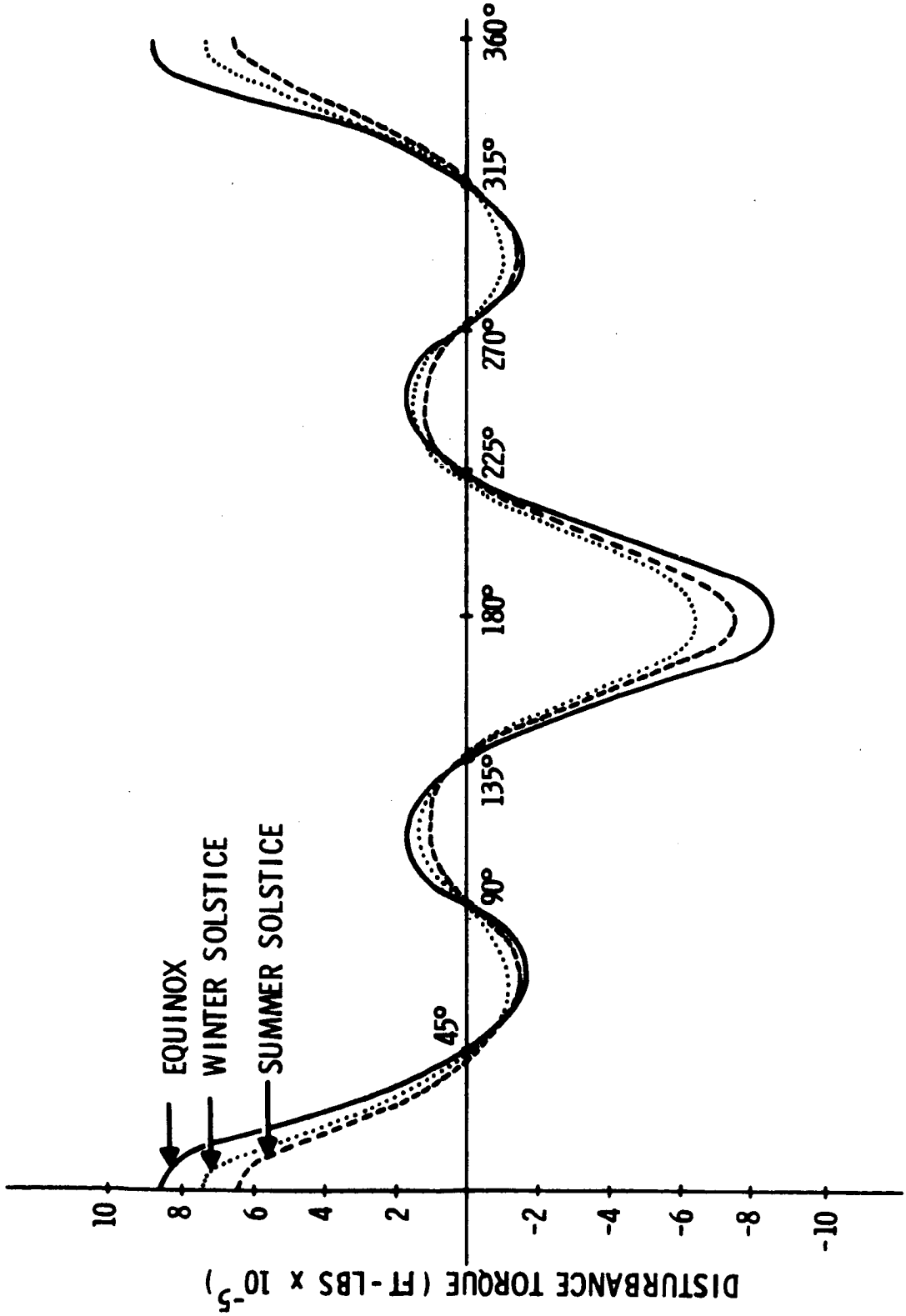

Figure 6-9. Roll Axis Solar Pressure Disturbance Torque Due to Fixed Solar Panels Only

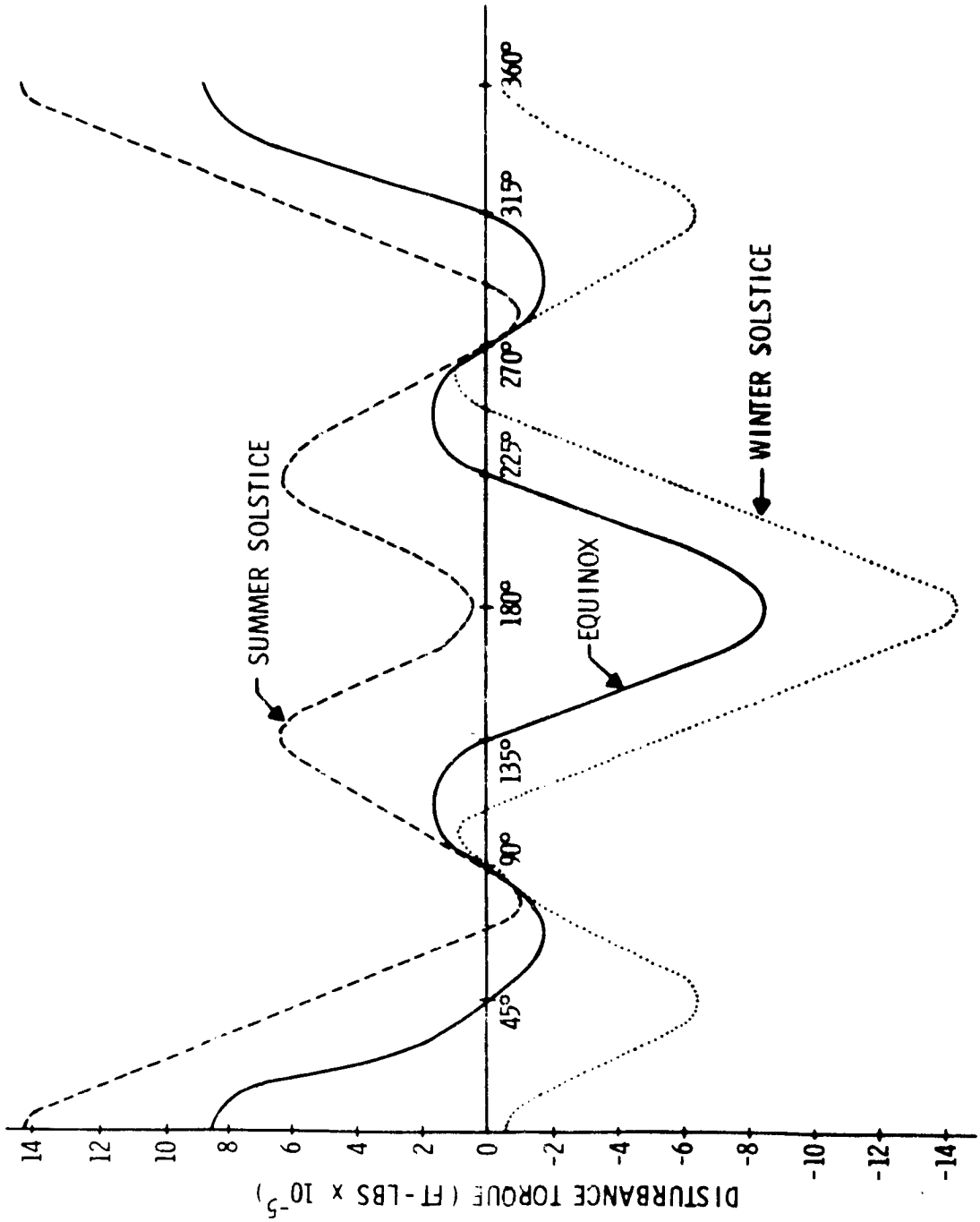

Figure 6-10. Roll Axis Solar Pressure Disturbance Torque

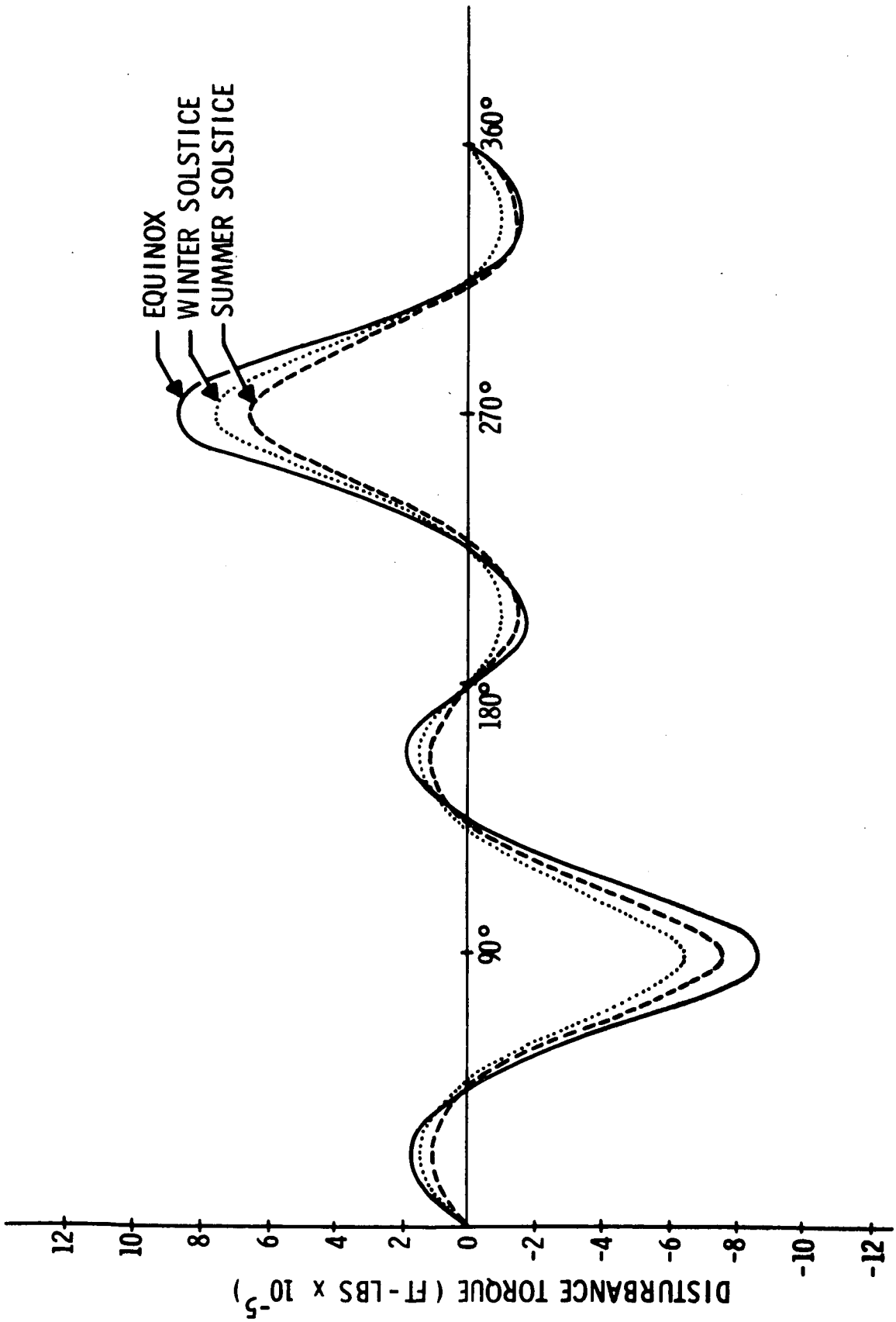

Figure 6-11. Yaw Axis Solar Pressure Disturbance Torque

6.4 TORQUER SUBSYSTEM

6.4.1 Control Torquer Requirements

The requirements on the control torquers took into account the disturbance torque models shown in subsection 6.3. (Preliminary control impulse calculations for alternate vehicle configurations are presented in Appendices 6A and 6B.) The reaction jet subsystem is designed to provide:

a) Tumbling arrest

b) Acquisition (15 times)

c) Unload wheels (as result of average disturbance torque)

d) Holding attitude during station keeping

The inertia wheels are sized to store the cyclic disturbance torque and maneuver the satellite to offset points. Antenna experiment maneuvers also will be conducted by the wheels; however, they were not a prime requirement in the sizing of the wheels. Rather, the antenna maneuvers will be configured to the wheel capability.

The satellite parameters which influence sizing of the control torquers are listed below.

Tumble Rates (Initial)

Roll	1°/sec	17.4×10^{-3} rad/sec
Pitch	0.5°/sec	8.7×10^{-3} rad/sec
Yaw	1°/sec	17.4×10^{-3} rad/sec

Search Rates during Acquisition

Roll	0.2°/sec	3.49×10^{-3} rad/sec	(earth acquisition)
Pitch	0.2°/sec	3.49×10^{-3} rad/sec	(sun and earth acquisition)
Yaw	0.2°/sec	3.49×10^{-3} rad/sec	(sun acquisition)
	0.05°/sec	0.87×10^{-3} rad/sec	(star acquisition)

Field of View (minimums for acquisition)

Fine Sun Sensor	±10°	±0.175 rad
Horizon Sensor	±10°	±0.175 rad
Star Tracker	± 1°	±0.0175 rad

Vehicle Inertia

Roll	2150 slug ft^2
Pitch	1226 slug ft^2
Yaw	1677 slug ft^2

Jet Moment Arm (all axes) 2.5 ft

Auxiliary Propulsion System

ΔV engines - 1 lb_f (NS engine on y axis, EW engines

CG variance ±0.6 inch

Total ΔV impulse 15,000 lb sec

Thrust Levels

Several considerations must be satisfied in selecting the thrust levels. These are as follows.

1) The thrust must be large enough to balance the misalignment torques resulting from the firing of the APS engines.

2) The thrust must be large enough to acquire the references within the field of view of the sensors with the required search rates. The search rates are dictated by the time allowed for acquisition of the references.

3) The thrust should be small enough to allow the wheels to maintain control of attitude during the unloading periods. The wheel torque may be increased but at the expense of increased peak power consumption and some increase in wheel weight.

The selected jet thrust provides a torque of 0.075 ft lbs. (The maximum misalignment torque due to the firing of ΔV engines is 0.05 ft lbs.) Phase plane plots show that this is adequate torque to allow acquisition of the star and earth in the field of view of the sensor. This jet torque is slightly above the stall torque of the wheel at zero velocity; however, with the wheel at unload speed the reverse torque of the wheel will be greater than the jet torque, so that the wheels can maintain control of the vehicle attitude. Unloading of the wheels will be stopped before the wheel torque is less than the jet torque.

The roll and pitch jet thrust is 0.03 pounds and the yaw jet thrust is 0.015 pounds. The yaw jets are fired in couples whereas roll and pitch are single jets. The results of preliminary studies to determine jet size for alternate ATS-4 configurations are given in Appendix 6B.

Total Impulse

The momentum or impulse capability of the reaction jet system is detailed below:

1. Arrest Tumbling

Roll	$2150 \times 17.4 \times 10^{-3}$	= 38 ft lb sec
Pitch	$1226 \times 8.7 \times 10^{-3}$	= 11 ft lb sec
Yaw	$1677 \times 17.4 \times 10^{-3}$	= 29 ft lb sec

2. Acquisition

Acquisition of the sun from any random orientation requires rotation about the pitch and yaw axis at 0.2°/sec. This will be done simultaneously. Acquisition of the earth requires rotation about the roll axis at 0.2°/sec and most likely will require some pitch rate when earth presence is detected. Acquisition of the star requires a rotation about the yaw axis at 0.05 degrees per second. The number of acquisitions is assumed to be 15. The gas requirements for

acquisition were determined from phase plane plots assuming that the gas system was supplying the entire impulse for acquisition. Since the wheels will be operating in parallel with the reaction jets, the gas required is less than that shown.

Roll	15 x 49.3	= 740 ft lb sec
Pitch	15 x 27.6	= 414 ft lb sec
Yaw	15 x 34.7	= 520 ft lb sec

3) Disturbance Torque

The momentum required to unload the wheels due to the steady state components of disturbance torque is set by solar radiation pressure, gravity gradient at offset pointing and magnetic moments. The latter two are insignificant compared to solar radiation torque, but have been included in the required gas storage. The analysis of wheel momentum requirements show a steady build up in momentum of the roll and yaw wheels. This momentum must be removed by the reaction jet system. Half of this momentum will be removed by the roll jets and half will be removed by the yaw jets.

The momentum to be removed by the yaw and roll jets is:

4.3×10^{-5} ft lb x 63.1×10^{6} sec = 2710 ft lb sec

therefore,

Roll = 1355 ft lb sec

Yaw = 1355 ft lb sec

The steady state component of the pitch torque due to solar radition was assumed to be 5 percent of the peak value. The momentum to be removed by the pitch jets is:

(0.05) (1.5×10^{-4} ft lbs) (63.1×10^{6} seconds) = 474 ft lb sec

The momentum due to gravity gradient was found by assuming a 0.1 radian offset in pitch and roll for a total of one year. The values are:

Roll	30 ft lb sec
Pitch	24 ft lb sec

A magnetic moment of 4000 dyne cm/gauss was assumed for the vehicle (this is the value used for AOSO). In a 200 gamma field this results in a total of 38 ft lb sec per axis for the two year period.

4. Misalignment torques due to ΔV engine

A total impulse of 15,000 lb sec is assumed for ΔV corrections. It is assumed that one-half of this total impulse is in each of the engines. Firing of the EW engine can cause torques about the y and z axis and the NS engine can cause torques about the x and z axis. The momentum required is:

Roll	(1/2) (15,000) (0.6/12) (1)	= 375 ft lb sec
Pitch	(1/2) (15,000) (0.6/12) (1)	= 375 ft lb sec
Yaw	(1) (15,000) (0.6/12) (1)	= 750 ft lb sec

The total requirements are summarized in the following table.

It is noted that the indicated APS impulse of 15,000 lb sec is based on early study results. The latest requirement for the recommended ATS-4/APS system is 29,600 lb sec. To resize the SCS jet system for this increased requirement, again using the conservative approach of combining the maximum 3 - σ APS impulse value with the 3 - σ alignment error for the APS engine, an additional 5.9 lbs of propellant (including a 50% contingency margin) would be required for the recommended hydrazine torquer subsystem. In addition, since similar propulsion approaches are proposed for the APS and SCS, it is recommended that provision be made to divert some of the APS propellant for the use of the SCS should the latter experience extreme impulse requirements. (The North-South station keeping or East - West station repositioning capabilities of the APS would be thereby reduced.)

Mode	Momentum (ft lb sec)		
	Roll	Pitch	Yaw
1. Arrest Tumbling	38	11	29
2. Acquisition	740	414	520
3. Disturbance Torque (Solar)	1355	474	1355
(Gravity and Magnetic)	68	52	
4. Attitude Hold	375	375	750
Totals	2576	1326	2654

The total impulse required is:

$$\frac{2576 + 1326 + 2654}{2.5} = \frac{6556}{2.5} = 2625 \text{ lb sec}$$

Assuming a 50 percent contingency due to uncertainties in disturbance torques and leakage the required storage in the reaction system is 3950 lb sec.

Jet on time during the unloading of the wheels is:

Roll 0.95 ft lb sec ÷ 0.075 = 12.7 seconds

Pitch 0.75 ft lb sec ÷ 0.075 = 10 seconds

Yaw 0.95 ft lb sec ÷ 0.075 = 12.7 seconds

During acquisition the jets on time may be on as long as:

Roll 181 seconds

Pitch 97 seconds

Yaw 120 seconds

For despin from the separation rates to the desired search rates the time could be:

Roll $\dfrac{1°/\text{sec}}{0.002°/\text{sec}^2} = 500$ seconds

Pitch $\dfrac{(0.5 + 0.2)°/\text{sec}}{0.0035°/\text{sec}^2} = 200$ seconds

Yaw $\dfrac{(1 + 0.2)°/\text{sec}}{0.00257°/\text{sec}^2} = 467$ seconds

6.4.2 Candidate Reaction Jet Types

Cold Gas

Cold gas systems are quickly eliminated from consideration due to low I_{sp} (60 seconds) and high system weight. The nitrogen tanks and plumbing for a cold gas system would be about 1.27 times as heavy as the fuel contained within.

Ion Engines

Electric or ion propulsion can provide very high specific impulse (I_{sp} = 500 to 4000 seconds) with correspondingly low system weight. However, the thrust levels attainable are on the order of 10 to 100 μ pounds; this is well below the ATS-4 thrust requirements.

Hypergolic Bipropellants

The hypergolic bipropellant thrusters can develop a high I_{sp} of 250 seconds in short pulses. However, the minimum thrust level of this type is greater than 0.3 pounds, and due to the dual valve and fuel line requirement, low reliability can be expected.

Ammonia Resisto-Jet

There are several types of decomposed ammonia resisto-jets available. The majority of the work being done in the development of resisto-jets is concentrated in three locations; AVCO, GE, and TRW. AVCO is developing an electrically heated, power-on-demand, decomposed ammonia resisto-jet in the millipound thrust class. The power scale factor is 8000 watts/lb_f with a

thermal time constand of one second. This development and test program is being performed under contract to GSFC for a 57 pound feed system. No flight experience exists, however. The GE system is also an electrically heated, power-on-demand, decomposed ammonia system in the millipound class. However, lower power is required by virtue of a lower power scale factor of 1400 watts/lb_f and a longer thermal time constant. Due to the low thrust capability of both the AVCO and the GE resisto-jet systems, their application to ATS-4 could only be possible if the thrusters were placed on long moment arms on the edge of the antenna. This would result in two major problems: 1) The fuel lines from the tank to the thrusters would have to include flexible joints to permit antenna deployment, thus, reducing system reliability; and 2) Placing the thrusters at a great distance from the inertia wheels and sensors would require the flexible body dynamics to be included in the inner loop of the control system, creating a stability and compensation complexity problem. Therefore, the AVCO and GE resisto-jet systems are removed from further consideration.

TRW has done a considerable amount of work in continuously heated resisto-jets with higher thrust levels and lower power consumption. In this design, the fuel is heated to 1500° continuously, by drawing about 5 watts per valve for a thrust level of 0.03 pounds. This resisto-jet design would therefore require about 40 watts heater power continuously plus valve actuation power for the ATS-4 mission. Alternatively, a radio-isotope heat source could be used if the half life of the radio-isotope could be sufficiently long to prevent a large thermal range in the 2-year period, and if AEC approval could be obtained.

TRW has developed and flown two electrically heated nitrogen resisto-jets on the VELA-3 program. The jets were continuously heated to 1000°F and developed .042 pound. Advanced VELA will be flown in early 1967 with two .02 pound thrusters using electrically heated nitrogen to 1300°F. TRW has also delivered an electrically heated decomposed ammonia resisto-jet to Wright Field and a radio-isotope heated decomposed ammonia resisto-jet to

Edwards AFB. These thrusters delivered 0.1 pound thrust and were used for test purposes only. The I_{sp} for decomposed ammonia heated to 1500°F or greater is in excess of 250 seconds.

From this investigation, it appears that the TRW electro-thermal decomposed ammonia resisto-jet could be considered for the ATS-4 application. Further trade-offs are recommended, however, to determine relative cost, development status, and reliability of the resisto-jet compared to other feasible approaches.

Hydrazine Mono-propellant

Recent advances in hydrazine mono-propellant thrusters using the Shell 405 catalyst make it a candidate for the ATS-4 application. Steady state I_{sp} is as high as 230 seconds while the reliability is much better than competitive bi-propellants. For a thrust size of .03 pound and jet on-times of 10 - 12 seconds, the I_{sp} of a hydrazine mono-propellant system is from 150 to 170 seconds. Although the fuel weight for hydrazine is therefore somewhat higher than for the TRW resisto-jet (I_{sp} = 250 seconds), electrical power is required for valve actuation only.

Each of the redundant hydrazine jet systems consist of two 0.03 pound jets in each of the three principle axes. The yaw jets, however, have split nozzles providing two 0.015 pound thrust outputs from one valve for a matched pair. In this manner, all valves are of the same design (0.03 pound thrust) for a total of 12 jets (6 primary and 6 standby redundant).

The thrust output of the hydrazine thruster is a function of catalyst bed temperature. The bed temperature increases from its initially cold state to 90 percent of its operating efficiency after about 0.5 seconds of thrusting. For the remainder of the 10 - 12 second thrust on time (wheel unload) maximum thrust output efficiency is obtained. The thrust output efficiency of a hydrazine thruster, designed for 0.03 pound thrust is shown in Figure 6-12.

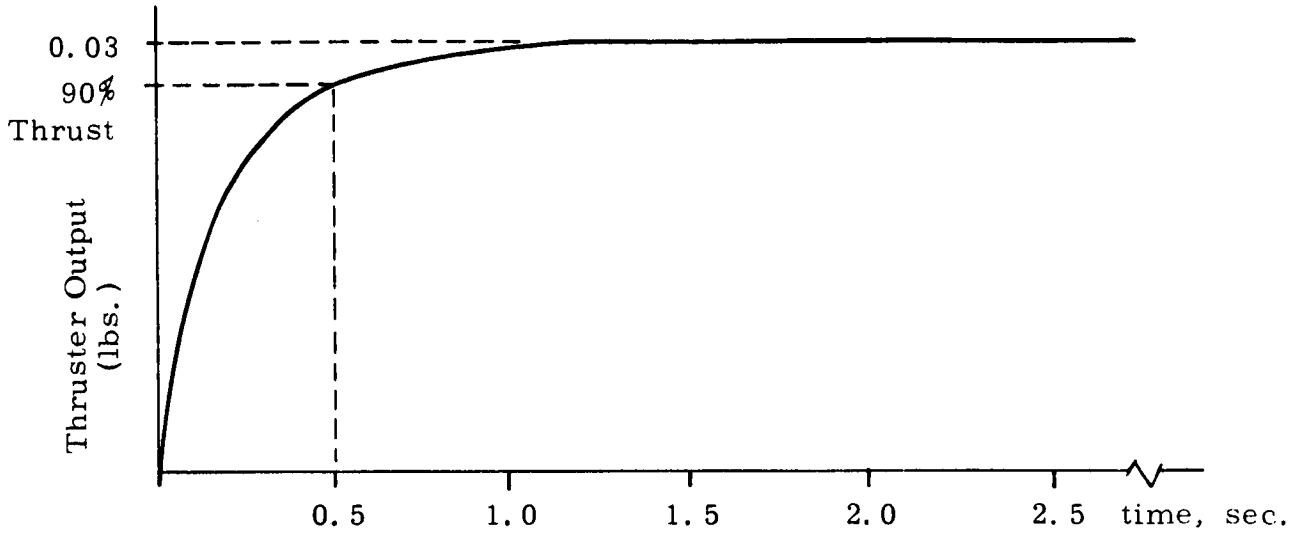

Figure 6-12. Hydrazine Thruster Output Efficiency

Hydrazine mono-propellant thrusters have been advanced by several reaction jet companies since the development of the Shell 405 spontaneous catalyst. The most significant hydrazine development appears to have been effected by Rocket Research Corporation, Seattle, Washington and Hamilton Standard, Windsor Locks, Connecticut. Rocket Research has developed and delivered a flightworthy hydrazine plenum system using the Shell 405 catalyst to General Dynamics. They also have a contract to develop and deliver a similar 0.5 pound blow-down system to the Naval Research Laboratory. This system is to be flown in May, 1967. In addition, they have demonstrated the reliability of hydrazine systems by pulsing a 0.05 pound jet 30,000 times for an accumulated 50,000 seconds of thrusting time.

Through significant company investment, Hamilton Standard has developed and tested flight weight hydrazine thrusters from 0.014 lbs to 0.4 lb. Endurance tests were performed by actuating the system with 125,000 pulses at sea level pressure and at a simulated 120,000 foot altitude, with a varying duty cycle of from 0.3 to 80 per cent.

From the standpoint of power, reliability, development status and fuel similarity with the APS, a hydrazine mono-propellant system is selected for attitude control. The vendor selection for this system can be made only after an evaluation of a firm proposal based upon firm system requirements. (See Appendix 6B for preliminary jet type considerations.)

The system weight for hydrazine mono-propellant thrusters assuming standby redundancy in valves and nozzles, fuel feed from either or both of two tanks, and hydrazine I_{sp} of 150 seconds is obtained as follows:

Fuel	26 lbs
Tanks and Plumbing	20 lbs
Valves and Nozzles	8 lbs
Total Weight	54 lbs

A schematic of the reaction jet subsystem is shown in Figure 6-13. A blow-down hydrazine system is represented, since it appears most attractive from weight and reliability considerations.

6.4.3 Inertia Wheel Subsystem

When inertia wheels are selected as the control moment devices for attitude control of a space vehicle it is generally done for two reasons. One, if the mission life of the spacecraft is long(such as the two year life required for the ATS-4)it is frequently possible to reduce the system weight from

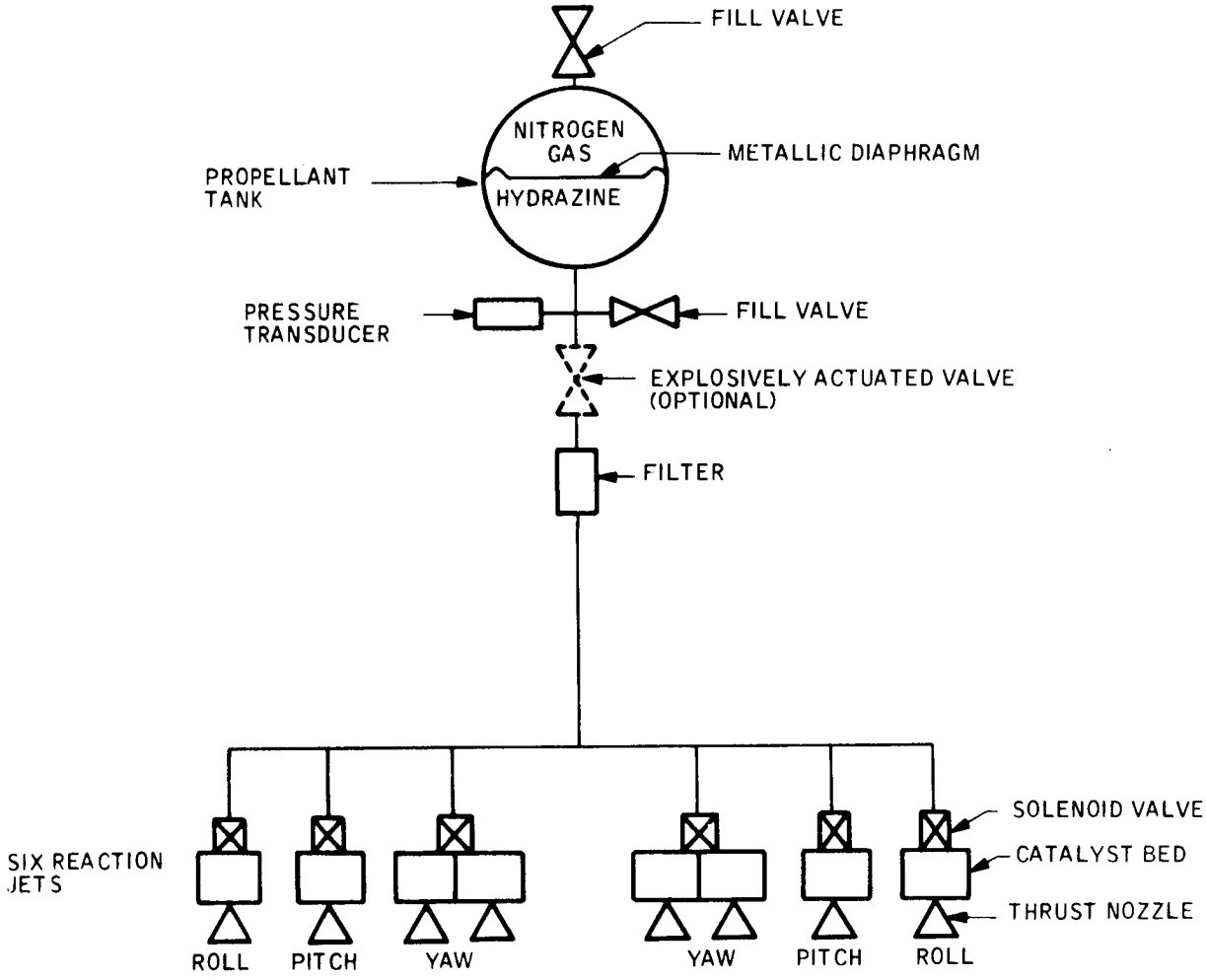

Figure 6-13. LIQUID HYDRAZINE SYSTEM SCHEMATIC (BLOW-DOWN)

that required for a mass expulsion system. Two, if precise attitude control is required (such as the ± 0. 1 degree specified for the ATA-4 system) it is necessary to provide the control torque with a finer resolution than is practical with a mass expulsion system.

In the case of the ATS-4 spacecraft the inertia wheels are selected for both of the above reasons; however, the attitude accuracy requirements make it necessary that inertia wheels be considered whether or not their application results in a saving in system weight. (See Appendix 6C for results of preliminary wheel studies for alternate spacecraft configurations.)

In reviewing the operating modes for ATS-4 it appears that inertia wheels may be used to advantage in the following modes.

- Attitude hold
- Tracking maneuvers
- Offset pointing maneuvers
- Antenna experiment maneuvers

In the attitude hold mode, the attitude control system must maintain the vehicle in a selected orientation relative to the local vertical, orbit plane reference with an accuracy of ±0. 1 degrees. Since the spacecraft will be subject to disturbances resulting from solar radiation and other causes, some control action will be required to hold to the desired attitude accuracy. If mass expulsion reaction jets were used to generate the control torque, it would be necessary to have a deadband of the order of ±0. 01 degrees. Experience indicates that such a small deadband results in excessive jet operation and fuel consumption because of noise. The use of reaction wheels to generate the control moment will eliminate not only the excessive fuel consumption but also the undesirable limit cycle oscillations between the limits of the deadband. This is a result of the continuous control moment available from the inertia wheel as contrasted with the one discrete level available from the reaction jets.

The tracking maneuver consists of keeping the vehicle yaw axis pointed at a satellite in a 90 minute orbit as it passes below the ATS-4 spacecraft. It is desired to track with an accuracy of ±0.5 degree. Since the tracking line of sight will have a sinusoidal angular acceleration the attitude control system must have the capability of producing a smooth angular acceleration of the vehicle in roll and pitch in order to track with suitable accuracy. The torque produced by inertia wheels is continuous within their range and would be compatible with this requirement.

The offset pointing maneuver requires that the vehicle axis be pointed at any point on the earth's disk with an accuracy of ±0.1 degree. Since the inertia wheels are required to obtain suitable accuracy during attitude hold and tracking maneuvers, a relatively small increase in the wheel size makes them suitable for performing the offset maneuver. The end result is saving of jet fuel that otherwise would be consumed.

The inertia wheels were resized based upon the disturbance torque model generated for the preferred configuration* The curves showing the disturbance torques are shown in subsection 6.3. The curves were broken down into their various components to simplify the analysis. The following values (lb ft.) were used:

Roll (antenna and feed)	$4 \times 10^{-5} + 4 \times 10^{-5} \cos 2w_o t$
Roll (solar paddles)	$4.3 \times 10^{-5} \cos w_o t + 4.3 \times 10^{-5} \cos 3w_o t$
Yaw	$-4.3 \times 10^{-5} \sin w_o t + 4.3 \times 10^{-5} \sin 3w_o t$
Pitch	$15.9 \times 10^{-5} \sin w_o t + 5.9 \times 10^{-5} \sin 3w_o t$

During holding at local vertical, the vehicle rates and accelerations are held at zero so the external disturbance torques can be equated directed to the wheel torques. Since roll and yaw are coupled by the orbital rate, w_o, they must be examined together. The equations are:

*Initial wheel design data are presented in Appendices C and D.

$$M_x = \dot{H}_x - w_o H_z$$

$$M_z = \dot{H}_z + w_o H_x$$

The resulting solution for H_x and H_z (ft. lb sec), the roll and yaw moment a, is: are:

$$H_x = 0.514 \sin w_o t + (4.3 \times 10^{-5}) t \cos w_o t + 0.368 \sin 2 w_o t + 0.148 \sin 3 w_o t$$

$$H_z = 0.55 + 0.514 \cos w_o t - (4.3 \times 10^{-5}) t \sin w_o t + 0.184 \cos 2 w_o t - 0.148 \cos 3 w_o t$$

The -0.55 ft. lb sec on the yaw wheel is due to the steady state value of the roll disturbance torque. The sinusoids (orbital, double and triple orbital frequency) are the cyclic values which are to be stored by the wheels. The remaining term, $(4.3 \times 10^{-5}) t \cos w_o t$, shows a steady increase in momentum which must be removed by the jets.

The pitch wheel momentum is found by equating:

$$\dot{H}_y = A \sin w_o t + B \sin 3 w_o t \quad (A = 15.9 \times 10^{-5},\ B = 5.9 \times 10^{-5})$$

The cyclic component which the pitch wheel must store is:

$$H_y = 2.18 \cos w_o t - 0.27 \cos 3 w_o t$$

The peak to peak values of momentum over one period is the + to- momentum which must be stored in the wheels.* In addition the transients due to maneuvers and the offset momentum should be stored in the wheels to avoid use of the reaction jets. The build up per orbit which must be removed by the roll and yaw reaction jets is 3.7 ft. lb sec. This can be removed four times per orbit, twice in yaw and twice in roll.

* This statement and the previous expression for wheel storage momentum (Hy) are based upon the approach of unloading wheel momenta at relatively high wheel speeds twice per orbit to remove momentum buildup effects.

The momentum excursion characteristics (between + and - unload points) for the wheels are tabulated below, together with the actual storage requirements:

Item	ft. lb sec		
	Roll	Pitch	Yaw
Cyclic (peak to peak)	1.72	4.90	1.08
Offset	--	--	1.10
Maneuver	1.90	1.08	--
Unload Increment	1.90	1.50	1.90
Contingency	0.48	0.52	0.52
	6.0*	8.0*	4.6*
Required Storage (one side)	3.0	4.0	2.3

* Between unload points at the + and - momentum storage maximums

In accordance with the wheel design procedure described in Appendix C, the wheel moments of inertia are established so that the required momentum storage can be achieved at a wheel speed (unload level) of 1000 RPM. The associated roll, pitch and yaw inertias (I) are 0.0286, 0.0382, and 0.0220 slug-ft^2, respectively.

The estimated reaction wheel weights (W) are then calculated by an emperical formula given in reference 12:

$$W \text{ (lbs)} = 6.3 + 170\ I \text{ (slug-ft}^2\text{)}$$

The estimated wheel weights are thereby determined as:

Roll 11.3; Pitch 12.9; Yaw 10.0; Total 34.2 pounds

The desired wheel torque is 10 ounce inches for each wheel. This is larger than required for maneuvering; however, there is no weight change due to motor size under 10 ounce inches. The 10 ounce inch (0.052 ft-lb) torque is obtained at zero wheel speed. Thus, when the jets are used to unload the wheels, the wheel deceleration torque will exceed the jet torque and allow the wheels to maintain control of the vehicle.

6.4.4 Selected Torquer Configuration

The selected configuration is a combination of wheels and jet system. Appendix 6D presents the results of preliminary wheel/jet trade-off studies which support this decision. Because of its proven design status, an ac wheel similar to that built by the Bendix Corporation for OAO, OGO and Nimbus is considered. The reaction jet system chosen is a hydrazine mono-propellant system.

The weight of a torquing system using only gas was investigated. It was assumed that a minimum bit impulse can be achieved by use of the proper pulse logic. It also was assumed that the disturbance torques will be large enough so that the vehicle doesn't limit cycle between the deadband limits. No attempt is made to assess the effect of noise on the narrow deadband in erroneous firing of the jets. The momentum to maintain attitude in presence of the disturbance torques for two years is:

Roll (cyclic)	2510 ft. lb sec
Pitch (cyclic)	7150
Yaw (cyclic)	1576
Roll (average)	2520
ΔV misalignment	1500
Acquisition	1752
Maneuvers	300
TOTAL	17,308 ft. lb sec

With a 50 per cent contingency the total impulse is 25,962 ft. lb sec (10,400 lb sec). This results in a gas system weight of 120 pounds. The wheels and jet system as configured for ATS-4 weighs 111.8 pounds, including the inverter and wheel drive electronics.

There is a small weight advantage for a wheels/gas torquer system over an all-gas system. This weight advantage could be improved further if dc brushless motors were used for in the inertia wheels. The ac wheel was chosen because of its development and flight status. Also, the 50 per cent gas contingency should be enlarged for the all-gas system to account for the increased gas consumption caused by the noise with a narrow deadband.

Using a reaction wheel to store the momentum due to cyclic disturbances and maneuvers, the number of jet actuations is greatly reduced. Thus, presently designed valves can meet the life and the reliability requirements for a wheel/gas torquer subsystem whereas they would be questionable for an all-gas torquer subsystem with its excessive number of required valve actuations.

These considerations, added to the primary one of the improved pointing accuracy of which it is capable, led to the choice of a combined wheels/gas torquer subsystem for the ATS-4.

6.5 COMPUTATION AND DATA HANDLING

6.5.1 On-Board Computation

On-board computation are required to generate the following commands and/or bias signals:

- Figure 8 bias for horizon sensor
- Diurnal star motion for yaw gimbal control
- Components of orbital rate in body coordinates for torquing the gyros
- Drift compensation signals for gyros
- Error correction signals for horizon sensor

6.5.2 Up-Data Commands

The commands required by the SCS are shown in Table 6-6.

6.5.3 Down-Data Monitor

The signals to be telemetered to the ground for monitoring purposes are shown in Table 6-7.

Table 6-6. SCS Command Requirements

Function	Objective	Type of Command	Remarks
1. Spacecraft orientation	Acquire sun	Pulse	Despin is also accomplished
2. Spacecraft orientation	Acquire earth	Pulse	Roll rate is commanded
3. Spacecraft orientation	Pos. direction of Polaris search	Pulse	
4. Spacecraft orientation	Set S.T. roll gimbal position	Series of pulses	Number of pulses determine gimbal position
5. Spacecraft orientation	Set S.T. yaw gimbal position	Series of pulses	Number of pulses determine gimbal position
6. Spacecraft orientation	Neg. direction of Polaris search	Pulse	
7. Spacecraft orientation	Set time of Polaris search	Series of pulses	
8. Spacecraft orientation	Pitch offset command (HS)	12 bits	
9. Spacecraft orientation	Roll offset command (HS)	12 bits	
10. Mode control	Horizon sensor control	Pulse	
11. Mode control	Monopulse control	Pulse	
12. Mode control	Gyro control	Pulse	Antenna maneuvers, station keeping
13. Mode control	Jets only	Pulse	Station keeping
14. Spacecraft maneuver	Positive roll rate command	Pulse	
15. Spacecraft maneuver	Negative roll rate command	Pulse	
16. Spacecraft maneuver	Positive pitch rate command	Pulse	
17. Spacecraft maneuver	Negative pitch rate command	Pulse	
18. Excitation	Gyro power off	Pulse	
19. Excitation	Gyro power on	Pulse	
20. Excitation	Horizon sensor power off	Pulse	
21. Excitation	Horizon sensor power on	Pulse	
22. Redundant switching	Switch standby star tracker Sec. No. 1	Pulse	
23. Redundant switching	Switch standby star tracker Sec. No. 2	Pulse	
24. Redundant switching	Switch standby horizon sensor	Pulse	
25. Redundant switching	Switch standby sun sensors	Pulse	
26. Redundant switching	Switch standby roll wheel drive elect.	Pulse	
27. Redundant switching	Switch standby pitch wheel drive elect.	Pulse	
28. Redundant switching	Switch standby yaw wheel drive elect.	Pulse	
29. Redundant switching	Switch standby inverter wheel drive elect.	Pulse	
30. Redundant switching	Switch standby roll jet valves	Pulse	
31. Redundant switching	Switch standby pitch jet valves	Pulse	
32. Redundant switching	Switch standby yaw jet valves	Pulse	
33. Redundant switching	Switch standby controller Sec. No. 1	Pulse	
34. Redundant switching	Switch standby controller Sec. No. 2	Pulse	
35. Redundant switching	Switch standby controller Sec. No. 3	Pulse	
36. Redundant switching	Switch standby controller Sec. No. 4	Pulse	
37. Redundant switching	Switch standby controller Sec. No. 5	Pulse	
38. Redundant switching	Switch standby controller Sec. No. 6	Pulse	
39. Redundant switching	Switch standby controller Sec. No. 7	Pulse	
40. Redundant switching	Switch standby controller Sec. No. 8	Pulse	
41. Redundant switching	Switch standby controller Sec. No. 9	Pulse	
42. Compensate gyro drift	Drift trim roll gyro	8 bits	
43. Compensate gyro drift	Drift trim pitch gyro	8 bits	
44. Compensate gyro drift	Drift trim yaw gyro	8 bits	

Table 6-7. SCS Telemetry Requirements

Measured Parameters	Type	Accuracy	Sampling Rate	Sampling Period	Frequency	Remarks
1. Positive yaw jets on	On-Off	---	Sample and Hold		Read hold once per two hours or upon investigation	
2. Negative yaw jets on	On-Off	---				
3. Positive pitch jets on	On-Off	---				
4. Negative pitch jets on	On-Off	---				
5. Positive roll jets on	On-Off	---				
6. Negative roll jets on	On-Off	---				
7. Gas Tank No. 1 pressure	Analog	± 3%	1 per 2 hour		12 per day	Monitor gas supply
8. Gas Tank No. 1 temperature	Analog	± 3%				
9. Gas Tank No. 2 pressure	Analog	± 5%				
10. Gas Tank No. 2 temperature	Analog	± 5%				
11. Star Tracker No. 1 sun shutter position	On-Off	- -	1 per 2 hour		12 per day	Monitor star tracker status
12. Star Tracker No. 2 sun shutter position	On-Off	- -				
13. S.T. yaw gimbal position	Digital	8 bits				
14. S.T. roll gimbal position	Digital	4 bits				
15. S.T. star pressure	On-Off	- -				
16. S.T. error signal	Digital	8 bits	1 per sec.		Continuous	Monitor system performance
17. Roll error signal (altitude)	Digital	12 bits				
18. Pitch error signal (attitude)	Digital	12 bits				
19. Coarse sun sensor pitch error	Analog	± 5%	1 per sec.	2 hour	One two hour period during acquisition	Acquisition may occur 20-30 times during two year period
20. C.S.S. yaw error	Analog	± 5%				
21. Fine sun sensor pitch error	Analog	± 5%				
22. F.S.S. pitch error	Analog	± 5%				
23. Roll gyro output	Analog	± 5%	1 per sec.		Continuous (while energized)	Gyros to be used 500 hours during two years
24. Pitch gyro output	Analog					
25. Yaw gyro output	Analog					
26. Earth presence - pitch	On-Off	- -	1 per hour		24 per day (while energized)	Horizon sensors to be energized one year
27. Earth presence - roll	On-Off	- -				
28. Sun presence - CSS	On-Off	- -	1 per sec.	2 hour	One two-hour period acquisition	Acquisition may occur 20-30 times during mission
29. Sun presence - FSS	On-Off	- -				
30. Roll inertia wheel speed	Digital	6 bits	1 per sec.		Continuous	Monitor performance
31. Roll inertia wheel current	Analog	± 5%				
32. Pitch inertia wheel speed	Digital	6 bits				
33. Pitch inertia wheel current	Analog	± 5%				
34. Yaw inertia wheel speed	Digital	6 bits				
35. Yaw inertia wheel current	Analog	± 5%				

Table 6-7. SCS Telementry Requirements (Continued)

Measured Parameters	Type	Accuracy	Sampling Rate	Sampling Period	Frequency	Remarks
36. Standby star tracker Sec. No. 1 on	On-Off	- -				
37. Standby star tracker Sec. No. 2 on	On-Off	- -				
38. Standby horizon sensor on	On-Off	- -				
39. Standby sun sensor on	On-Off	- -				
40. Standby roll wheel electronics on	On -Off	- -				
41. Standby pitch wheel electronics on	On-Off	- -				
42. Standby yaw wheel electronics on	On-Off	- -				
43. Standby inverter on	On-Off	- -				
44. Standby roll jet valves on	On-Off	- -				
45. Standby pitch jet valves on	On-Off	- -				
46. Standby yaw jet valves on	On-Off	- -	1 per 6 hr.		4 per day	Monitor status
47. Standby controller Sec. No. 1 on	On-Off	- -				
48. Standby controller Sec. No. 2 on	On-Off	- -				
49. Standby controller Sec. No. 3 on	On-Off	- -				
50. Standby controller Sec. No. 4 on	On-Off	- -				
51. Standby controller Sec. No. 5 on	On-Off	- -				
52. Standby controller Sec. No. 6 on	On-Off	- -				
53. Standby controller Sec. No. 7 on	On-Off	- -				
54. Standby controller Sec. No. 8 on	On-Off	- -				
55. Standby controller Sec. No. 9 on	On-Off	- -				
56. Sun acquisition logic activated	On-Off	- -				
57. Earth acquisition logic activated	On-Off	- -	1 per sec.	2 hour	One two-hour period during acquisition	Acquisition may occur 20-30 times
58. Star acquisition logic activated	On-Off	- -				
59. Power on - gyros	On-Off	- -	1 per 6 hr.		4 per day	Monitor status
60. Power on - horizon sensor	On-Off	- -				
61. Inverter output	Analog	± 5%	1 per sec.		Continuous	Monitor system performance
62. Power supply voltage	Analog	± 5%				
63. Horizon sensor mode	On-Off	- -				
64. Gyro mode	On-Off	- -	1 per 2 hr.		12 per day	Monitor system status
65. Monopulse mode	On-Off	- -				
66. Station keeping mode	On-Off	- -				

6.6 SYSTEM OPERATIONAL DESCRIPTION

6.6.1 Control Mode Operation

Ascent and Injection

After Centaur has reoriented the spacecraft to the inertial attitude required for apogee thrusting, the vehicle is spun at about one rpm and the Centaur stage is separated. At this time, spin-up jets on the payload are fired to increase the spin rate to 60 rpm. This spin rate exists during the 15.75 hour coast and through injection at the second apogee. After injection, the spacecraft is yo-yo despun, the spent injection engine is jettisoned, the antenna petals are deployed, and the sun acquisition sequence begins. Preliminary spin rate and control calculation are shown in Appendix 6E.
During the ascent phase, from Centaur separation through synchronous injection, disturbances due to spin-up misalignments, gravity gradient, solar pressure, and injection engine misalignments will exist. These disturbances will produce coning and precession of the momentum vector requiring active coning and nutation control.

To spin-up the spacecraft to 60 rpm about its body z-axis, two solid fuel spin-up jets mounted on five foot momentum arms will be used. A total of 377 lb-sec total impulse is required, which can be obtained from two 10 lb engines thrusting for 19 seconds. Using an I_{sp} of 200 seconds, the two jets including fuel and nozzles will weigh 3.8 lbs.

During spin-up thrusting, 3σ jet misalignments of 0.25 degree will produce a 0.4 ft-lb disturbing torque. This will result in a coning half-angle of 0.2 degree.

At Centaur burnout, which is perigee of the transfer orbit, either a sunrise or a sunset condition will exist. Depending on the time of year, a 20 to 30

minute occult will occur. This occult will occur once if the transfer orbit perigee occurs at a sunrise condition; but will occur twice if the transfer orbit perigee occurs at a sunset condition.

Body attitude reference will be determined in a manner similar to that used by Hughes for the Early Bird satellite. A sun sensor will be mounted on the body and aligned prior to launch to the body-to-sunline angle desired at apogee injection and throughout the transfer ellipse. As the vehicle rotates, the sun sensor will prescribe a cone in space. With each rotation, the cone will intersect the sunline providing one axis reference; however, since the sun may be anywhere on the sun sensor cone, a means of determining the other axis orientation is required. This is accomplished by telemetry polarization information received at the controlling ground station. Body attitude information is then determined on the ground, and attitude commands are sent to the spacecraft via a data link. By this means, body axis orientation relative to the desired inertial orientation is known, allowing spin precession control.* During occulted phases, however, there is a loss of solar reference for 20 to 30 minutes.

The resulting drift in yaw during this phase, is within the limits of solar reacquisition.

During the coast phase, the primary disturbance forces resulting in vehicle coning and spin axis precession are gravity gradient, aerodynamic (near perigee), and jet thrust misalignments. Solar pressure torques are considered negligible in this phase of the mission, being on the order of 1×10^{-7} lb_f/ft^2 whereas aerodynamic pressure is about 1×10^{-5} lb_f/ft^2 at 100 nautical miles, decreasing to 1×10^{-7} lb_f/ft^2 at about 300 nautical miles. Gravity

* Coning and nutation control is provided by the lateral rate damping loop subsequently described.

gradient torques are a function of vehicle attitude and inertia configuration. The peak gravity gradient torque imposed on the vehicle occurs when the vehicle spin axis is 45 degrees from local vertical on either side of the perigee crossing. The torque is given as follows:

$$T = \frac{3}{2}(\omega_o)^2 (I_y - I_z) \sin 2\theta$$

$$T = (1.5)(1.5 \times 10^{-3})^2 (1140 - 303)(\sin 90 \text{ degrees})$$

$$T = (1.5)(2.25 \times 10^{-6})(837)(1)$$

$$T = 2.8 \times 10^{-3} \text{ ft. lbs}$$

Also, in the vicinity of the perigee crossing, the aerodynamic torque could be as high as 0.5×10^{-3} ft. lbs based on a 10-foot diameter cylinder and an estimated 0.5 foot center-of-pressure moment arm from the c. g.

These gravity gradient and aerodynamic external torques will produce spin-axis precession and also body coning. A rigid rotating body, with spin velocity ω_s about either a maximum or a minimum axis of inertia, will maintain its orientation in inertial space in the absence of external moments or forces. If the total angular momentum vector H_S initially coincides with the spin axis, and then an impulse angular momentum H_η is added normal to the spin axis, the body spin axis will assume a new inertial position (precess) and then nutate about the new total angular momentum vector, at a frequency $\omega_S I_S / I_T$. Also, a cone angle will exist whose half-cone amplitude is given as

$$\Omega = \frac{I_T \omega_\eta}{I_S \omega_S}$$

where

I_T = Inertia, transverse axis (1140 slugs-ft^2)

I_S = Inertia, spin axis (303 slugs-ft^2)

ω_S = body spin rate, 60 rpm

ω_η = imposed rate about normal axis = $\frac{H_\eta}{I_T}$

H_η = Imposed normal angular momentum

If it were conservatively assumed that gravity gradient torque produced a 2.8×10^{-3} foot-lb disturbance throughout the 16 hour coast period, the total spin axis precession would not exceed one degree.

$$\theta_p = \frac{(2.8 \times 10^{-3})(3600)(16)}{(303)(60)(2\theta)} \cong 1 \text{ degree}$$

To balance this torque, a control impulse at a five foot moment arm is

$$\text{Impulse} = \frac{(2.8 \times 10^{-3})(3600)(16)}{5} = 32 \text{ lb-sec}$$

During synchronous injection thrusting, the thrust misalignment angle will be 0.25 degrees acting at a five foot moment arm at the nozzle throat of the 9000 lb engine. This results in a body oriented torque.

$$\text{Torque} = (9000)(0.004)(5) = 180 \text{ ft-lbs}$$

This will result in a half cone angle of 0.05 degree at a spin rate of 60 rpm.

Therefore, the use of 60 rpm spin rate results in a stable configuration with a minimum of control impulse needed to preserve the inertial orientation

after Centaur separation (control spin axis orientation during vehicle spin-up and damp out any coning or spin axis precession due to imposed disturbance torques). The total impulse for a single jet control system is summarized as follows:

Centaur separation rate (1.8°/sec pitch)	35 lb-sec
Centaur separation rates (0.4°/sec yaw)	8 lb-sec
Spin-up jet misalignment	5 lb-sec
Disturbance torques during coast phase	34 lb-sec
Synchronous injection thrust misalignments	1 lb-sec
Impulse subtotal	83 lb-sec
Assumed 100 per cent contingency	83 lb-sec
Total impulse	166 lb-sec

Using a cold gas reaction jet system with an I_{sp} of 60 seconds, results in a gas weight of 2.8 lbs for a total jet system weight of 6.3 lbs (assuming a tank and plumbing factor of 125). This could be accomplished with a 0.5 lb engine at a moment arm of five feet with 100 ms pulses.

After injection, the vehicle is despun by yo-yo's, consisting of two masses on the ends of two wires. Despin can be accomplished with 2.6 pounds of weight and wrapping the wires twice around the vehicle. The wire tension will be 126 pounds. Despin is initiated by firing a pyrotechnic squib on command. After despin, the yo-yo's are released by self-releasing latches.

The ascent and injection control system will employ the gyro reference unit and a portion of the SCS controller for control electronics and jet drive logic. The remainder of the system will be housed in the injection engine adaptor and will be jettisoned with the injection engine. The weight for that portion of the system which will not remain with the operational spacecraft is as follows:

Spin-up jets	3.8 pounds
Control jets	6.3
Sun sensor	1.5
Despin yo-yo's	2.6
Cabling and connectors	1.0
Total Weight	15.2 pounds

Rate Arrest and Acquisition

This section describes a sequence of maneuvers to establish acquisition of the space reference coordinates. The maneuver sequence considered is sun-earth-polaris. This sequence of maneuvers is described as follows:

- The IRP senses angular rates around the spacecraft x, y, and z axes and develops proportional signals. This signal is then used to command the reaction jet thrust in the proper direction and arrest the spacecraft motion.

- The sun sensor torques the IRP to drive the vehicle at the proper rate toward the sun. The x axis is oriented toward the sun at the completion of this maneuver.

- At a pre-determined time of day, the vehicle is rolled about the x axis (sunline) allowing the earth to be acquired by the horizon sensor. Having acquired the earth, pitch and roll control is transferred to the horizon sensor leaving yaw control on the gyro.

- Based on the ephermeris data, a yaw maneuver is commanded through the IRP by torquing the yaw gyro at a fixed rate for a specified period of time. This maneuver will cause Polaris to be directly in the field of view of the Polaris star tracker (PST), and yaw control will be transferred from the yaw gyro to the PST.

Attitude Maneuvers

The attitude maneuvers required of the SCS include:

- Offset pointing

- Satellite tracking

- Antenna pattern study

Offset Pointing -- The ATS-4 satellite will be required to point its antenna toward selected earth-based locations on the visible hemisphere for extended periods of time.

Offset point can be accomplished by commanding the required offset angles through the horizon sensor, or by torquing the gyros. Since the gyros will be de-energized for the major part of the mission, the usual mode will be the horizon sensor. While at an offset point, the monopulse can supply the error signals to control pitch and roll. The yaw axis will continue to be controlled by the star tracker. If it is expected to remain at the offset point for an extended period, the horizon sensor may be deenergized.

Maneuvering to an offset point will be made at a commanded rate of 1 degree per minute. The wheels have sufficient momentum storage to perform this maneuver.

Satellite Tracking -- Satellite tracking is a special case of offset pointing, however it has several added system requirements. The antenna must be pointed to the edge of the earth disc (up to 9.0 degrees in pitch and roll) where it is to acquire a close-earth orbiting satellite. Pitch and roll control is then switched from the horizon scanner to the antenna. The vehicle then is commanded to track the satellite across the full earth disc (17 degrees) via signals from the antenna. This maneuver will be made using wheels. The vehicle must follow a varying tracking rate which the wheels will be able to follow smoothly. The maximum acceleleration required to follow the satellite is 14.8×10^{-6} degrees/sec^2 which is well within the wheel capability even near unload speed.

Antenna Pattern Maneuvers -- The antenna pattern maneuver is performed to measure the antenna pattern over various angular displacements for the different transmission frequencies. The maneuver consists of a rotation first in one direction to the desired positive angle, then a rotation in the opposite direction to the desired negative angle, and then back to zero.

Two of the pattern maneuvers require rotation of ±15 degrees at 1 degree/minute and ±5 degrees at 4 degrees/minute. These maneuvers are to be made using the inertia wheels. The wheels have been sized to allow maneuvers of 1 degree/minute in addition to the storing of the cyclic momentum. The 4 degrees/minute maneuver can also be made on the wheels without activating the jets; however, this will require monitoring wheel speed before making the maneuver. The direction of the maneuver can then be chosen to reduce the wheel momentum, and, thus, avoid firing of the jets.

In a pulse torque rebalance gyro system each pulse is an increment of attitude; so, gyro pulse history will be recorded to provide the attitude of the vehicle. The attitude-rate trajectory for the ±5 degree maneuver is shown in the following sketch:

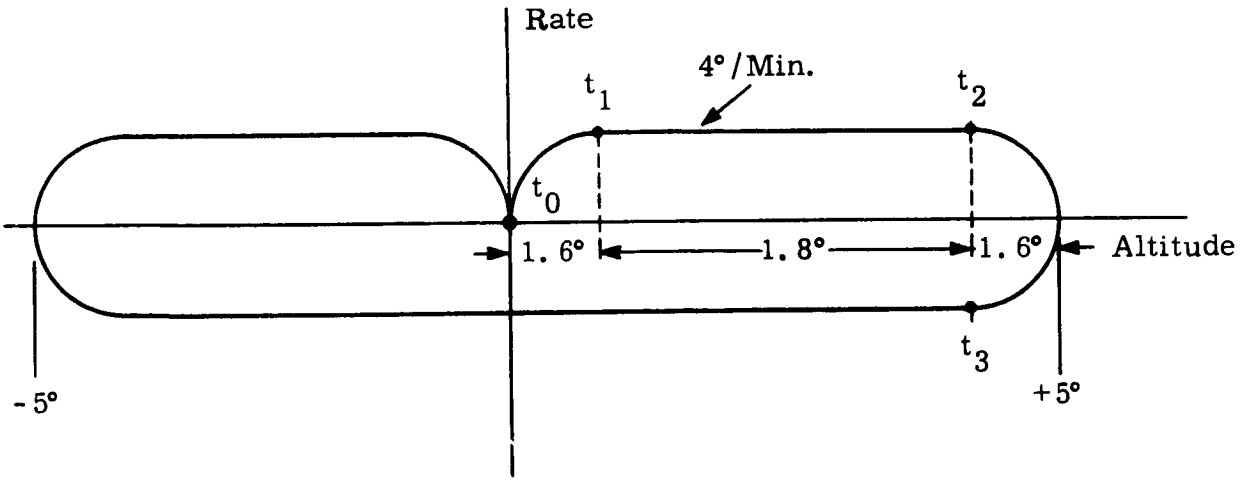

At t_o the command is initiated. The vehicle is accelerated until t_1, when the desired rate is achieved. A constant rate is maintained until t_2 when the vehicle is decelerated. Application of torque continues until at t_3 the reverse rate is achieved. Because of the acceleration periods, the time to complete the above maneuver for the roll axis is 7.4 minutes. Gyro drift for 0.1 degree/hr gyro will be less than 0.0123 degrees for this period.

The time for the ±15 degree maneuver is 60.6 minutes. Gyro drift during this time is slightly over 0.1 degree.

The pitch axis maneuvers will require slightly less time because the pitch inertia is lower, resulting in a higher acceleration capability.

Station Keeping Mode

East-west stationkeeping must be performed at regular intervals to maintain the longitudinal location of the satellite. North-south stationkeeping must be performed to control the inclination error. East-west stationkeeping is performed by use of an engine on the x axis; North-south stationkeeping is performed by use of an engine on the y axis. Vehicle center of gravity misalignment with the thrust axis creates a torque on the vehicle. The SCS must control attitude in presence of these disturbance torques. These torques are estimated to be 0.05 pounds.

The reaction jet system will be used in this mode to maintain attitude. The acquisition logic with deadbands of 0.1 to 0.2 degrees will be used for controlling attitude from the horizon sensor and the star tracker. Attitude excursions as large as 0.5 degree are expected during stationkeeping; however, this will not significantly affect the thrust axis impulse.

6.6.2 System Block Diagram

Ascent Control System

The block diagram for the ascent control mode is shown in Figure 6-14. The logic for the ascent mode will be contained in the SCS controller. During launch and injection only that part of the controller will be energized.

The required rate information will be obtained from the gyro reference unit which is part of the SCS.

The telemetered data provides the error signal to control the pitch attitude of the vehicle, and the sun sensor provides the control signal for the yaw attitude.

Operational Spacecraft Control System

The SCS Block Diagram is shown in Figure 6-15. A short description of the blocks on the diagram is given below.

The command data input is the link by which commands are introduced into the attitude control system to select modes and offset points.

The outputs of the X-Band monopulse provide the roll and pitch error signals to hold attitude at an offset point. This would also be the input channel if the vehicle were tracking a cooperative satellite.

The Polaris star tracker provides the yaw error information, and also a star presence signal which indicates that a star of the proper magnitude is in the field of view. The roll gimbal drive electronic resets the field of view to keep the star in view, when commanding antenna maneuvers or holding at offset points. The yaw gimbal drive resets the yaw axis null to account for the apparent diurnal motion of Polaris.

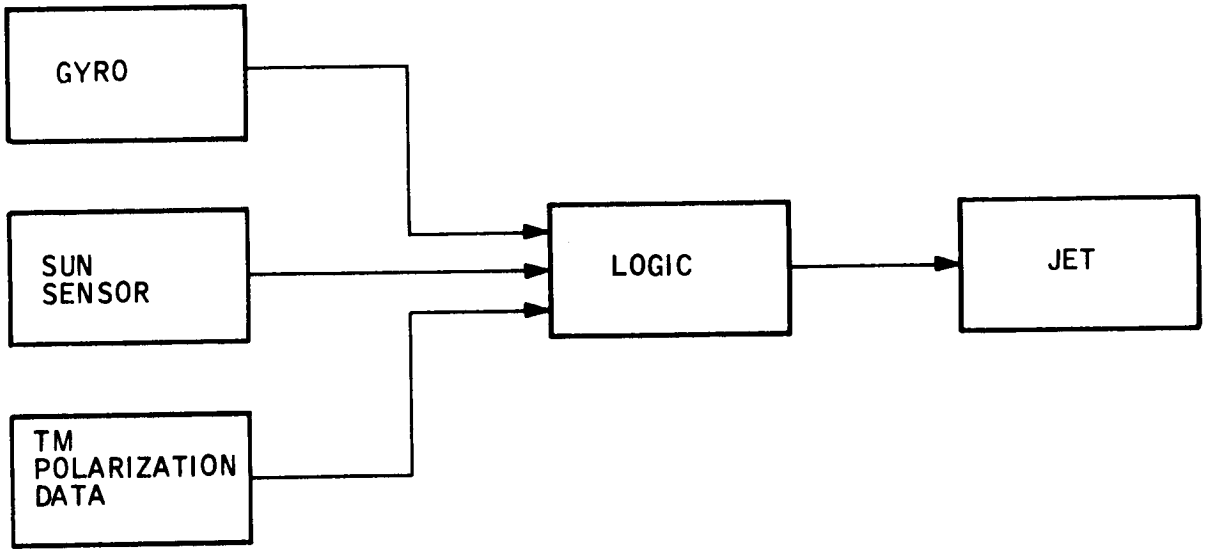

Figure 6-14. Block Diagram - Ascent Control

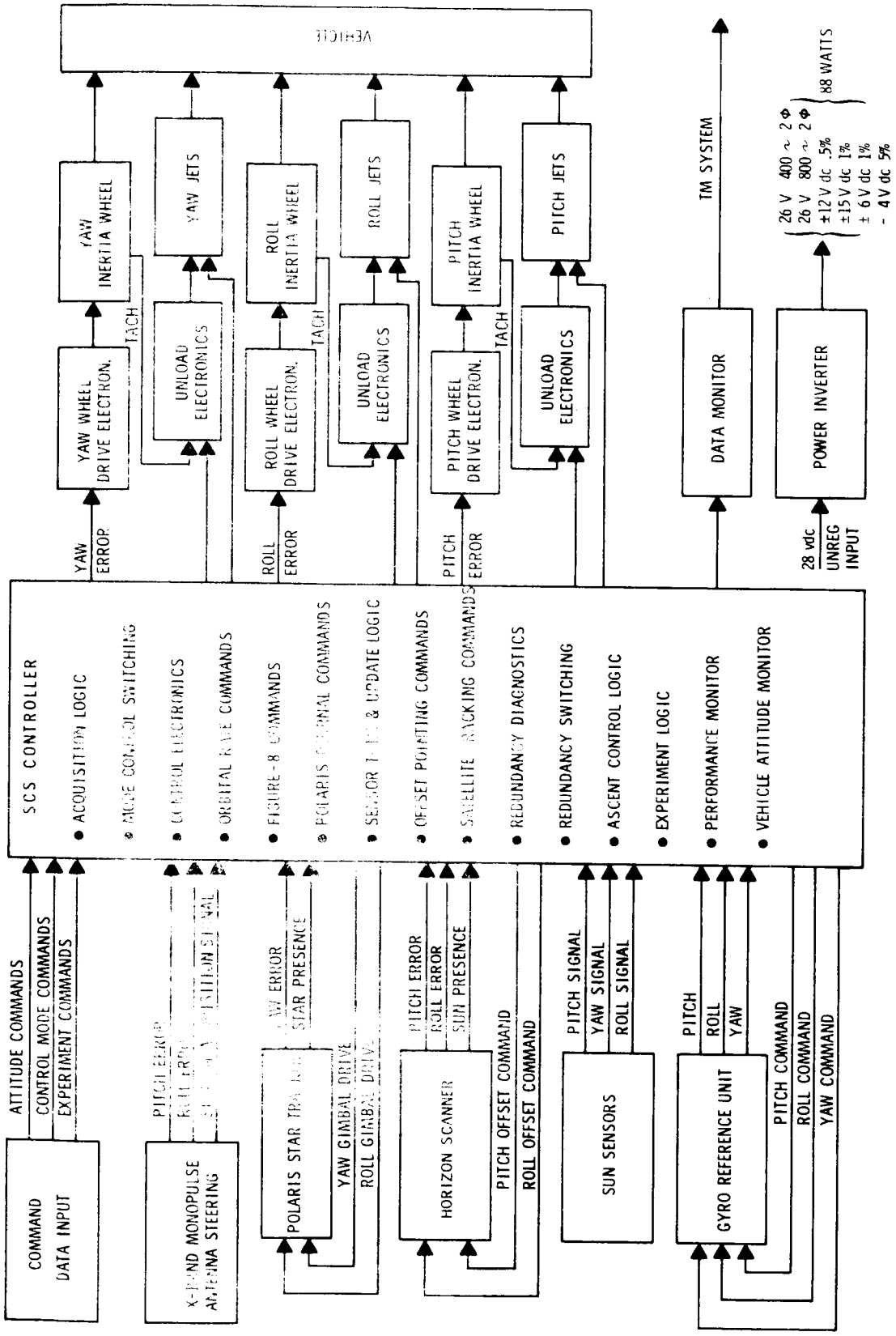

Figure 6-15. SCS Block Diagram

The horizon scanner provides a pitch and roll error signal to stabilize the vehicle at local vertical or at the offset points. A sun presence signal is generated whenever the sun is in the horizon sensor field-of-view. The pitch and roll offset commands are provided for pointing off of the local vertical.

The sun sensors provide the error signals to drive the vehicle x axis toward the sun for the first step of the acquisition sequence.

The gyro reference unit provides the pitch, roll and yaw attitude and rate signals in form of pulses. Each pulse is an increment of attitude, and the pulse frequency is a measure of the body rate. The pitch, roll and yaw commands are those required to torque the gyros to establish the various maneuver rates, to compensate for gyro drift, or to compensate for various components of orbital rate.

The SCS contains the necessary logic, compensations and computations to accept signals from the sensors and drive the torquers accordingly. The unit stores the compensation or calibration signals needed for the gyros, horizon scanner, and star tracker. The SCS also contains logic needed for the ascent mode. All of the switching of redundant units is accomplished within this unit.

The drive electronics contains those power electronics needed for running the wheels. The unload electronics takes the wheel tachometer signal and fires the reaction jet whenever the wheel momentum unload level is exceeded. The unload electronics also serve as a jet driver for the other modes where the wheels are not used.

The jets and the wheels are the torque producers and are used depending upon the mode of control as commanded by the controller.

6.6.3 Sensor Update

Because of the accuracy required for the ATS-4 mission, calibration of the sensors may be required to achieve the accuracy, or may be desirable to check the performance of the sensor. These sensors include the following:

- Gyro
- Horizon Sensor
- Star Tracker

All of these sensors can be monitored while the control system is being driven by the monopulse system at an offset point. The time history of the gyro drift, horizon sensor and star tracker outputs can be obtained. It is proposed to store the values obtained in the computer memory. Then, when ever the signals from these sensors are used, the computer will not only process the command, but will incorporate the proper correction signal in the computation.

6.7 SYSTEM PERFORMANCE

6.7.1 Pointing Accuracy

An allocation of errors for the various error sources was made. The error budgets are tabulated in Table 6-8 for roll and pitch and in Table 6-9 for the yaw axis. An analysis was made to allocate the error among the possible sources within the sensors; offset pointing using either the horizon scanner or the monopulse error signals is considered.

Error sources which may need some explanation are discussed below. The errors associated with the electronics are considered to be noise, null offsets and drifts. The alignment error is the misalignment of the optical axis with the mounting surfaces of the unit. The temperature allocation is the effect of temperature variation on both the electronics and the mechanical alignment. The long term variation due to degradation over the life of the unit is listed under life.

It is assumed that commands to go to offset points will be digital; thus, the number of bits in the command will determine how close the vehicle can be pointed to a particular point. Ten bits (including a sign bit) are sufficient to provide this command resolution.

The error contributed by the wheel drive amplifier is a null offset. The unload error is that required to command a wheel torque to balance the jet torque while unloading.

The yaw coupled error is an error resulting in one axis with an offset angle in the other axis. It is a function of the magnitude of the offset angle and the yaw error. For pointing at the center of the earth this error is zero in the roll and pitch axes. A yaw error of 0.2 degrees was allowed, since there appears to be no difficulty in achieving this accuracy with present state-of-the-art equipment.

Table 6-8. Roll-Pitch Pointing Error (Degrees)
(Maximum 3-σ Value)

Error Contributor	Horizon Scanner	Antenna Monopulse	
		Arriving at Offset	Holding at Offset
Horizon Scanner			
Electronics	0.03	0.03	--
Alignment	0.04	0.04	--
Temperature	0.03	0.06	--
Life	0.03	0.03	--
Horizon Definition	0.01	0.01	--
Command Resolution	0.01	0.01	--
Computer	0.01	0.01	0.01
Wheel Drive Electronics	0.03	0.03	0.03
Unload Error	0.04	0.04	0.04
Yaw Coupled Error	0.03	0.03	--
Antenna Signal	--	--	0.003
Other	0.02	0.1	--
RSS Value (three sigma)	0.0916	0.144	0.052

Table 6-9. Yaw Pointing Error

(Maximum 3-σ Value)

Error Contributor	Error - Degrees
Star Tracker	
Electronics	0.1
Alignment	0.05
Temperature	0.1
Life	0.1
Computer	0.02
Resolution (gimbal)	0.02
Wheel Drive Electronics	0.05
Unload Error	0.05
Other	0.04
RSS Value (three sigma)	0.2

All of the errors are assumed to be Gaussian and the 3-σ value is given. Some of the errors could be predicted or measured; thus, they could be eliminated from the total pointing error by modifying the point offset commands. It is noted that when the antenna monopulse error signals are used to control offset pointing, many error sources are eliminated. The increased value for the "other" error source in arriving at the offset point for the chosen ground station is caused by command angle inaccuracies not included in the other pointing modes.

The error budget also assumes that the yaw gimbal (for following diurnal motion of Polaris) is repositioned as a function of the pitch offset angle.

6.7.2 Acquisition

Phase plane plots were constructed showing acquisition of the references from the specified search rates. A lead-lag compensation of $\frac{10S + 1}{S + 1}$ was used. Deadbands of ±0.1 degrees were used for pitch and roll. A deadband of ±0.2 degrees was used for yaw. It was also assumed that the acquisition maneuver was performed using jets only. With the wheels operating in parallel, acquisition can be accomplished in a shorter time and with less gas. The phase plane plots are shown in Figures 6-16, 6-17, 6-18, and 6-19.

6.7.3 Control System Dynamics

Wheel Control

The control system for pointing and maneuvering the vehicle is shown simply in the following block diagram:

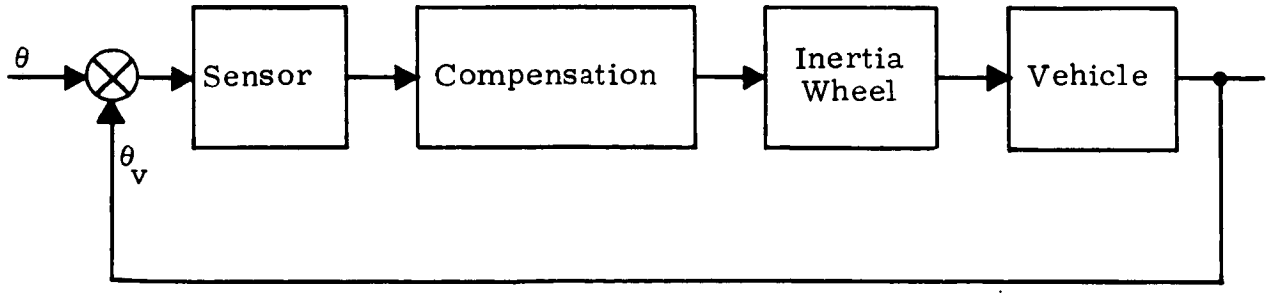

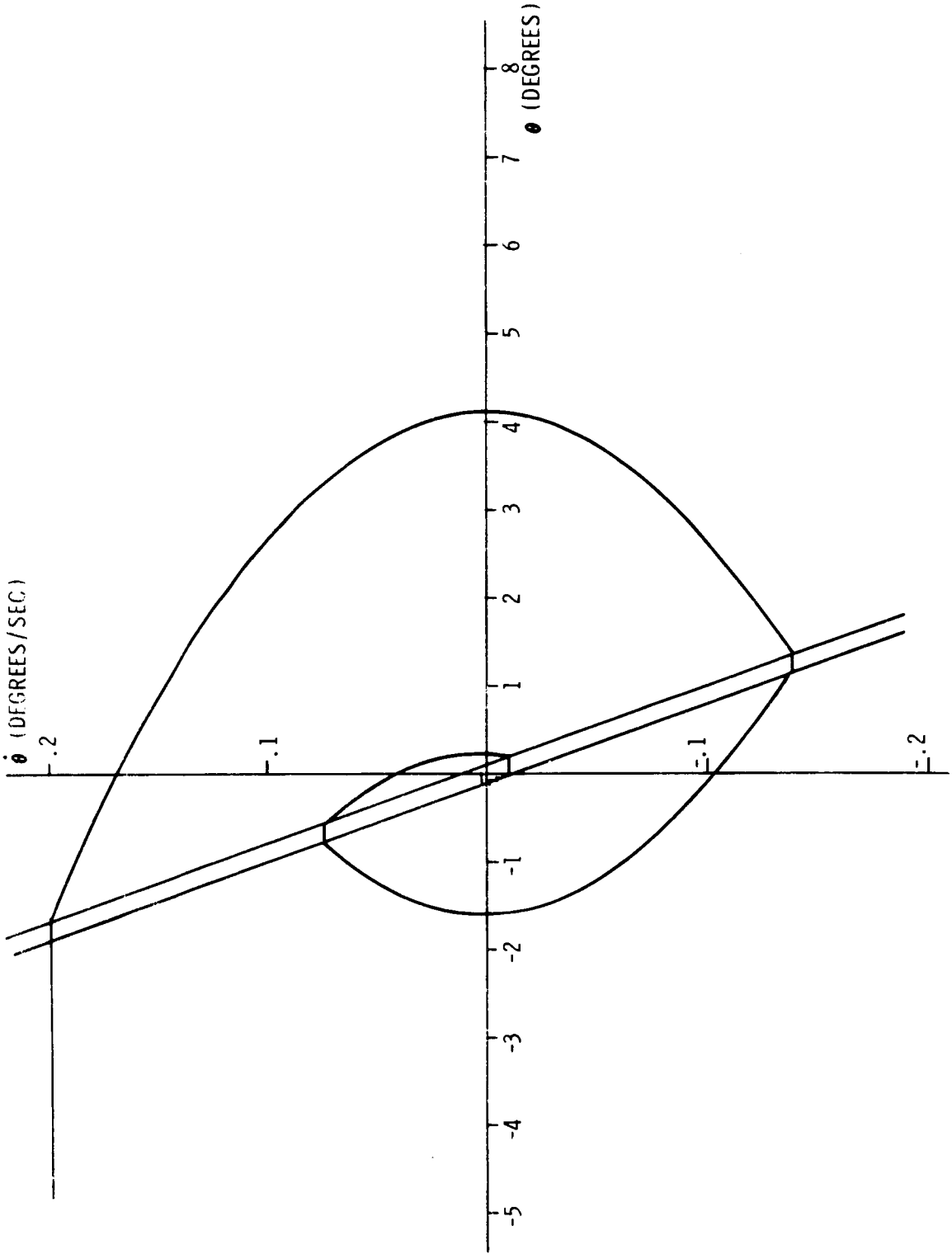

Figure 6-16. Phase Plane Plot Sun Acquisition - Pitch Axis

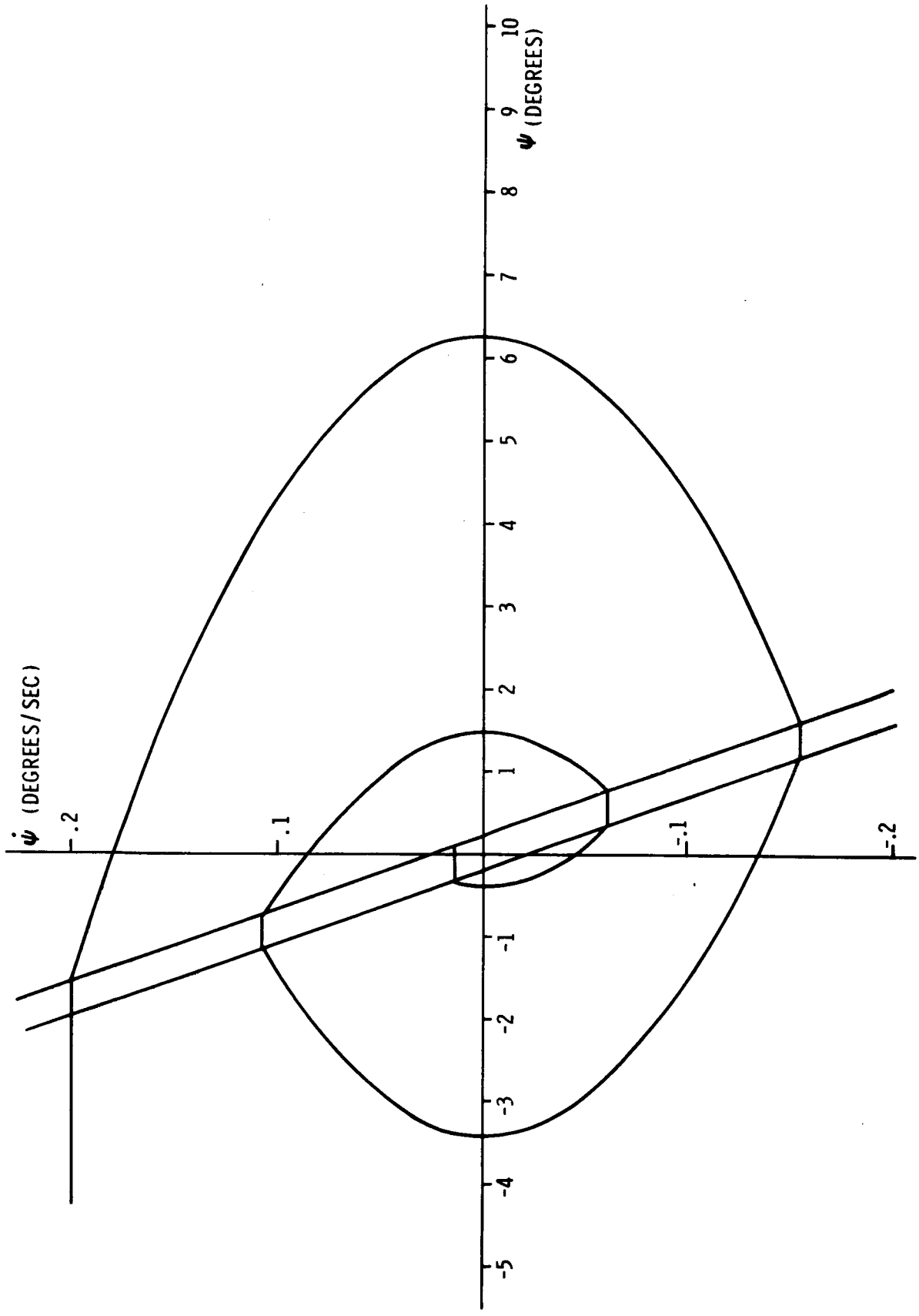

Figure 6-17. Phase Plane Plot Sun Acquisition - Yaw Axis

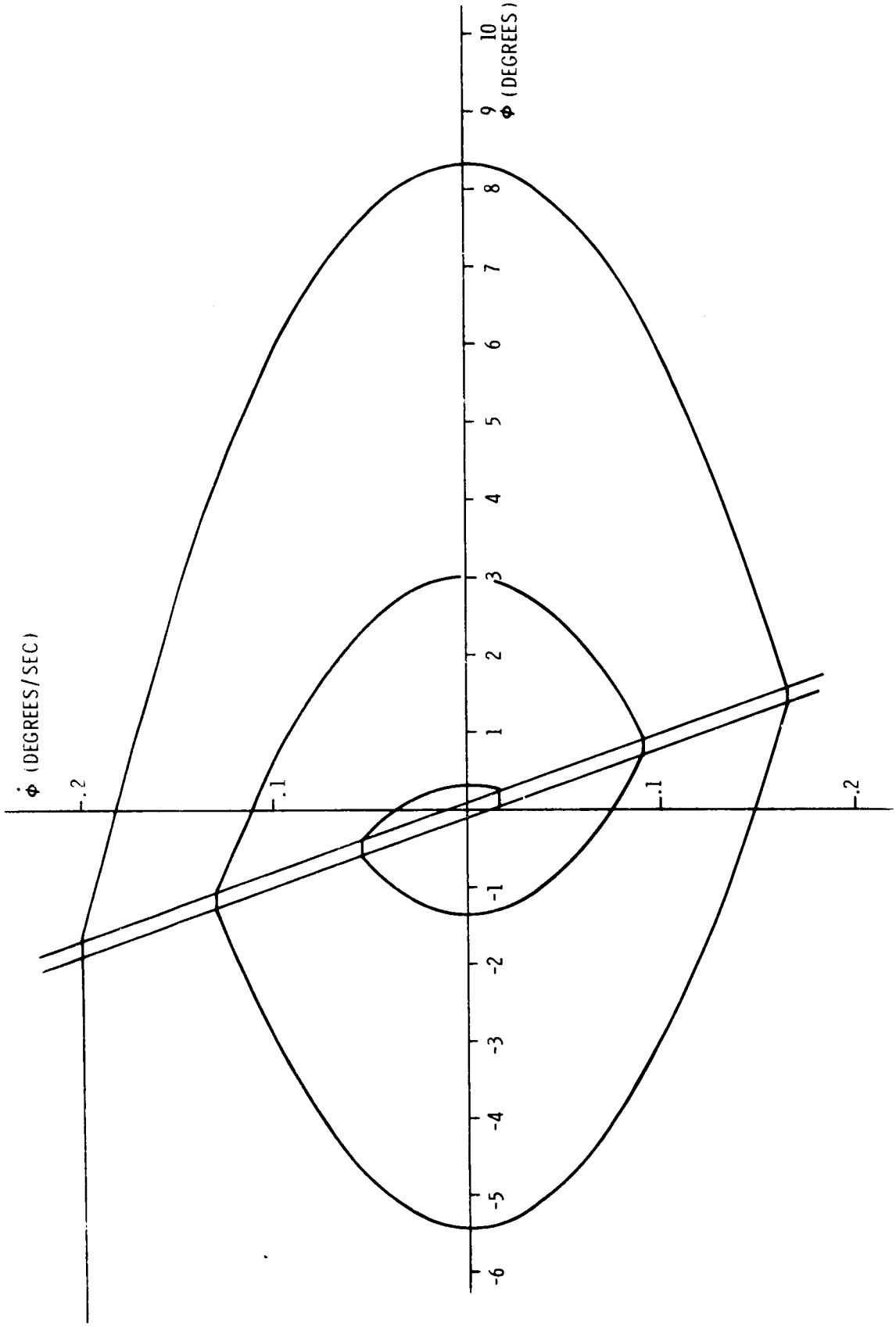

Figure 6-18. Phase Plane Plot Earth Acquisition Roll Axis

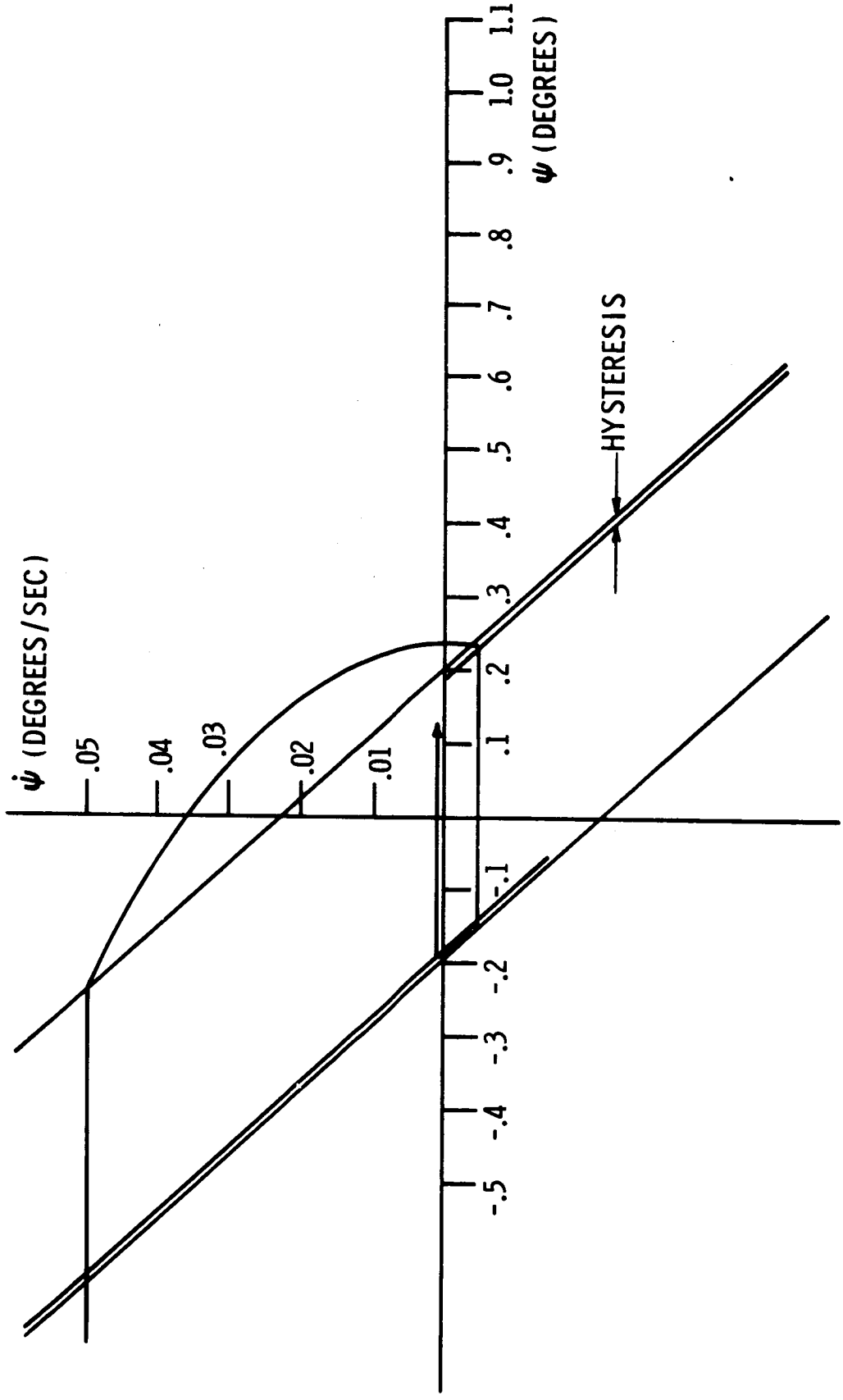

Figure 6-19. Phase Plane Plot Star Acquisition Yaw Axis

The sensor in the pitch and roll axis is the horizon sensor and in the yaw axis is the star tracker. The compensation is a lead-lag network to provide the required phase lead.

Open loop Bode plots were made for the three axes to establish the compensation required. The gain was set at 120 ft lb/rad. This value of gain allows the SCS to maintain the attitude error within the accuracy requirements while unloading the wheels with the jets. The Bode plots are shown in Figures 6-20, 6-21, and 6-22. The transfer function used for the sensor is $\frac{1}{0.4S + 1}$. The transfer functions for the inertia wheels are:

Roll $\quad \frac{58\,S}{58S + 1}$

Pitch $\quad \frac{77S}{77S + 1}$

Yaw $\quad \frac{55\,S}{55S + 1}$

The transfer functions of the compensation networks are shown on the graphs. The open loop Bode plots show that adequate phase and gain margins exist for the rigid body.

To assess the effects of the flexible antenna and solar paddle structure on the pitch and roll loops, a simple model was constructed for computer simulation.* The model consists of the antenna and paddle inertia coupled through a spring (K_s) and viscous (F_m) restraint to the module which houses the SCS. The block diagram of this model is shown in Figure 6-23. The transfer function of the overall body is given by:

*These loops would be most affected by dynamic structural coupling effects, since the associated structural mode frequencies are lower.

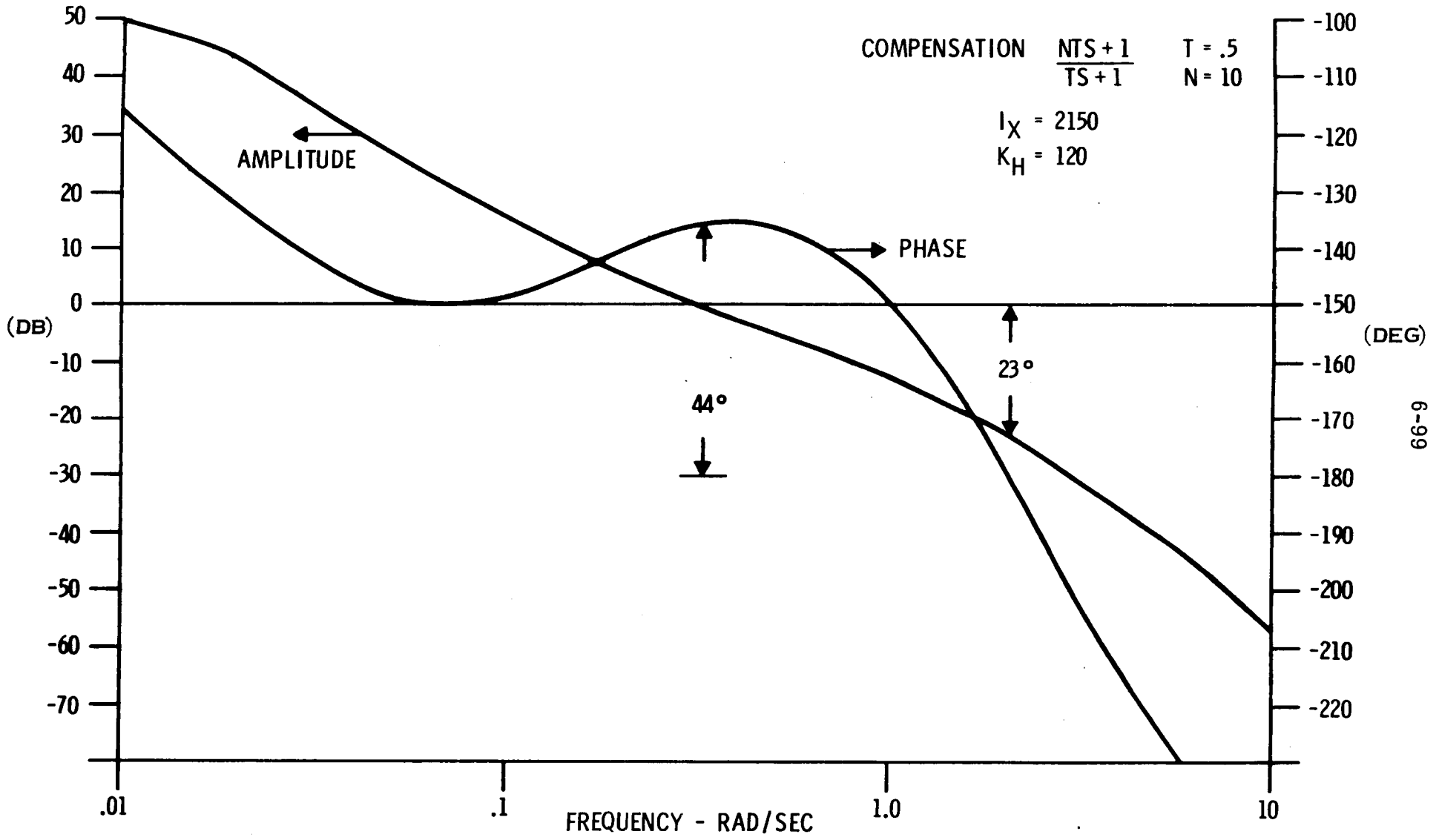

Figure 6-20. Open Loop Bode Plot - Roll Axis

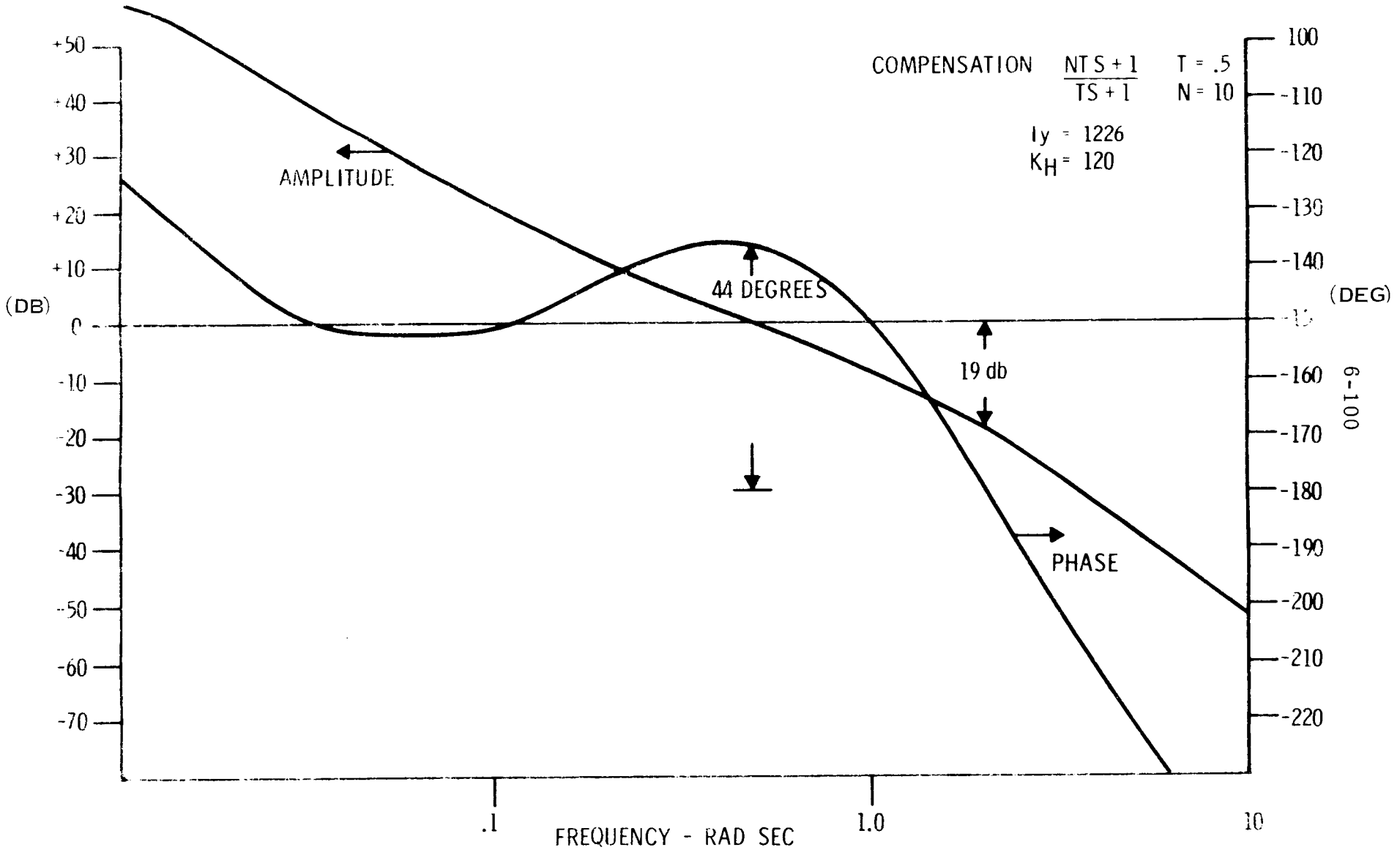

Figure 6-21. Open Loop Bode Plot - Pitch Axis

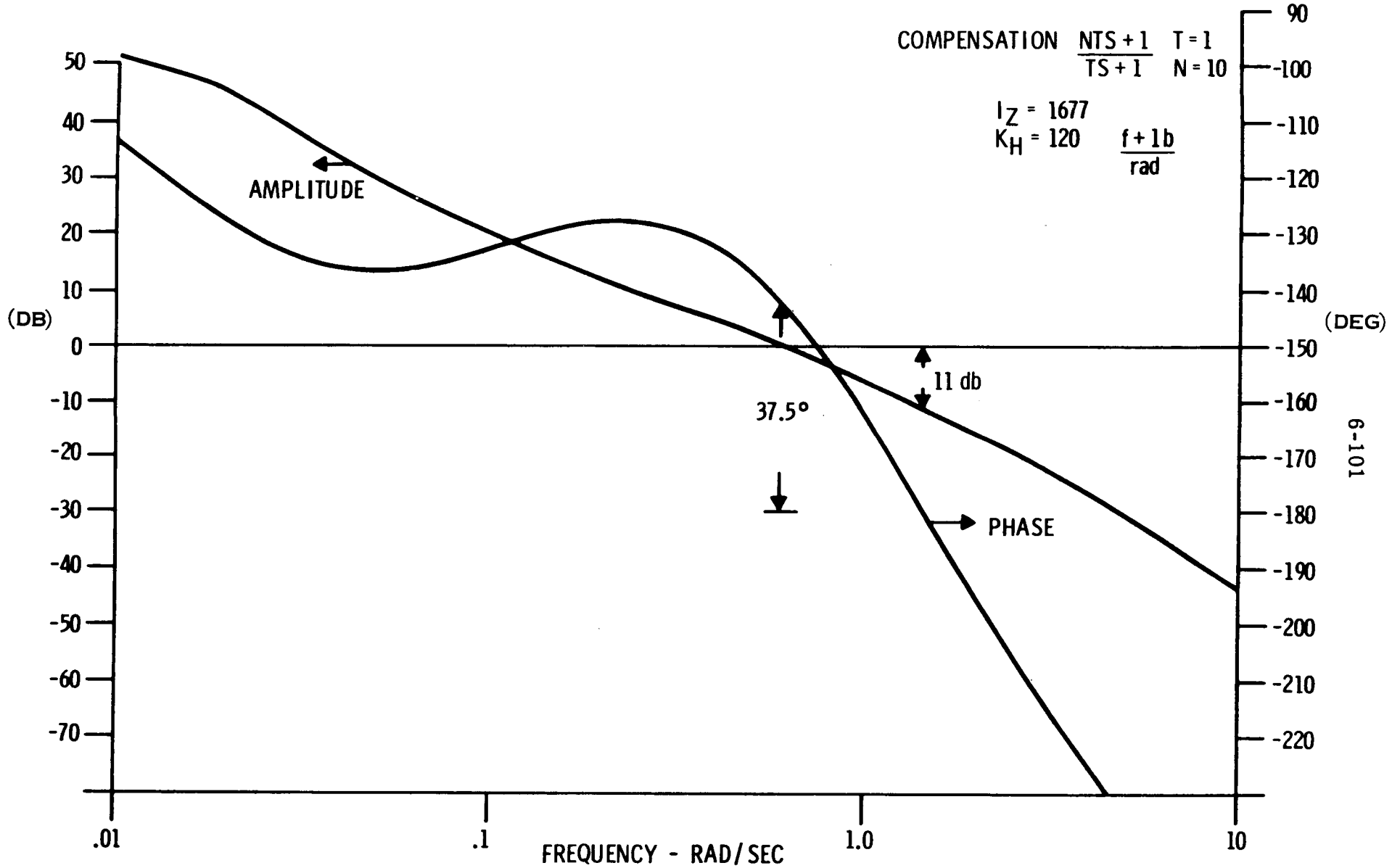

Figure 6-22. Open Loop Bode Plot - Yaw Axis

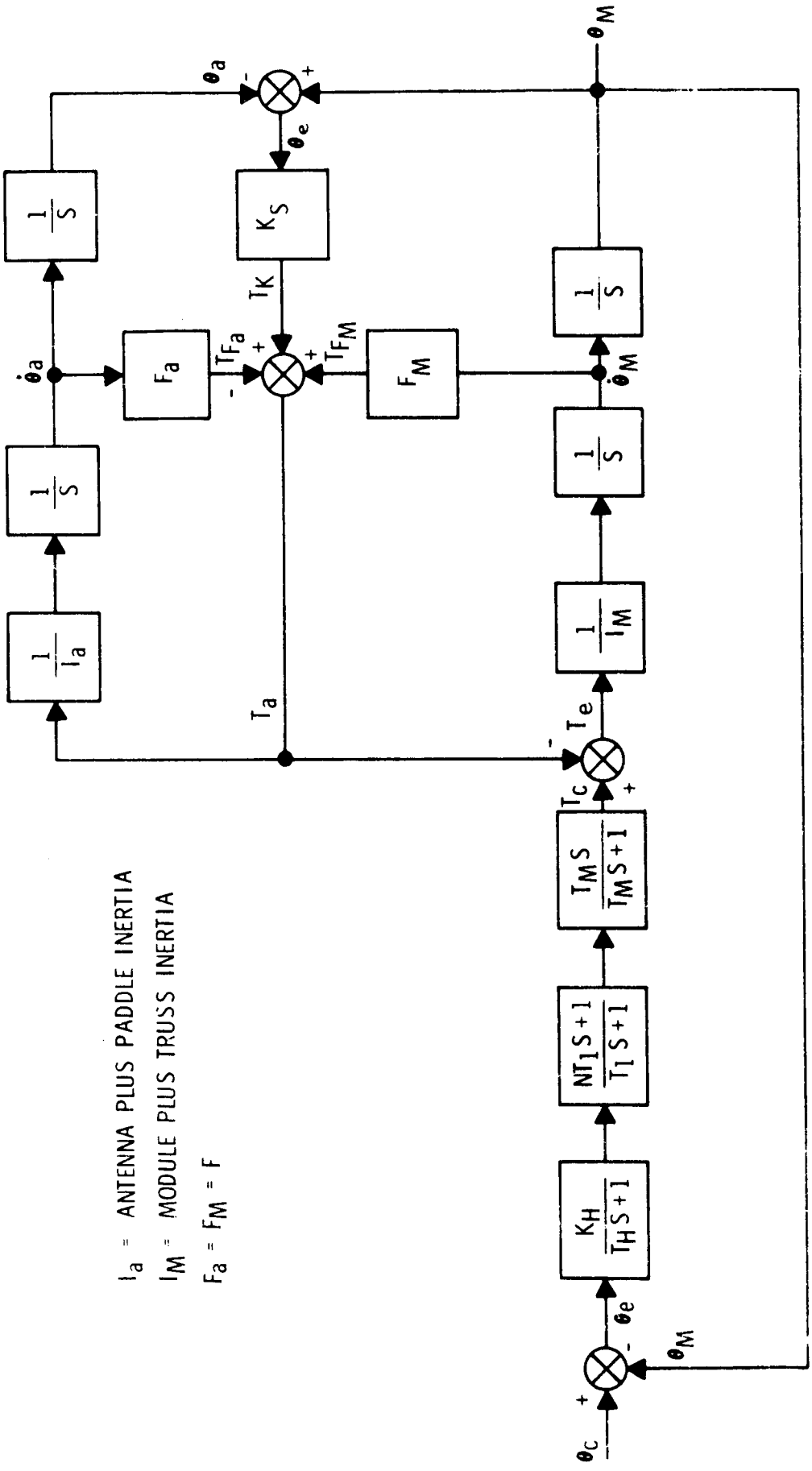

Figure 6-23. SCS and Vehicle Dynamics Block Diagram

$$\frac{\theta_M}{T_C} = \frac{S^2 + \frac{F}{I_a} S + \frac{K_s}{I_a}}{I_M S^2 \left(S^2 + \frac{I_M + I_a}{I_M} \times \frac{F}{I_a} S + \frac{I_M + I_a}{I_M} \times \frac{K_s}{I_a} \right)}$$

To evaluate the transfer function, $\frac{F}{I_a}$ is considered to equal $2\zeta\omega_n$ and $\frac{K_s}{I_a}$ equal ω_n^2. The first bending mode frequency is considered to be ω_n and the damping is considered to be ζ.

The complete transfer function was derived and used in a digital computer program to generate the closed loop frequency response, i.e., θ/θ_c $(j\omega)$.

The rigid body responses for the roll and pitch axes are shown in Figures 6-24, 6-25, 6-26, and 6-27. The responses with the flexible effects are shown in Figures 6-28, 6-29, 6-30, and 6-31 using a damping ratio of 0.01. Figures 6-32, 6-33, 6-34, and 6-35 show the response with a damping ratio of 0.005.

The natural frequency of the roll and pitch axes is 0.46 radians/sec and 0.67 radians/sec respectively. In comparing the rigid versus the flexible responses there is little difference in the response below four radians/second. Likewise, there is an insignificant difference in control system response for the different structural damping in the frequency range of concern. The high frequency resonance effects are not critical stability wise.

There is more than three octaves separation between the control system frequency and the first structural mode. With this degree of separation, no control problems are anticipated. Should structural frequencies become lower, the gain of the pitch and roll axes could be decreased. With a lower

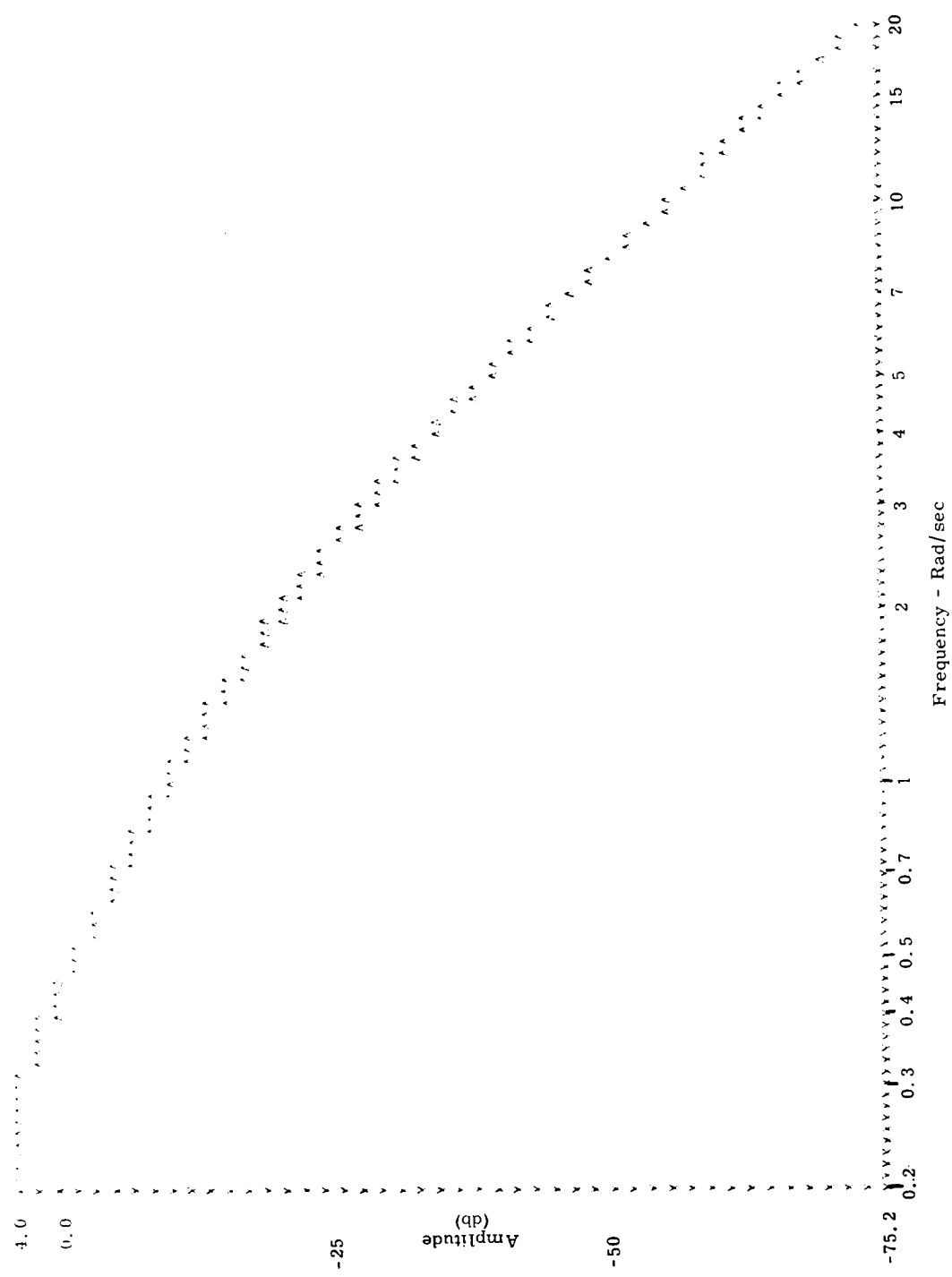

Figure 6-24. Roll Axis-Rigid Body Amplitude Response

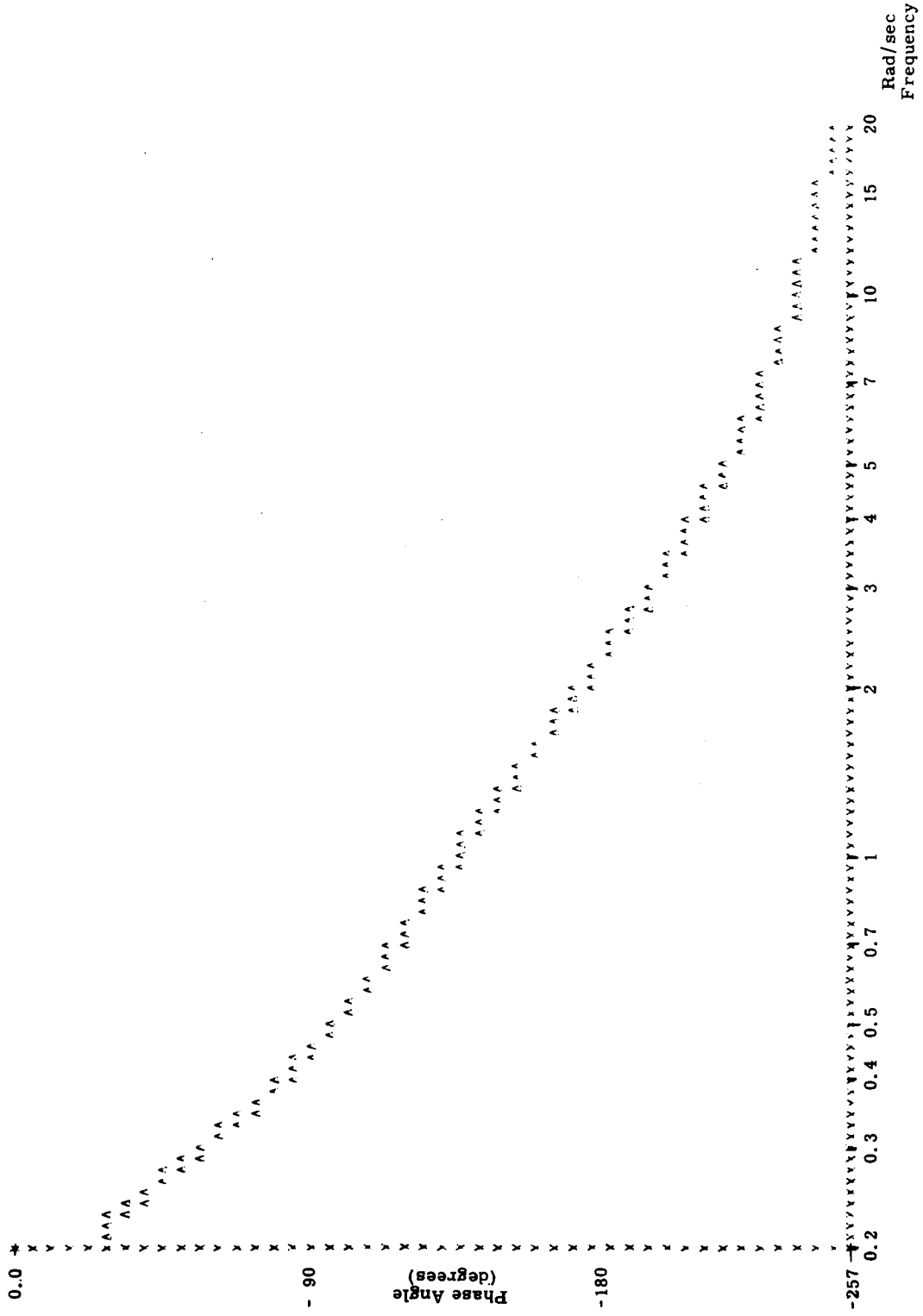

Figure 6-25. Roll Axis-Rigid Body Phase Response

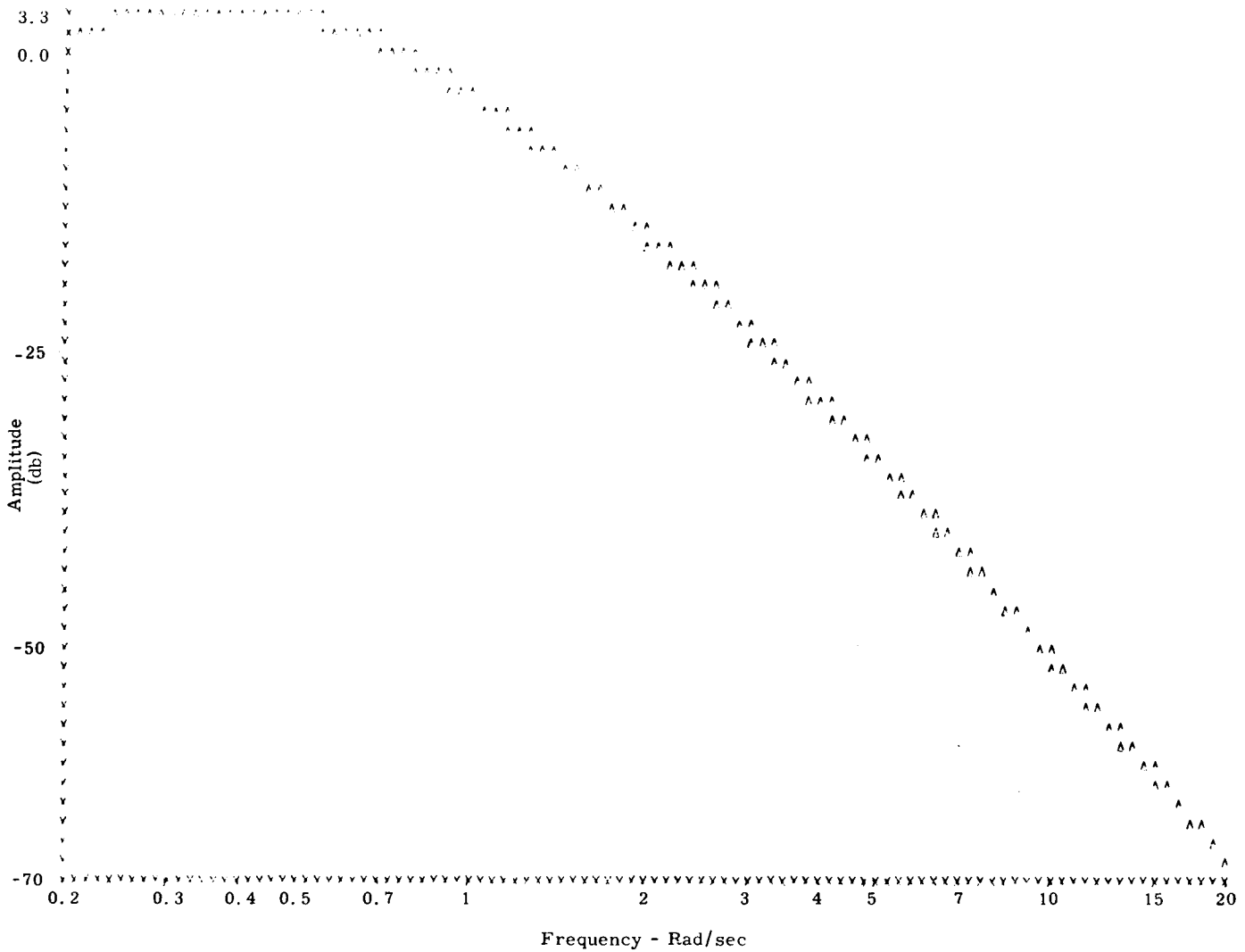

Figure 6-26. Pitch Axis-Rigid Body Amplitude Response

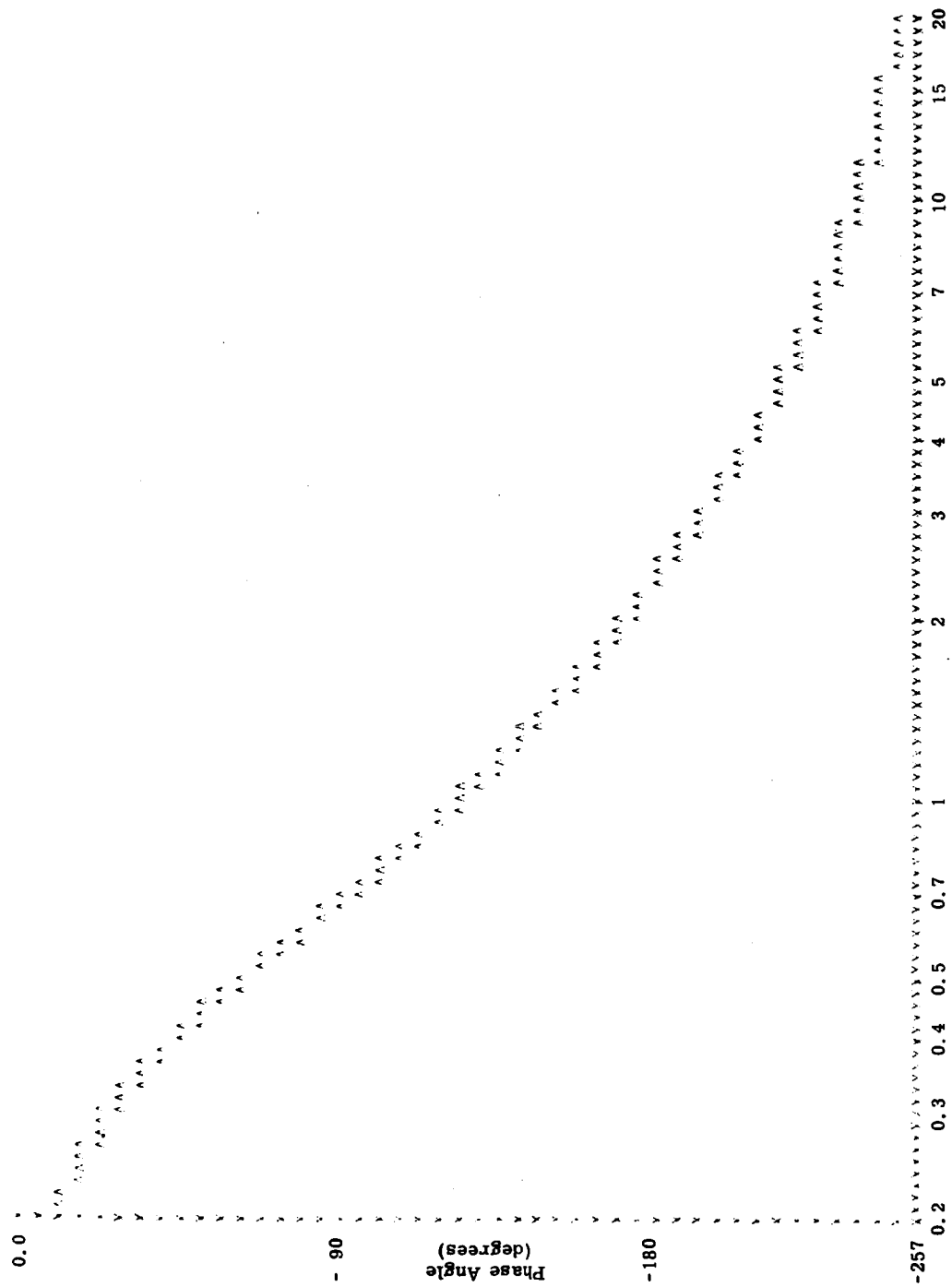

Figure 6-27. Pitch Axis-Rigid Body Phase Response

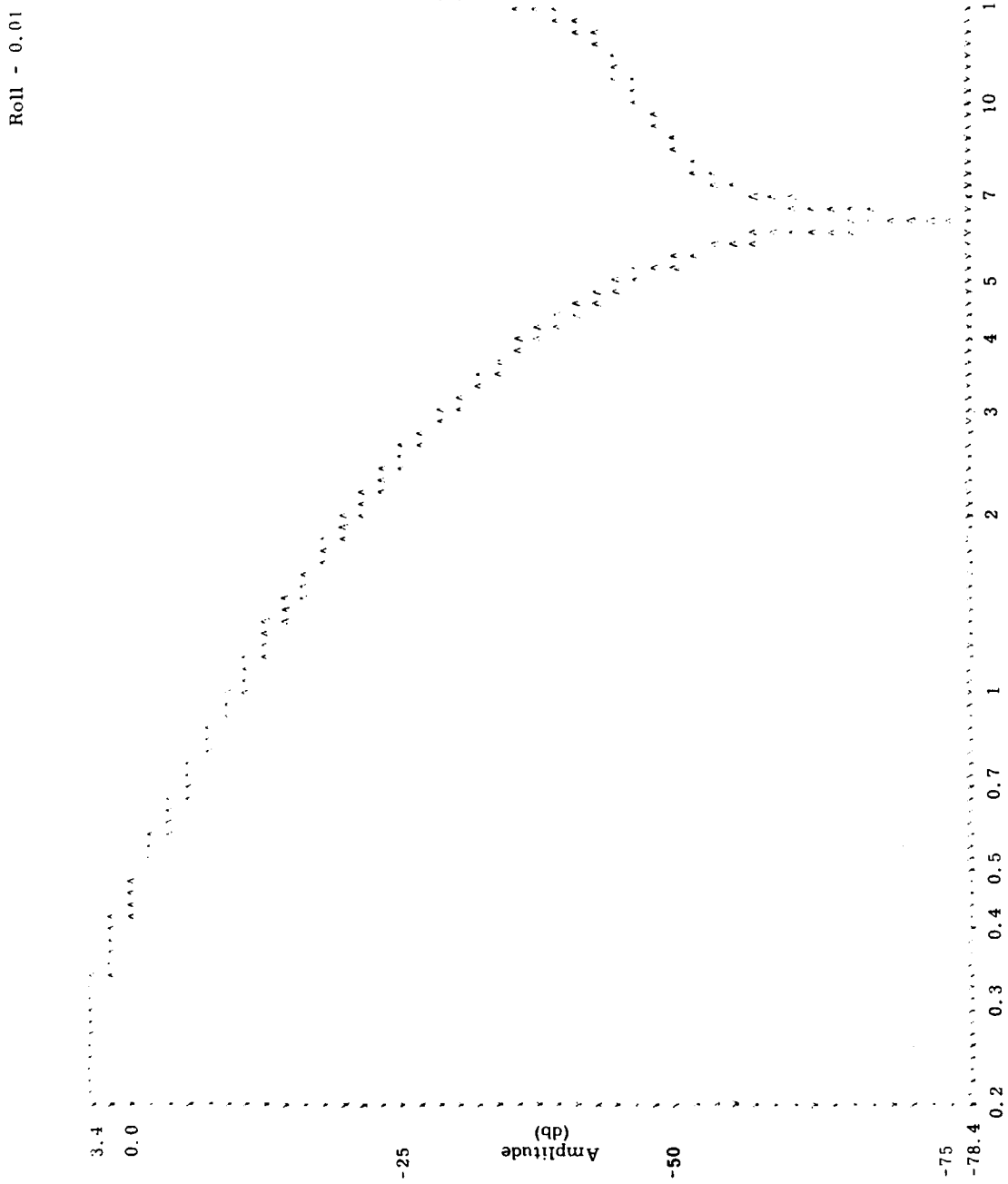

Figure 6-28. Amplitude Response Roll Axis-Flexible (.01)

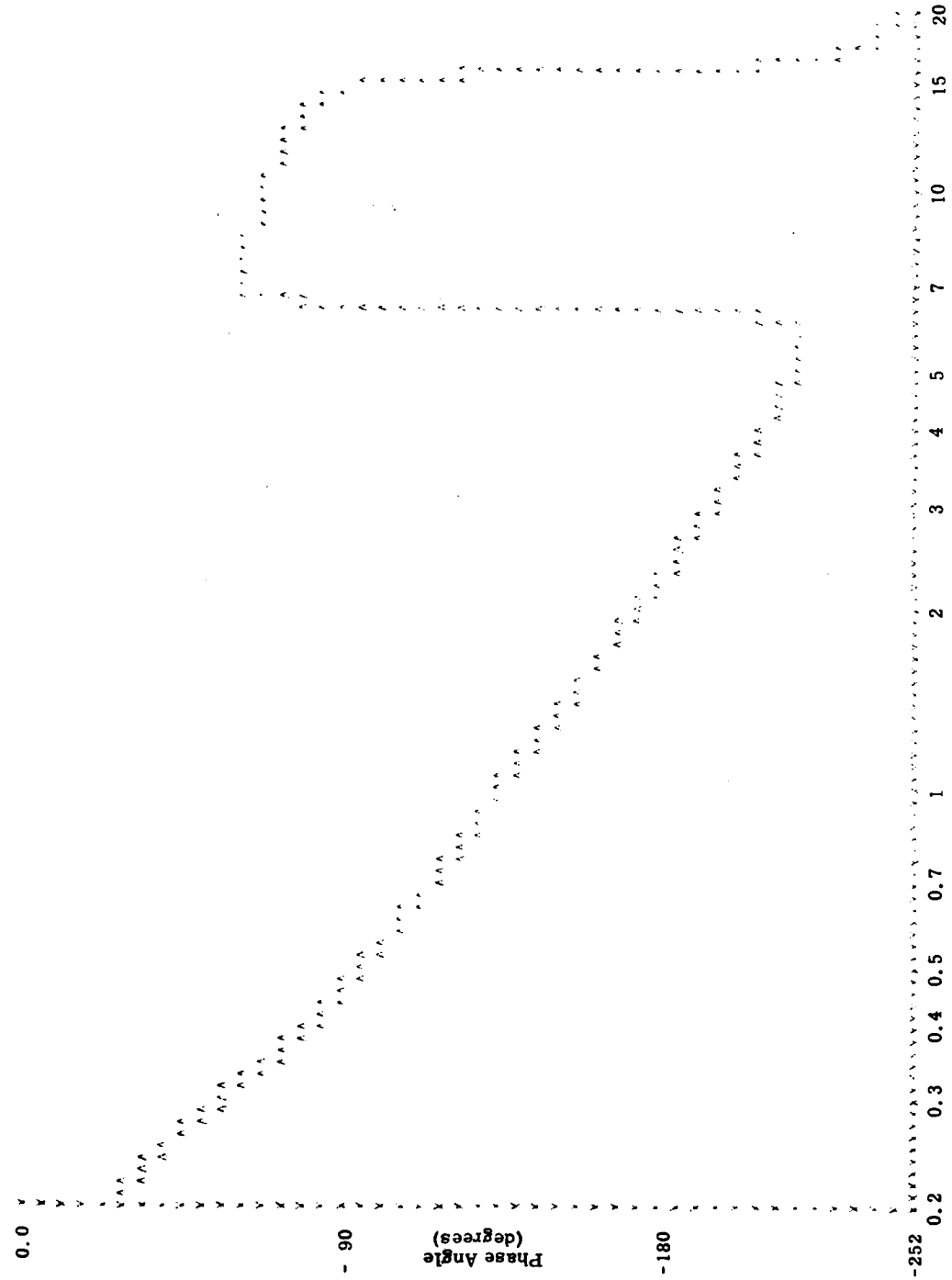

Figure 6-29. Phase Response Roll Axis-Flexible (.01)

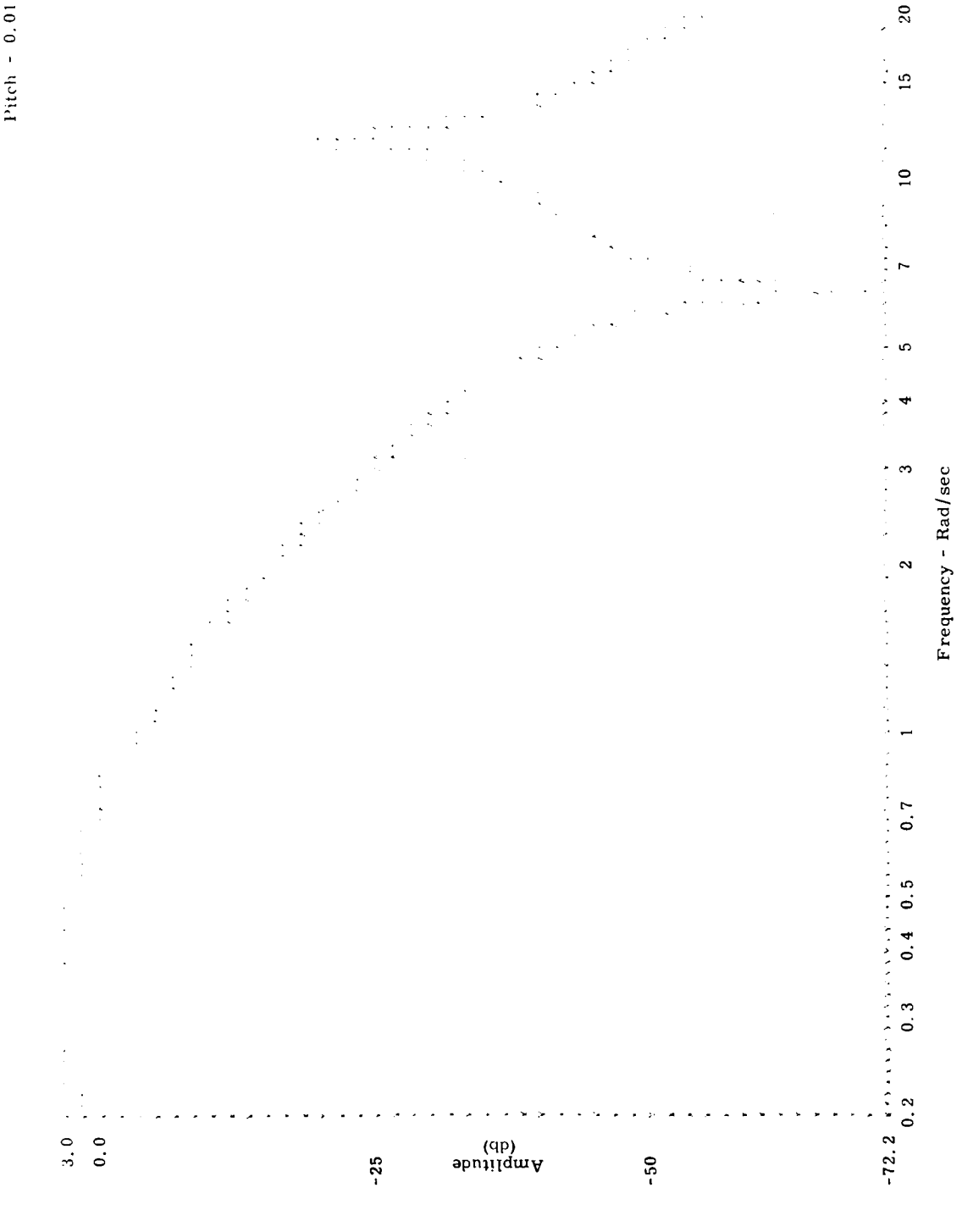

Figure 6-30. Phase Response Pitch Axis-Flexible (.01)

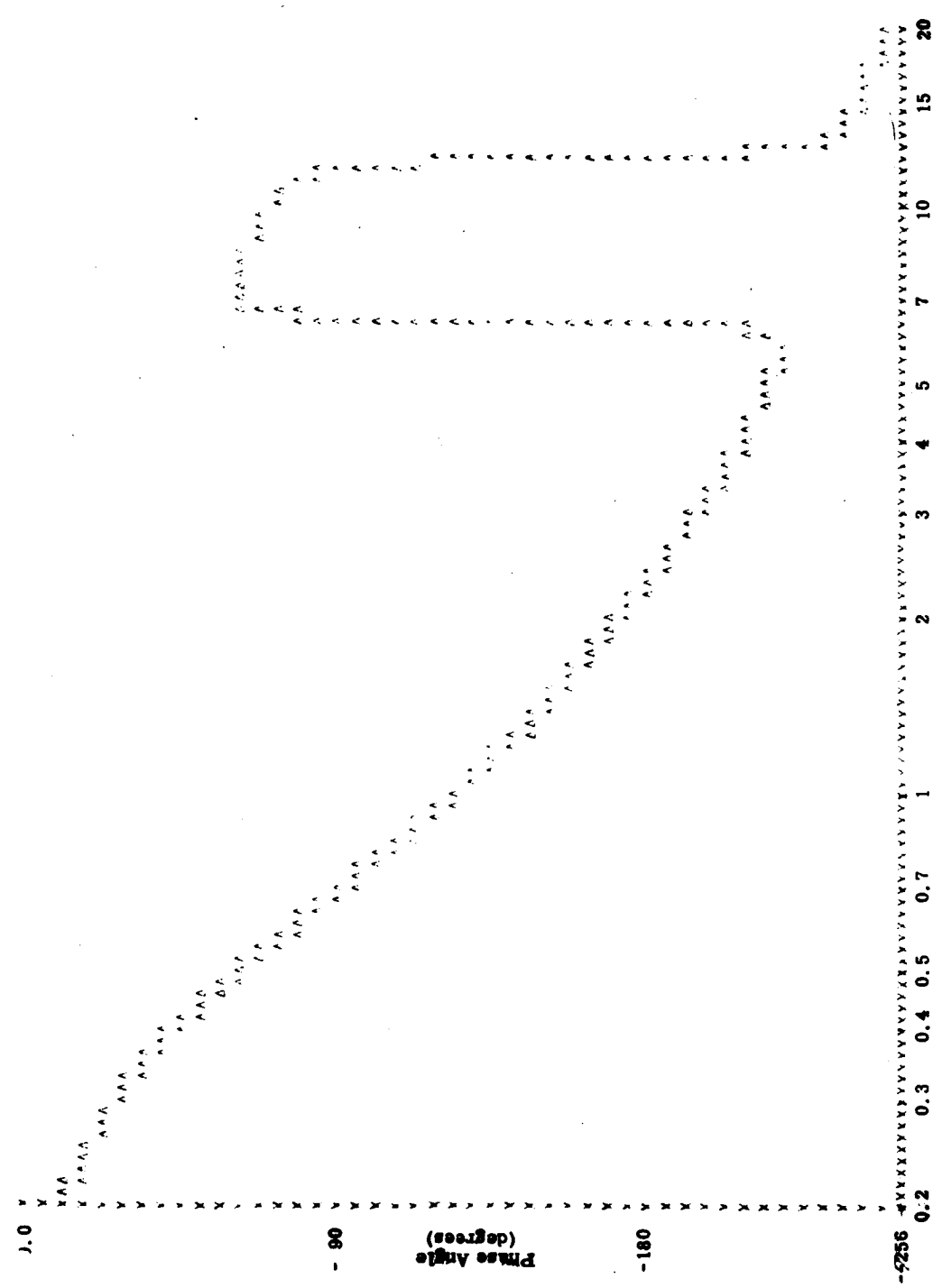

Figure 6-31. Phase Response Pitch Axis-Flexible (.01)

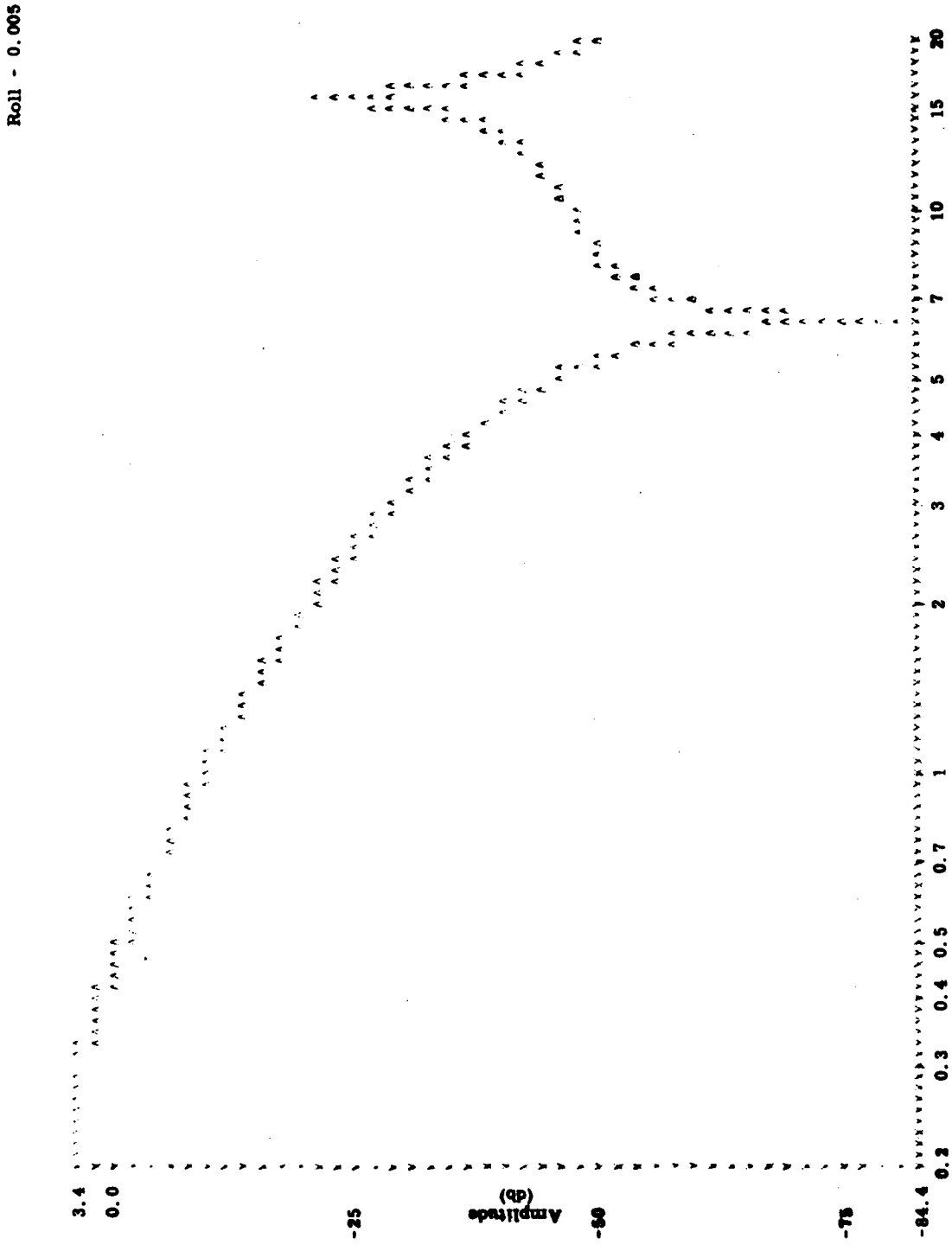

Figure 6-32. Amplitude Response Roll Axis-Flexible (.005)

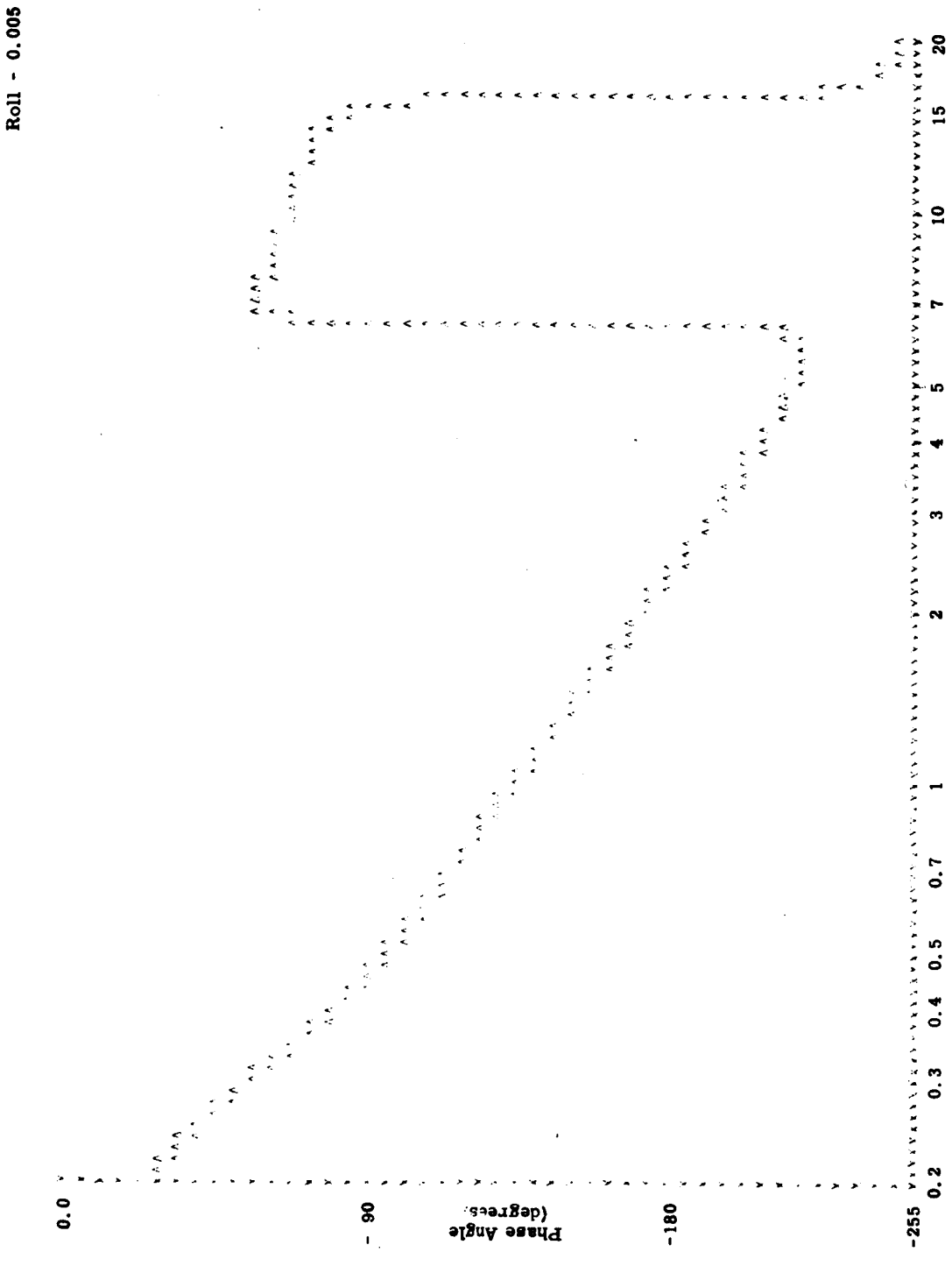

Figure 6-33. Phase Response Roll Axis-Flexible (.005)

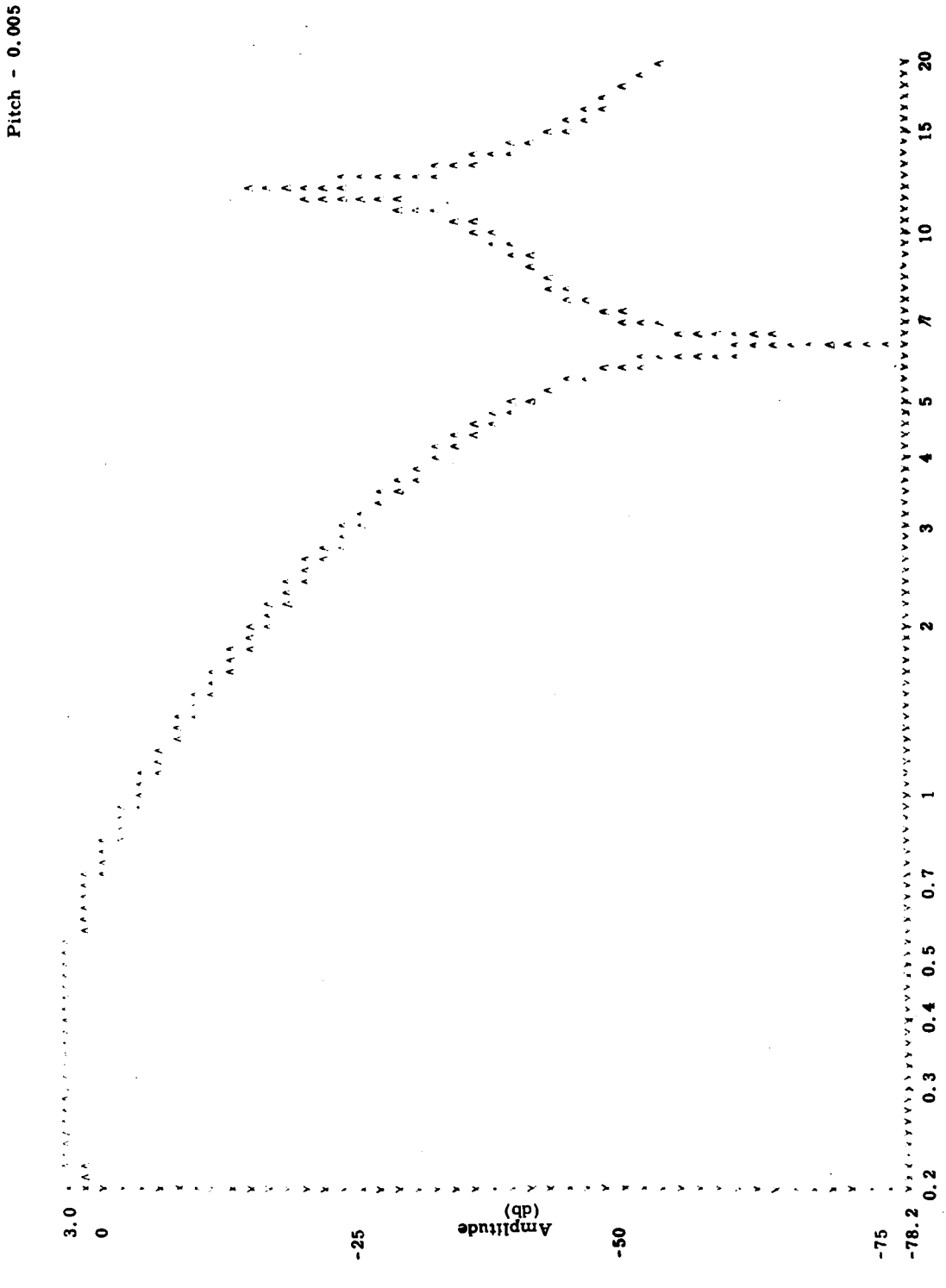

Figure 6-34. Amplitude Response Pitch Axis-Flexible (.005)

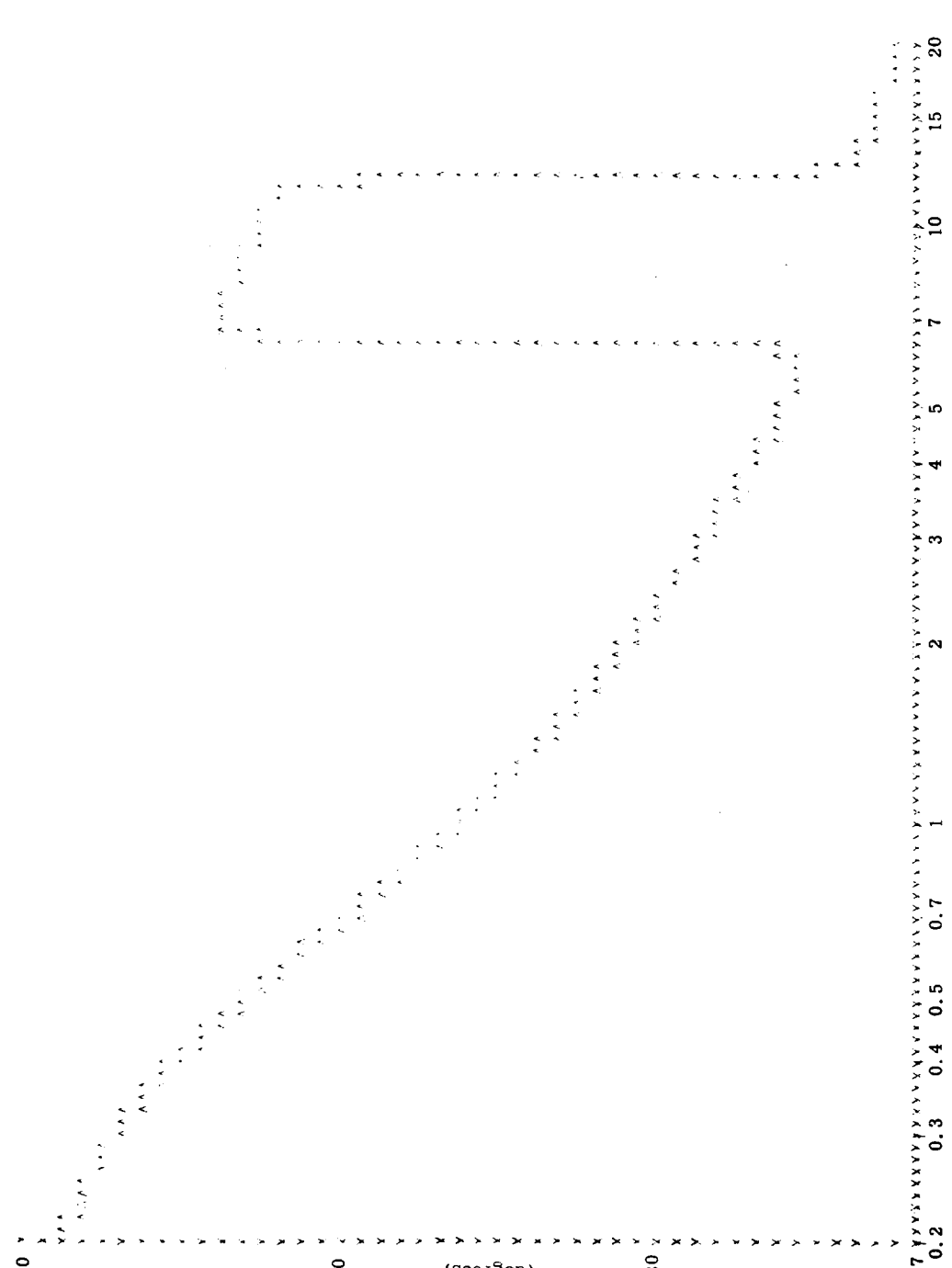

Figure 6-35. Phase Response Pitch Axis-Flexible (.005)

gain the attitude error during unloading of the wheels would exceed the accuracy requirements. However, unloading will ordinarily occur four times per day for about 12 seconds for each unload period. Exceeding the attitude accuracy for these short intervals should not be objectionable. Also additional or more optimum compensation can be used to reduce the amount of coupling.

The yaw axis was not simulated since there are no maneuvering requirements for yaw. Further, the gain can be reduced in yaw considerably without affecting the system performance, and the structural mode frequencies are higher.

Jet Control

During the station-keeping mode, the firing of the ΔV engine can cause misalignment torques of 0.05 ft. lbs. To counteract this torque the reaction jets will be thrusting. With a control torque of 0.075 ft. lbs the torque versus time on the vehicle could look as follows:

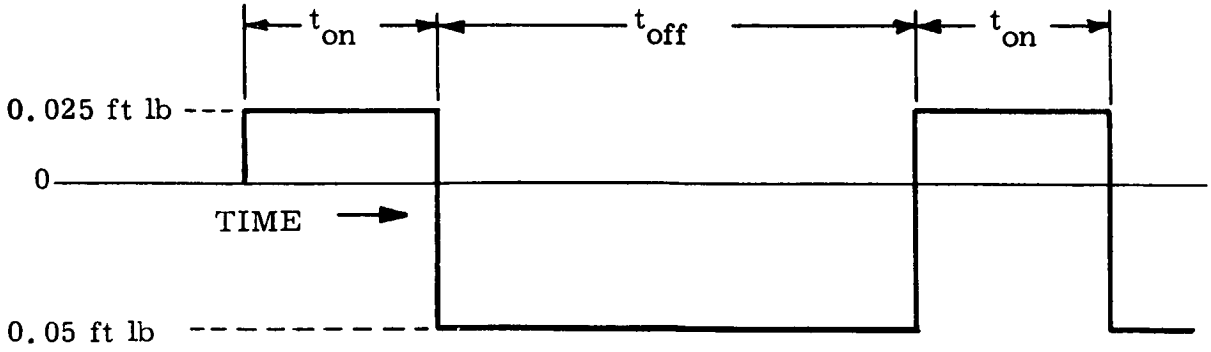

If the $t_{on} + t_{off}$ equals some multiple of the period of the bending mode, a possibility of exciting the structure exists. It is not likely that t_{off} will settle to a constant value due to the number of variables in the control system and the value of the disturbance torque itself. To protect against this possibility the time between consecutive pulses could be monitored by the computer. If two consecutive times were the same, the logic could command a momentary pulse during the off time. This would perturb the limit cycle and change the overall period length. Once this happens a series of pulses would occur before the system would settle down to a constant period. At this time, another perturbing pulse could be commanded.

A phase plane plot is shown in Figure 6-36, of attitude during a ΔV maneuver with a misalignment of 0.05 ft. lbs. In this example, five on times were required before the system settled down to a sequence of equal pulses. The time involved is approximately 16 minutes. With the longest ΔV thrusting time of 48 minutes, only several perturbing pulses need be applied.

6.7.4 Reliability

The reliability goal for the SCS is 0.9. A reliability block diagram is shown in Figure 6-37, incorporating the required redundancy to meet this goal.

To meet the overall system reliability requirements, the star tracker is divided into two parts, power supply and signal electronics. Standby redundancy is provided for each section. The quoted failure rate is 0.649 per cent per 1000 hours. The tracker is divided into sections with failure rates of 0.337 and 0.312. The resultant reliability for a two-year period is 0.997.

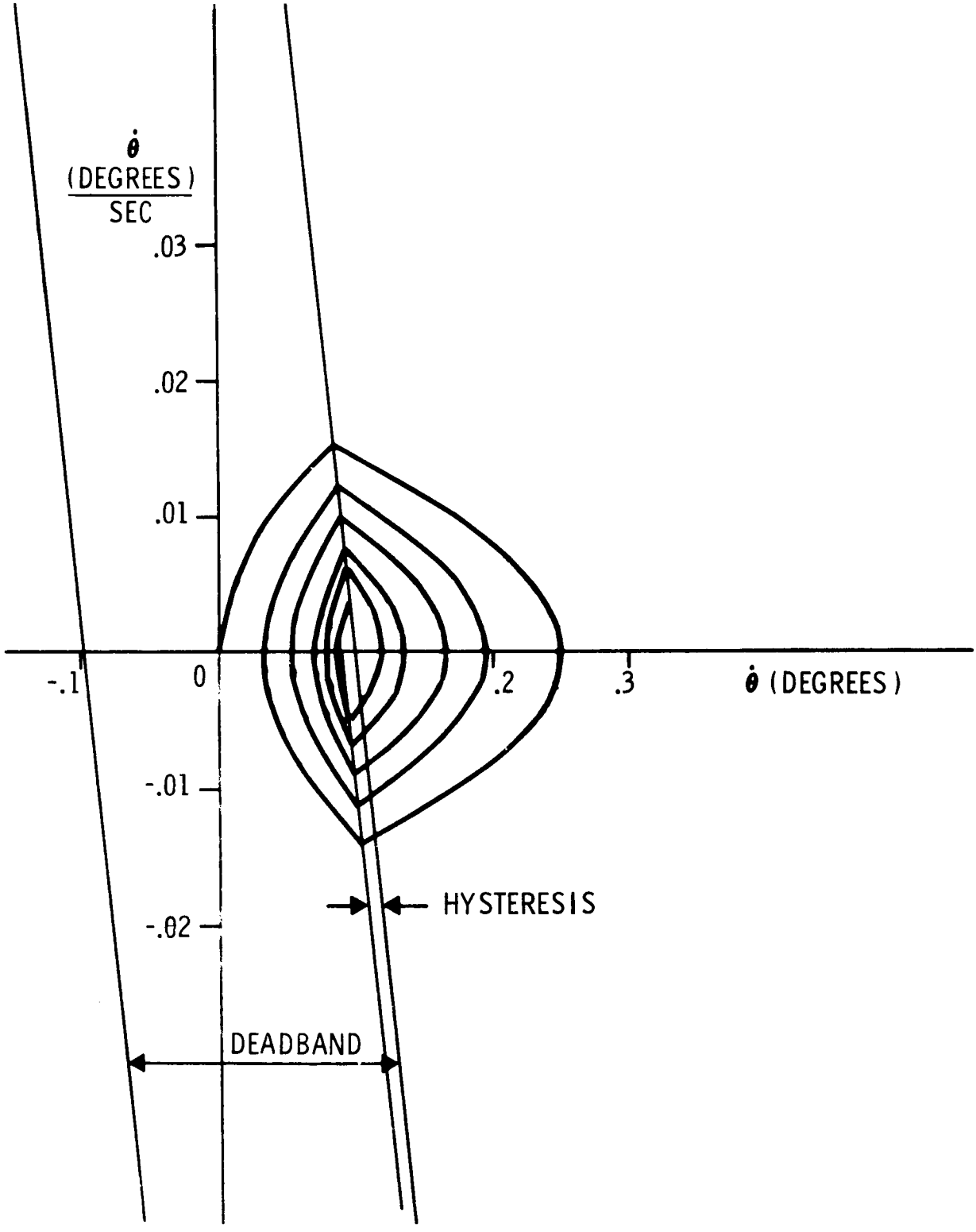

Figure 6-36. Phase Plane Plot Attitude Control During Station Keeping

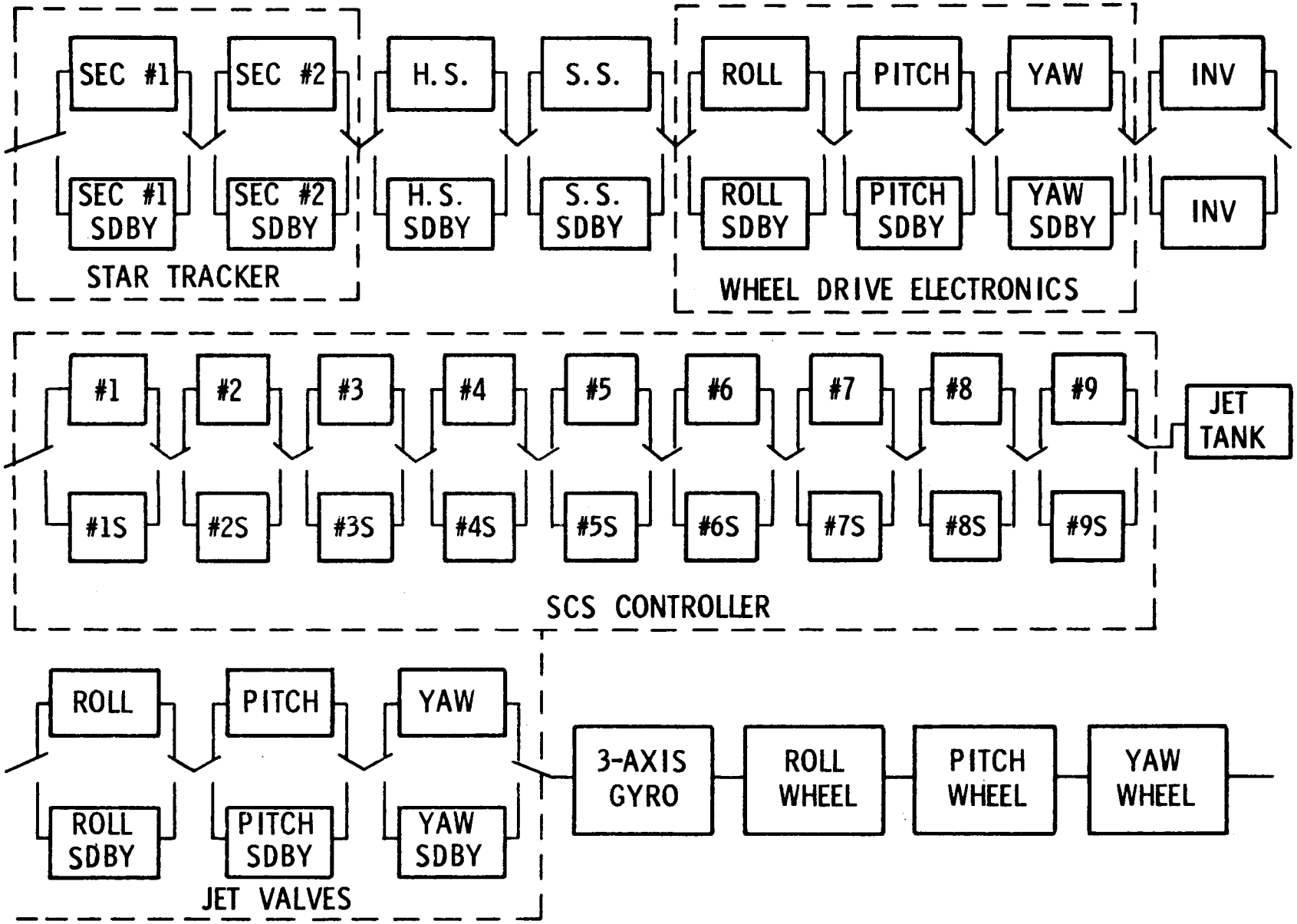

Figure 6-37. Reliability Diagram

Since the horizon scanner is not required to operate at all times, it can be de-energized. The total operating time is considered to be 1/2 of the total mission. The non-redundant reliability for one year is quoted as .91478 so standby redundancy is employed, resulting in .9928 for the horizon scanner.

The Acquisition Sun Sensors are simple photo cells with required electronics to complete the interface with the SCS controller. The sensors and electronics are switched as a block to the standby redundant sensors and electronics to provide a reliability of .9975 for a two-year period. A failure rate of .4 percent per 1000 hours was used for the sensors and electronics. The sensors are considered to be in use for the entire mission. The sensors are photo voltaic devices which require no power, consequently, cannot be de-energized. Also reverting automatically to sun oriented control in event of a malfunction is desirable and is the first step in the reacquisition sequence.

The gyros will be de-energized for most of the two-year period. An operating time of 500 hours was assumed. With a failure rate of 1.96 percent per 1000 hours, the reliability is .9934. Thus, redundancy was not provided for the gyros.

The Inertia Wheels are not redundant. They are ac powered similar to wheels developed for the NIMBUS, ADVENT, OAO and OGO satellites. These wheels have passed accelerated life tests to meet a three-year life requirement. A reliability of .999 is quoted for a wheel with a resultant of .997 for the three wheels.

The wheel drive electronics consists of the power transistors necessary to drive the wheels. Also included in this block for purposes of standby redundancy is the wheel unload electronics. A failure rate of .4 percent per 1000 hours is used for each axis. Providing standby redundancy in each axis results in a reliability of .9925.

Since the jets are being used primarily to unload the wheels, the firing time will be relatively long (compared to limit cycle control). With wheels as the prime means of control, the number of jet actuations will be much less. To achieve a reliability of .9796, standby redundant jet valves are provided.

The SCS Controller is broken up into nine sections with standby redundancy provided for each section. With a failure rate of .6 percent per 100 hours for each section the reliability is .9515 for two years.

The inverter is a solid state unit providing 400 cps power for driving the inertia wheels. Interlocks will be provided to prohibit more than one wheel from being unloaded at a time and overloading the inverter. A redundant standby inverter is required to achieve the reliability of .9975. The failure rate used for an inverter is .4 percent per 1000 hours.

A total system reliability of .902 is achieved with the above configuration. No attempt has been made at this time to determine reliability based on use of alternate modes. The horizon scanner can be considered a backup to the monopulse signal and the gyros for going to and holding an offset point. Other alternate modes such as wheels backing up the reaction jets or vice versa may also be deserving of consideration.

A tabulation of the reliability for each component is summarized in Table 6-10.

Table 6-10. System Reliability

System Component	Number of Units	Operating Time (hours)	Reliability
Polaris Star Tracker	2 (1 Stby)	17, 520	.997
2-Axis Horizon Scanner (gimballed)	2 (1 Stby)	8, 760	.9928
Acquisition Sun Sensors	2 (1 Stby)	17, 520	.9975
3-Axis Gyro Package	1	500	.9934
Inertia Wheels	3	17, 520	.997
Wheel Drive Electronics	6 (3 Stby)	17, 520	.9925
Reaction Jet Subsystem	1 (Jets Stby)	17, 520	.9796
SCS Controller	2 (1 Stby)	17, 520	.9515
Inverter	2 (1 Stby)	17, 520	.9975
			System Rel. .902

6.8 SYSTEM PHYSICAL DESCRIPTION

The weight, volume and power characteristics of the SCS are shown in Table 6-11

Table 6-11. SCS PHYSICAL CHARACTERISTS

SCS Components	Weight (pounds)	Power - (watts) Peak	Average	Volume (cu. in.)
Polaris Star Tracker	20	20	4	1000
Two-axis Horizon Scanner (electronic gimballed)	18	6	3	500
Acquisition Sun Sensors	3	-	-	28
Three-axis Gyro Reference	10	30	20	300
Inertia Wheels (Roll, Pitch, Yaw)	34.2	60	21	1060
Wheel Drive Electronics	5	12	4.5	140
Reaction Jet Subsystem	54	20	0.5	2800
SCS Controller	30	30	30	860
Inverter	18.6	20	5	520
Totals	192.8	198	88.0	7208

References

1. "Space Debris Hazard Evaluation," Davidson and Winslow, NASA TN-D-1105, December 1961.

2. "Distribution of Small Interplanetary Dust Particles in the Vicinity of the Earth," McCracker and Alexander, NASA TN-D-1349, July 1962.

3. "Attitude Perturbation of Space Vehicles by Meteoroid Impacts," G.J. Cloutier, AVCO Corp. Wilmington, Massachusetts.

4. "Meteoroids and Dust," F.L. Whipple, Symposium on Bio-astronautics and the Exploration of Space, December 1965.

5. "Preliminary Survey of Meteoroid Effects on Space Vehicles," North American Aviation, SID 62-658-2, 1962.

6. "The Radiation Environment", Fourth Weather Group, United States Air Force, 4WGP-80-6-1; 1 June 1965.

7. "Handbook of Chemistry and Physics", 39 Edition, Chemical Rubber Publishing Co.

8. "The Solar System", Vol. I "The Sun"; Edited by G. P. Kuiper, University of Chicago Press, 1953.

9. "The Physics of Solar Flares", AAS-NASA Symposium, NASA SP-50 Goddard Space Flight Center, 1963.

10. "Medium and High Altitude Horizon Sensor", Advanced Technology Division of American Standard, ATD-TM-102, 31 July 1965.

11. "Description of Earth Sensor Unit (MOGO) for High Altitude Horizon Sensing, 18,000 to 100,000 NM Useful Orbital Range", Advanced Technology Division of American Standard, ATD-R-1398, 1 June 1966.

12. "Reaction Wheel Catalogue", Bendix Engineering Report #6311-5, 1 November 1965.

APPENDICES

In the early conceptual phases of this study, numerous alternate vehicle and control concepts were considered. To permit a final configuration selection, preliminary systems analyses of the alternate concepts was performed. This preliminary data, which was used in the initial trade-off studies, provides much of the generic background which lead to the recommended system. However, the data was generated to indicate relative magnitudes of quantities for trade-off purposes and hence simplifying assumptions were permitted. The analyses were rerun in considerably more detail for the recommended configuration.

The preliminary configuration data used in the initial trade-off studies is presented in these Appendices to provide the background data on each of the alternate configurations considered in the study.

It is noted that rotating sub-oriented solar paddles were assumed for configuration #1 to #14; while fixed solar paddles were studied for the final configurations #17 and #18.

APPENDIX 6A

PRELIMINARY CONTROL TORQUE AND IMPULSE REQUIREMENTS

Control Impulse

Initial control impulse requirements for four alternate vehicles with either a wire mesh or solid surface antenna configuration was computed to illustrate the relative impulse requirements for each configuration. These initial calculations were performed assuming a pure jet control system. The control impulse requirements shown in Table 6A-1 are based upon a preliminary disturbance torque model, limit cycle operation, initial orientation, offset pointing maneuvers and station keeping. These calculations assume a two-year mission and that all control impulse is provided by a mass expulsion system acting at selected moment arms for each candidate configuration.

In Table 6A-1 the estimates for the required impulse for maneuvering and maintaining the limit cycle are based on the following assumptions:

1) It was assumed that the limit cycle deadband was 0.02 degrees wide in roll and pitch and 0.1 degree in yaw.

2) It was assumed that the jets were sized and operated so as to cause an angular velocity in roll and pitch equal to the velocity in roll and pitch equal to the velocity that would result if the estimated disturbance torque acted during one pass through the deadband.

3) The limit cycle rate in yaw was assumed to be 1°/hr.

4) It was assumed that stationkeeping required 3-90° maneuvers.

This is required if the stationkeeping engine is located along the body z-axis, requiring 90° reorientiation to permit an appropriate station-keeping impulse.

5) It was assumed that offset pointing was required 100 times during the mission of two years and that the pointing was at the edge of the earth's disk. Also it was assumed that the offset pointing maneuver was done with rates of 1°/min in both pitch and roll.

6) Also it was assumed that the satellite would be required to track another satellite across the earth's disk 100 times during the two-year mission. It was assumed the tracking rate would be 0.123×10^{-3} rad/sec.

In this phase of the study, several alternate vehicle configurations are being considered. To assist in this design and selection, control impulse data is provided which parametrically relates the impulse per axis per year to the mission and vehicle configuration variables.

The control impulse required to perform a limit cycle operation in an undisturbed condition for a period of one year is shown in Figure 6A-1.

$$\text{Impulse/axis/year} = \frac{2tI\dot{\theta}^2}{10}$$

where:

$t = 31.5 \times 10^6$ seconds per year

I = Inertia, slugs-ft^2

l = moment arm, feet

$\dot{\theta}$ = limit cycle attitude rate, rad/sec

θ = deadband full width, rad

For these calculations, I/l was assumed to be 1×10^{-3} and the impulse is derived for varying limit cycle rates and deadband widths . A change in I/l would result in a proportionate change in the impulse required.

Figure 6A-2 illustrates the impulse required per axis per year to balance a steady state disturbance torque for various control moment arms. The steady state disturbance torque is defined as the average torque over a period of time which has the same integrated area as the calculated disturbance toque model. The impulse equation is as follows:

$$\text{Impulse/axis/year} = \frac{tT}{l}$$

where:

T = steady state disturbance torque

To determine the control impulse required to perform close-earth satellite tracking and offset pointing maneuvers, several assumptions are made. A complete tracking maneuver will require slewing in both pitch and roll from the vertical to the horizon (8.5°), then across the full earth disk (17°) and then back to local vertical. This will require six pulses of the jets to impart the necessary angular rate in each axis. Offset pointing will require a total of four pulses per cycle. The time between pulses

will vary, depending upon the actual angle to be slewed in each axis. For simplicity it is assumed that the tracking rate is a constant and 30 minutes is allowed for the 17° maneuver (34°/hr.). Also it is assumed that this same rate is sufficient for the initial maneuvers to the edge of the disk. To impart the required rate, the impulse in each pulse is given by:

$$\text{Impulse per pulse} = \frac{\dot{\Theta} I}{1}$$

For the tracking maneuver, six pulses are needed. Hence the total impulse per axis per year (shown in Figure 6A-3) is the product of the impulse per pulse times six pulses times the number of maneuvers per year.

$$\text{Impulse/axis/year} = \frac{6N\dot{\Theta} I}{1}$$

The impulse required for offset pointing maneuvers can be obtained by reducing the data shown in Figure 6A-3 by a factor of 2/3.

SYSTEM CONFIGURATION	INITIAL ORIENTATION			REQUIRED REACTION JET IMPULSE LB-SEC (2 yrs) DISTURBANCE TO UL												STATIONKEEPING	ATTITUDE MANEUVERS (2yrs)		
				ROLL		PITCH		YAW		LIMIT CYCLE (2 yrs) ROLL		PITCH		YAW			ROLL	PITCH	YAW
	ROLL	PITCH	YAW	Solid	Mesh	Solid	Mesh	Solid	Mesh	Solid	Mesh	Solid	Mesh	Solid	Mesh				
SK-513-9																			
SK-513-10	45.9	29.3	28.4	240	108	400	126	0	0	1920	479	2540	670	780	780	530	608	286	
SK-513-11	44.9	31.7	42.4	1285	494	2090	830	0	0	5600	2700	13200	5100	1170	1170	530	594	309	
SK-513-12	45.9	29.3	28.6	55	22	100	26	0	0	450	181	185	76	780	780	528	608	286	
SK-513-13	11.3	7.1	21.3	950	715	1190	365	0	0	6600	1700	7600	2340	585	585	315	156	69	

TABLE 6A-1

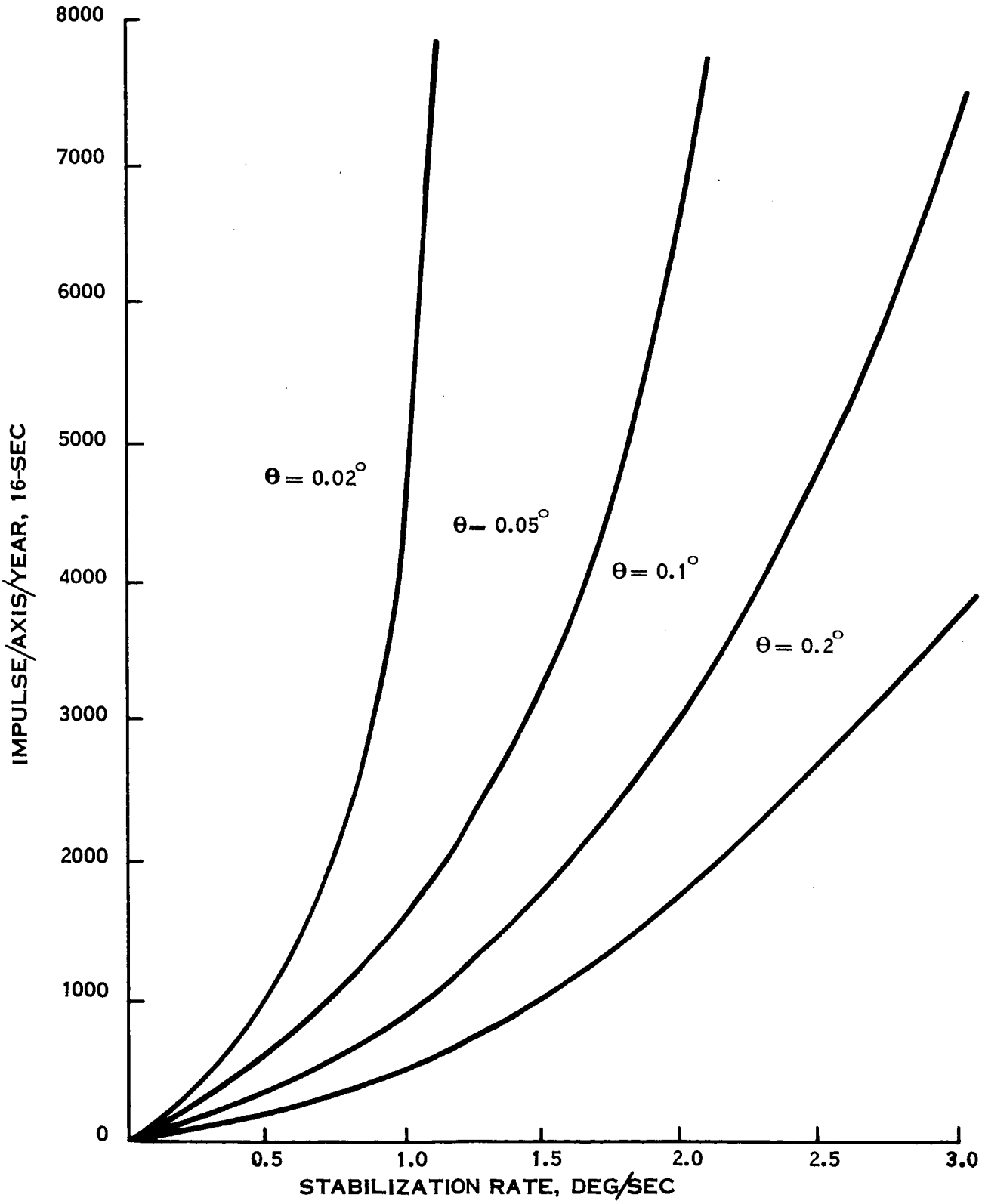

Figure 6A-1. Limit Cycle Impulse Requirements

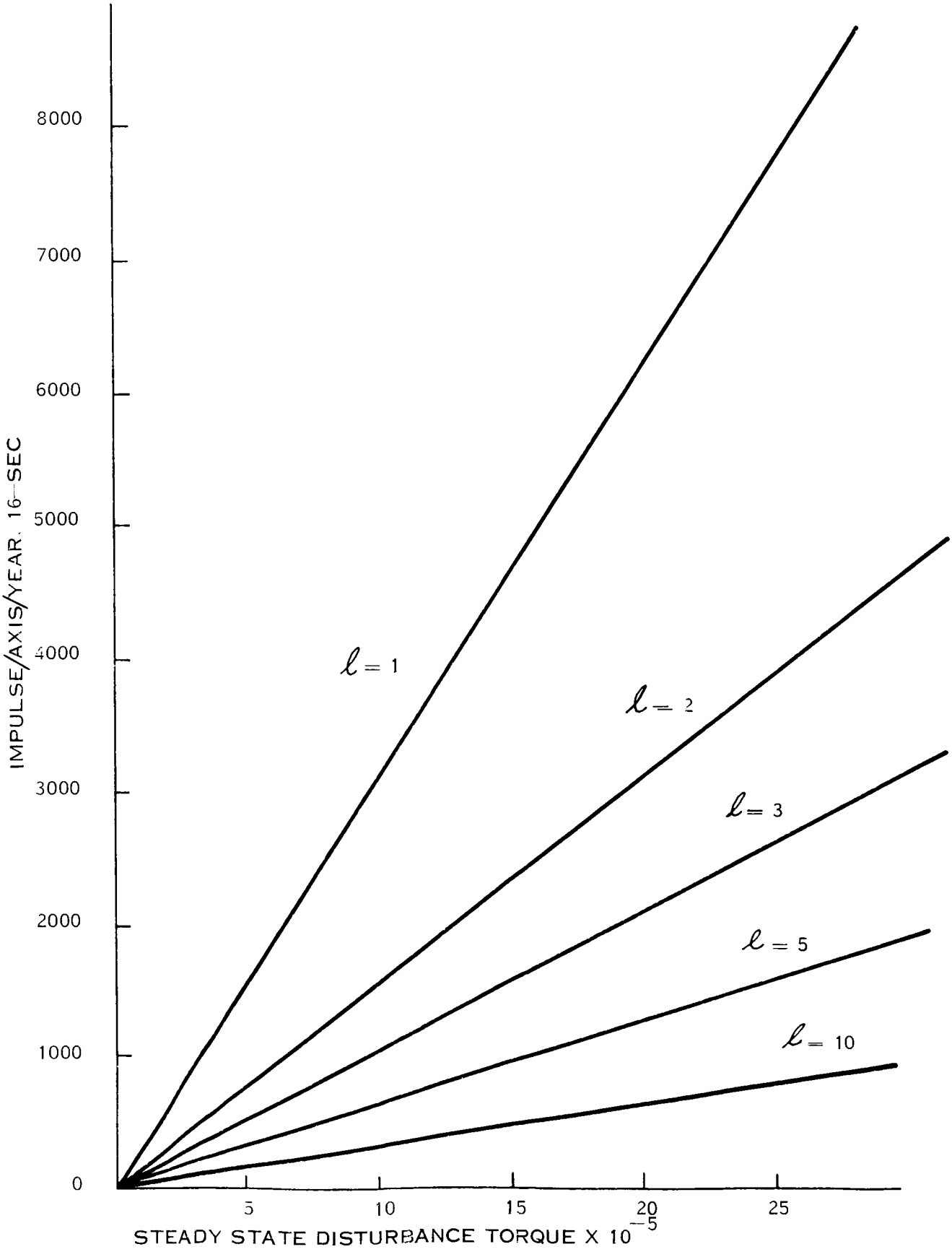

Figure 6A-2. Disturbance Torque Impulse Requirements

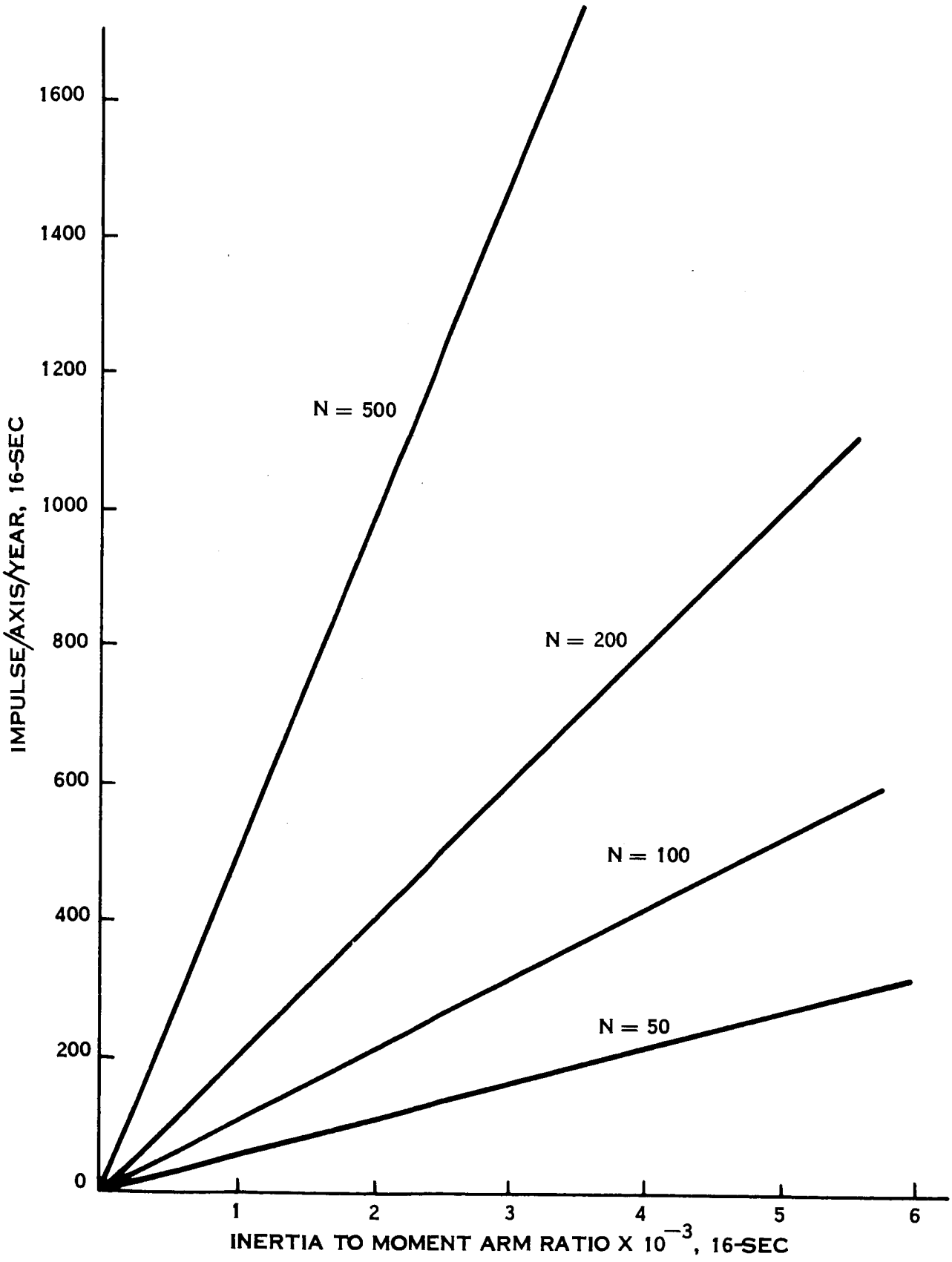

Figure 6A-3. Maneuver Impulse Requirements

APPENDIX 6B

PRELIMINARY REACTION JET CONSIDERATIONS

Reaction Control Jets

To initiate a preliminary reaction jet trade-off study, a set of preliminary bounds were placed on the control system requirements. These bounds were based upon the impulse requirements for the four initial vehicle configurations discussed in Appendix 6A and assumed a pure jet control system.

This discussion presents the results of a preliminary study of candidate mass expulsion torquing systems as applicable to the ATS-4 mission. Cold gas, hydrazine, hypergalic, subliming solid and heated ammonia systems are evaluated and their definitive trade-off parameters determined.

For this reaction jet system trade-off study the following ground rules are assumed:

Minumum Impluse Bit	.001 lb_f-sec
Total Impulse Range*	4000-32000 lb_f-sec
Thrust Level	0.1-1.0 lb_f
Rise-Decay Time	Assumed Not Critical
Pulse Repeatibility	Within 5% After 2 Years
Limit Cycle Duty Cycle	10-25ms On-Time Every 300-700 sec.
System Weight (Max)	125 lbs
System Volume	Assumed Not Critical
Power Limit	20 Watts

System Life*	Up to 500,000 Pulses Per Axis
System Reliability	.99 For 2 Years

From Figures 6B-1 and 6B-2 (Reference 1), it is apparent that for the thrust levels, duty cycle and total impluse range contemplated, the following systems are worthy of investigation:

1. Subliming Solids
2. Vaporizing Liquids
3. Electro-chemical
4. Cap Pistol
5. Cold Gas
6. Liquid Bipropellants
7. Monopropellant Plenum
8. Liquid Monopropellant

The subliming solids, vaporizing liquids and the electro-chemical systems may be eliminated from consideration because of the very high power requirements, ranging from 1,000 to 15,000 watts for each pound of thrust generated (Reference 1 and 2). The applicable thrust range for electro-chemical systems is from 1×10^{-5} to .1 lb_f. The GE resistance jet thruster which is in the electro-

* The range of total impulse and pulse lifetime required is dependent upon whether reaction wheels are used to balance the disturbance torques and remove the limit cycle operation.

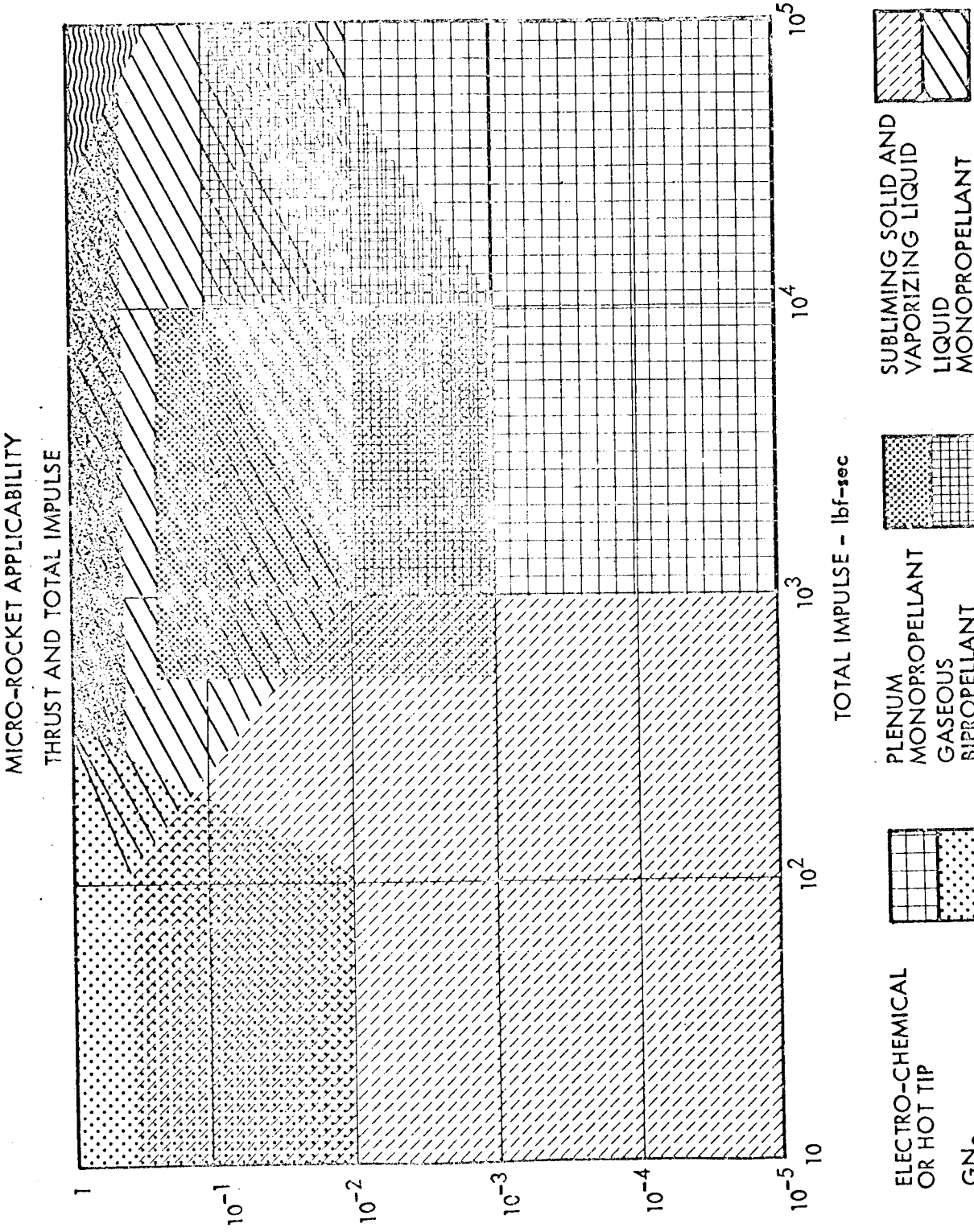
MICRO-ROCKET APPLICABILITY
THRUST AND TOTAL IMPULSE
1
10^{-1}
10^{-2}
10^{-3}
10^{-4}
10^{-5}
10
10^{2}
10^{3}
10^{4}
10^{5}
TOTAL IMPULSE - lbf-sec
ELECTRO-CHEMICAL OR HOT TIP
GN_2
LIQUID BIPROPELLANT
PLENUM MONOPROPELLANT
GASEOUS BIPROPELLANT
CAP PISTOL
SUBLIMING SOLID AND VAPORIZING LIQUID
LIQUID MONOPROPELLANT

Figure 6B-1.

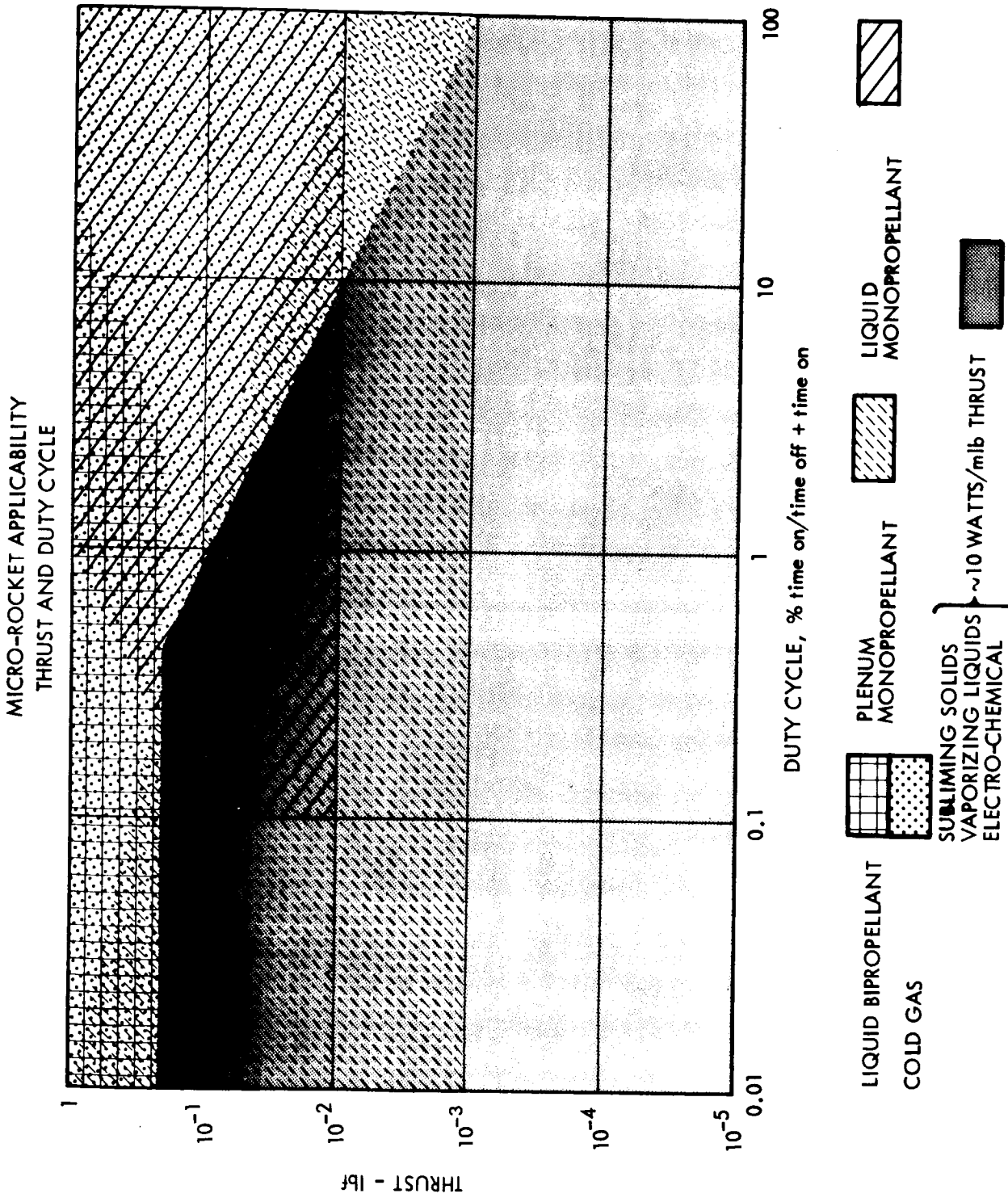
MICRO-ROCKET APPLICABILITY
THRUST AND DUTY CYCLE
THRUST - lbf
1
10^{-1}
10^{-2}
10^{-3}
10^{-4}
10^{-5}
0.01
0.1
1
10
100
DUTY CYCLE, % time on/time off + time on
LIQUID BIPROPELLANT
COLD GAS
PLENUM MONOPROPELLANT
SUBLIMING SOLIDS
VAPORIZING LIQUIDS
ELECTRO-CHEMICAL
~10 WATTS/mlb THRUST
LIQUID MONOPROPELLANT

Figure 6B-2.

chemical category, has a power requirement of ~ 1300 watts/lb of thrust generated for a single jet, and ~ 450 watts/lb of thrust generated for a cluster of five jets. The thrust range for this resistance jet is currently .015 to .05 lb_f. The specific impulse varies from 150 to 250 lb_f-sec/lb_m depending upon chamber pressure and gas temperature (Reference 3).

The cap pistol which is still under development, can provide 200 lb_f-sec/lb_m and repeatible impulse bits, but the disadvantages of its mechanical complexity and low volumetric efficiency for cap storage are too excessive to permit further consideration for ATS-4.

The cold gas systems which meet the thrust level and duty cycle requirements do not meet the maximum weight requirement of 125 pounds. Figure 6B-3 shows estimated system weight as a function of total impulse for the Freon 14 and nitrogen cold gas systems.

From Figure 6B-2, it appears that liquid bipropellants could be applicable from the duty cycle and thrust level considerations. Unfortunately, for short pulse widths (10-50ms) propellant utilization is quite poor due to mixing problems in the chamber. This eliminates any weight advantage that the system may have had over a liquid monopropellant system. Also, the mixing problem causes poor pulse repeatibility for short pulse widths. Also, from a reliability standpoint, the bipropellant system is not as good as the monopropellant system. A relative indication is given in Figure 6B-4 (Reference 4).

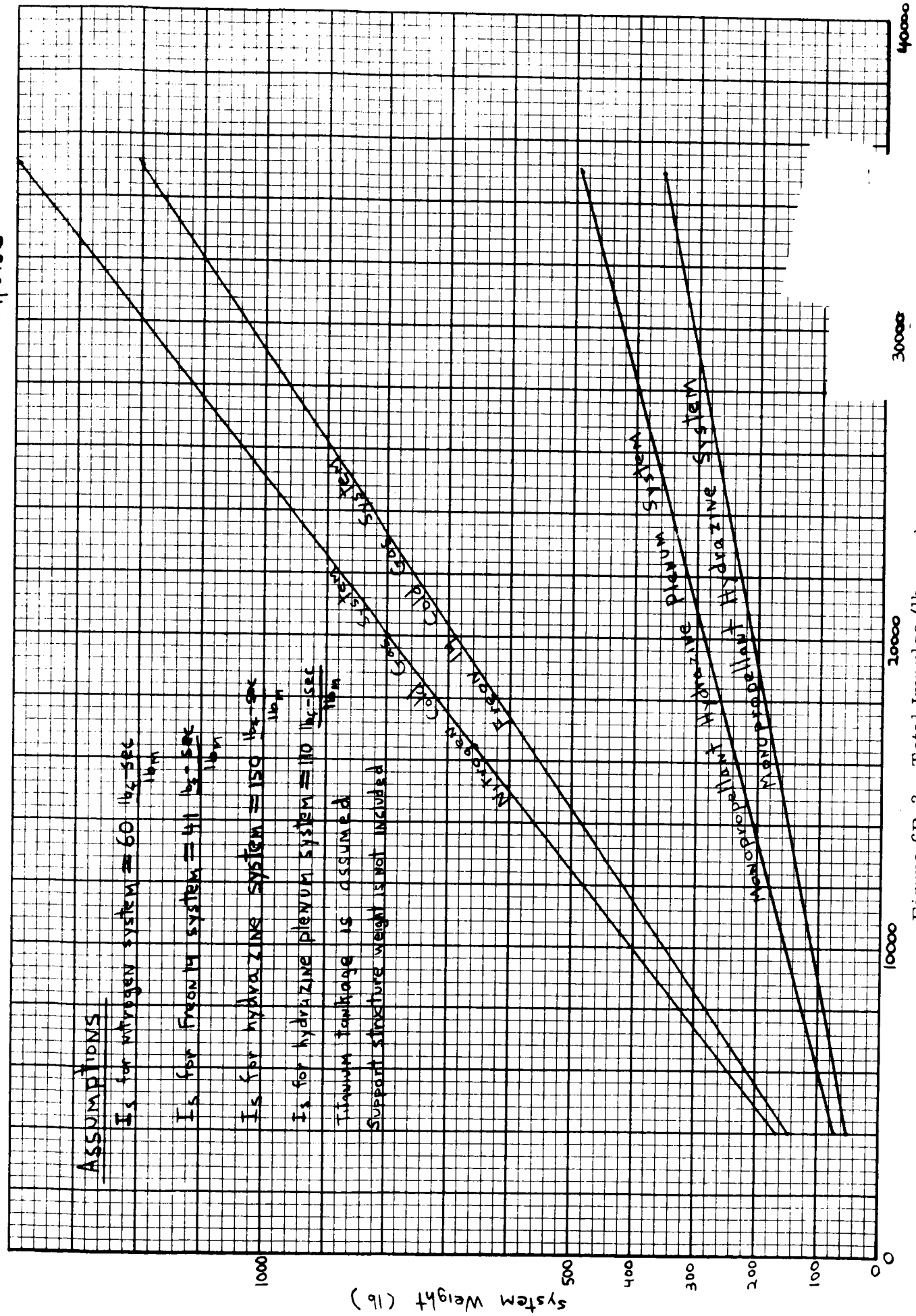

Figure 6B-3. Total Impulse (lb_f-sec)

	RELATIVE FAILURE RATE	RELATIVE COST
BIPROP.	3.53	10.0
MONO.	2.24	2.0
COLD GAS	1.0	1.0

Figure 6B-4.

Monopropellant hydrazine reaction jet systems can be divided into two categories: a) Monopropellant Plenum and b) Liquid Monopropellant.

The monopropellant plenum reaction jet system shown schematically in Figure 6B-5 looks quite attractive from the duty cycle, thrust level, total impulse, and impulse bit reproducibility aspects. Compared with a liquid monopropellant system, the major advantages are rapid response time ($\sim$ 10ms from signal to 90% thrust) and lower thrust levels (to $1 \times 10^{-3} lb_f$) while the chief disadvantages are additional weight as seen from Figure 6B-3, and the requirement of some form of thermal control for the plenum chamber. Since response time is assumed not to be critical for the ATS-4 application, it is recommended that this system be considered further only if; (1) the thrust requirements drop below .05 lb_f, (2) response time requirements are in the 5 to 15 ms range, and (3) the total impulse needed is less than 7,000 lb_f-sec. However, if the rise time becomes less critical and the minimum pulse width increases, as would be the case for a wheel unloading made, the liquid direct feed hydrazine monopropellant would be most attractive.

The liquid monopropellant system shown schematically in Figure 6B-6 is quite attractive from the thrust level and total impulse considerations, but is slightly less attractive from the duty cycle aspect. It is currently estimated that this system could supply a total impulse of 10,000 lb-sec and still be within the maximum weight limitation of 125 lb. When the system is compared with the monopropellant plenum system, it offers a weight advantage as mentioned

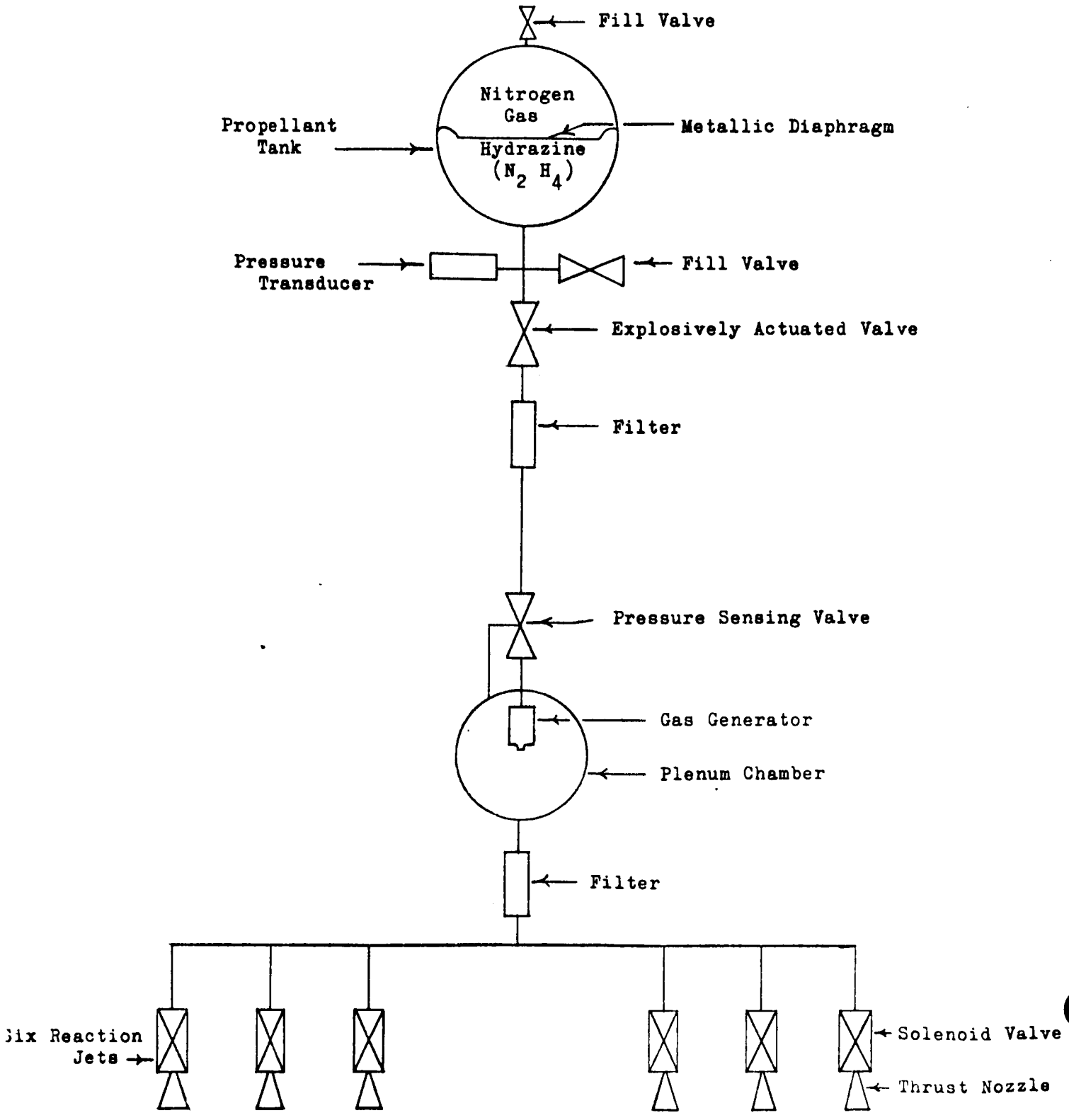

Figure 6B-5. Hydrazine Plenum System Schematic

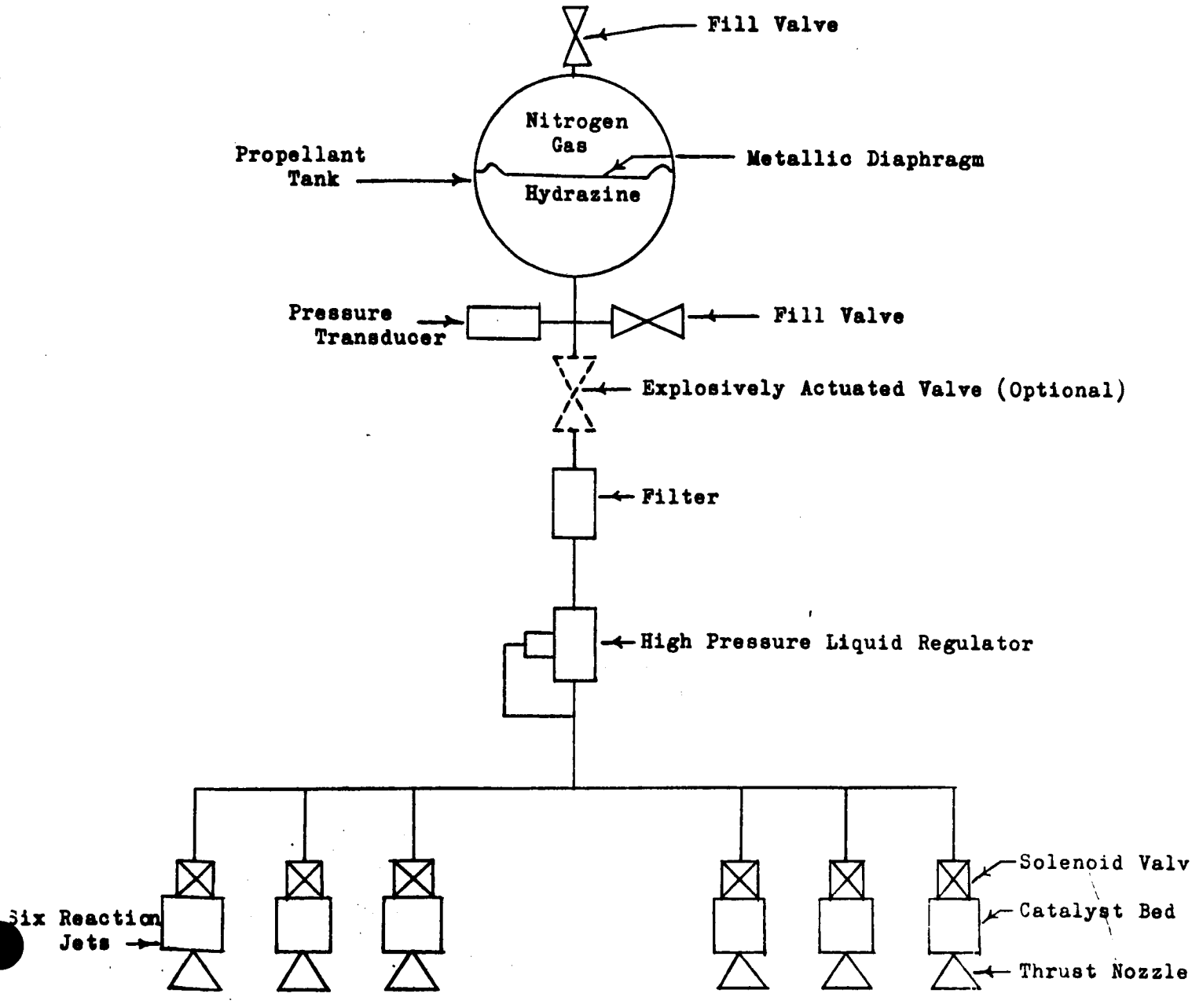

Figure 6B-6. Liquid Hydrazine System Schematic

previously and the possibility of a slight improvement in reliability.

In view of reliability improvement, a modification could be made to the system which would prevent propellant depletion due to sudden leakage across reaction jet solenoid valves in the event of a valve failure during the mission. This could be accomplished by installing normally-open explosively-actuated valves in series upstream of the solenoid valves. A concept which has been employed previously to reduce the probability of a complete system failure has been the use of dual systems which are two independent half-systems. However, this scheme involves a slight weight penalty.

It is assumed for this study that the specific impulse of the liquid mono-propellant hydrazine system will be 150 lb_f-sec/lb_m. This assumption may be marginal for cold bed pulse widths of 10 to 50ms. There may be a good possibility of increasing the specific impulse by using some passive technique of bed heating which employs radioistopes. This would also improve the pulse reproducibility by decreasing bad temperature variations which are a function of duty cycle. Hot bed pulse bit reproducibility has been reported by Rocket Research Corporation to be within 2% for short pulse widths of $\sim$ 25ms. Although it is not known for certain whether pulse bit reproducibility can be held within the 5% limit after two years, it is believed that this requirement should be achievable. The required minimum impulse bit of .001 lb_f-sec can be attained with an engine in the .05 to .1 lb_f thrust range. The smaller engine which would operate for a longer time to produce the minimum

impulse bit would be preferable from the standpoint of increased efficiency.

Hydrazine engines have currently been pulsed from 60,000 to 120,000 times with total on-times of 6,000 to 25,000 seconds (Reference 4 and 5). If it is assumed that each jet during limit cycle operation will fire once every 300 seconds for a 25 ms period during a two year span, then the on-time will amount to 5250 sec. If it is also assumed that the limit cycle operation accounts for one-half of the total firing time per thruster, the total firing time will be 10,500 seconds which is well within current limits.

To date, hydrazine engines have been tested for up to 120,000 pulses without a valve failure. Since the ATS-4 reaction jet system may require a pulse lifetime of up to 500,000 pulses or even one million pulses, serious consideration must be given to methods of reducing the number of pulses or providing a satisfactory valve design. It appears that standby redundancy alone may not be able to satisfy the pulse lifetime requirements.

As a result of this study, the liquid monopropellant hydrazine reaction jet system is recommended for primary consideration. If the thrust levels required are reduced to less that 0.02 to 0.05 lb_f, the hydrazine plenum system should be considered.

Reaction Jet Thrust Levels

This portion of the study presents the definition of the jet thrust levels, pulse width, and impulse requirements in the configuration which does not

employ inertia wheels or any passive means of attitude control. The data included therefore provides a basis for trade-off comparison between five candidate vehicle configurations, each with a wire mesh or a solid antenna surface.

The jet thrust level is determined by two opposing requirements:

a) The resulting vehicle torques must be high enough, so that:
   1) Acquisition of references can be accomplished in the field of view of the sensor and in the required time
   2) Maneuvers can be made in the required time
   3) Attitude control can be maintained in the presence of external torques
b) The resulting vehicle torque must be low enough so that low rates may be maintained in the limit cycle, thus avoiding excessive fuel consumption.

If one thrust level cannot meet both of the above requirements then two thrust levels must be used. If the vehicle is operating in the presence of disturbance torques and the total impulse is largely due to disturbance torque then the second consideration is not as important in determining thrust size. In other words, a large jet thrust with short pulse length is just as effective as a small jet thrust with a long pulse length in removing vehicle momentum caused by disturbance torques. With some types of systems the specific impulse decreases with a pulse length decrease, and thus efficiency may suffer with short pulses, so this must also be considered.

Preliminary calculations of thrust level and pulse width have been made and the results are shown on the attached charts. The approach used was to determine the minimum acceptable level for acquisition and for controlling in the presence of the external torque due to misalignment of the stationkeeping engines.

A search rate of 0.3 degree per second was used for each axis with the restriction that acquisition should be accomplished within 1/2 of the total field of view of the sensor. Using 1/2 the total field allows for variations in search rate, thrust levels. etc.

The acquisition thrust levels for each of the configurations were used for calculating impulse and time for the remaining control modes. A 0.015 second pulse width was selected for limit cycle control and the total impulse (upper set of numbers on chart for limit cycle mode) for roll and pitch axis are considerably less than calculated previously (lower set of numbers on the chart) where a limit cycle rate was assumed to determine total impulse. The resulting limit cycle rates are much smaller with the acquisition thrust levels and the pulse width selected. The yaw total impulse (upper set of numbers) is larger than previously (lower set of numbers) calculated. Here the resulting limit cycle rate was higher than previously assumed.

The total impulse for limit cycle operation in yaw can be reduced by reducing the search rate for acquisition of Polaris. This will reduce the thrust level which in turn reduces the limit cycle rate and the total impulse required.

The results of calculations for reducing the search rate by one half (0.15°/sec) are tabulated below.

Configuration	Yaw Thrust Level (pounds)	Total Impulse Yaw Limit Cycle (lb-sec)
SK-513-10	.046	74
SK-513-11	.069	115
SK-513-12	.046	74
SK-513-13	.035	55
SK-513-14	.046	73

The method of computation and rationale are discussed by control mode in the following paragraphs.

1. Initial Tumble Arrest - Because the rates are being damped to zero, the impulse per pulse is considered to be the same as the total impulse. To determine the pulse width or the jet on time the impulse per pulse is divided by twice the thrust size for yaw (jets are firing in couples) and the thrust size for roll and pitch (single jets).

2. Orientation - The thrust size was determined from the following formulas:

$$F = \frac{I\dot{\theta}^2}{4l\theta} \text{ (yaw)} \qquad F = \frac{I\dot{\theta}^2}{2l\theta} \text{ (roll pitch)}$$

where:

F = Jet thrust in pounds
$\dot{\theta}$ = Search rate in radians/sec
l = Moment arm - feet
θ = One-half the field of view - radians

The impulse per pulse was determined by dividing the total impulse by 2; one pulse to accelerate the vehicle and the second to decelerate

the vehicle. The pulse width or jet on time per pulse is determined by dividing impulse per pulse by twice the yaw thrust size and by pitch and roll size as given.

3. Limit Cycle Operation - The total impulse was found by using thrust level determined above with a minimum pulse width of 0.015 seconds.

$$\text{lb sec} = \frac{2PlF^2 \quad t_{on}^2}{\Theta_{DB} \quad I} \quad \text{(yaw)}$$

where $$\text{lb sec} = \frac{PlF^2 \quad t_{on}^2}{2\Theta_{DB} \quad I} \quad \text{(roll and pitch)}$$

P = Total mission period - 63.1×10^6 seconds
l = Jet moment arm - feet
F = Jet thrust - pounds
t_{on} = Minimum pulse width - 0.015 seconds
Θ_{DB} = Width of deadband - radians
I = Inertia of vehicle - slug-ft^2

Impulse per pulse was found by multiplying pulse width by twice the thrust level for yaw and by the thrust level in roll and pitch.

The lower set of numbers on the charts shows thrust level and impulse per pulse using the total impulse as determined previously with the minimum pulse widths.

4. Balance Disturbance Torques - The same size pulse width and jet levels were used for this mode.

5. Offset Pointing - Four pulses were considered for each offet pointing maneuver with a total of 100 offset points, so impulse per pulse was

found by dividing total impulse by 400. Pulse width was found by dividing impulse per pulse by twice the thrust for yaw and by the thrust level for roll and pitch.

6. Satellite Tracking - The impulse per pulse was determined in the same manner as offset pointing. The number indicated under thrust size is the thurst required to accelerate the satellite to track a low orbit satellite. It is expected that the acquisition thrust sizes determined above will also be satisfactory for this mode when using pulse widths of 0.015 seconds. With these thrust sizes the rate increment per pulse is 1.2 x 10-6 rad/sec.

7. East-West Station Keeping - For east-west station keeping a misalignment of .25 degrees is assumed for the two jets. One of the jets is the pitch jet used for attitude control. Misalignment is assumed into the roll and yaw axes with moment arms equivalent to the pitch jet moment arm.

$$\text{Yaw thrust requirements} = \frac{2(\text{thrust level-pitch})(.00435)}{2\ l}\ l_{cg}$$

$$\text{Roll thrust requires} = \frac{2(\text{pitch thrust level})(.00435)}{l}\ l_{cg}$$

where:

l_{cg} = Pitch jet moment arm
l = Roll or yaw moment arm

The pulse width shown in Tables 6B-1 through 6B-10 is the time for the jets of the size indicated which are just large enough to balance the torques from the station keeping engines. Using the thrust levels determined for acquisition will result in a series of short pulses.

8. 90° Roll for N-S Station Keeping - The maneuver rates are the same as for orientation so the same jet size and pulse width are adequate. Impulse was determined to start and stop the maneuver at 90 degrees and then return to normal orientation.

9. Attitude Control During Station Keeping Thrust - To determine thrust levels, and impulse the following assumptions were made:

a. Station keeping engine thrust - 5 pounds
b. Thrust time - 10 minutes
c. Misalignment - 0.25°
d. Moment arm (distance of engine from cg)

1.	SK-513-10	6 feet
2.	SK-513-11	12 feet
3.	SK-513-12	10 feet
4.	SK-513-13	2 feet
5.	SK-513-14	4.7 feet

The misalignment was assumed to act about an axis at 45° to the pitch and roll axis . The attitude control thrust is then found from

$$F = \frac{(T_{sk})(\text{sine misalignment angle})(\text{sine } 45°)\, l_{cg}}{l}$$

Where:

T_{sk} = Thrust level of station keeping engine

F = Thrust level of attitude control jet

l_{cg} = Distance between cg and station keeping engine

l = Moment arm of attitude control jet

The thrust levels are less than those determined for orientation control, thus the thrust level chosen for orientation control will be satisfactory.

The impulse per pulse will also be modified since by using larger jets than actually required a series of short pulses will occur in balancing the misalignment torque.

l). Antenna Pattern Study Maneuver - A rate of 0.1 deg/sec was assumed. This is 1/3 of orientation rates. Jet sizes chosen above are adequate. Impulse was determined to start the stop the maneuver for a total of 50 maneuvers.

CONTROL MODE	TOTAL IMPULSE (LB.-SEC)			IMPULSES PER PULSE(LB-SEC)			THRUST SIZE (LB)			PULSE WIDTH (SEC)		
	ROLL	PITCH	YAW	ROLL	PITCH	YAW	ROLL	PITCH	YAW	ROLL	PITCH	YAW
1. INITIAL TUMBLE ARREST	38.1	24.2	23.5	38.1	24.2	23.5	.06	.038	.185	635	638	63.5
2. ORIENTATION Assume 50 times	400	255	245	4.	2.6	2.5	.06	.038	.185	66.7	67.2	6.6
3. LIMIT CYCLE OPERATION	96 1920	66 2540	1185 780	9×10^{-4} 4×10^{-3}	5.7×10^{-4} 3.7×10^{-3}	5.5×10^{-3} 4.5×10^{-3}	.06 .266	.038 .245	.185 .15	.015	.015	.015
4. BALANCE DISTURBANCE TORQUES	240	400	0	9×10^{-4}	5.7×10^{-4}	0	.06	.038	0	.015	.015	0
5. OFFSET POINTING 100 maneuvers	91	58	0	.23	.15	0	.06	.038	0	3.8	3.8	0
6. SATELLITE TRACKING 100 maneuvers	37	24	0	.09	.06	0	$.2 \times 10^{-3}$	$.13 \times 10^{-3}$	0	.015	.015	0
7. EAST, WEST STATIONKEEPING 8 corrections	2.7	530	2.6	.34	66.3	.32	39.4×10^{-5}	.038	18.4×10^{-5}	873	873	873
8. 90° ROLL FOR N-S STATIONKEEPING 6 maneuvers	96	0	0	4.	0	0	.06	0	0	66.7	0	0
9. ATTITUDE CONTROL DURING STATION-KEEPING THRUST	37.8	32.4	0	6.3	5.4	0	.021	.018	0	600	600	0
10. ANTENNA PATTERN STUDY MANEUVERS 50 maneuvers	134	85	82	1.34	.85	.82	.06	.038	.185	22.3	22.4	2.2
$I_x = 3108$ $l_x = 4.2$ $I_y = 2424$ $l_y = 5.0$ $I_z = 2115$ $l_z = 4.5$												

CONFIGURATION: SK-513-10 (solid)

TABLE 6B-1

CONTROL MODE	TOTAL IMPULSE (LB-SEC)			IMPULSE PER PULSE (LB-SEC)			THRUST SIZE (LB)			PULSE WIDTH (SEC)		
	Roll	Pitch	Yaw	Roll	Pitch	Yaw	Roll	Pitch	Yaw	Roll	Pitch	Yaw
1. INITIAL TUMBLE ARREST	38.1	24.2	23.5	38.1	24.2	23.5	.06	.038	.185	635	638	63.5
2. ORIENTATION 50 Times	400	255	245	4	2.6	2.5	.06	.038	.185	66.7	67.2	6.6
3. LIMIT CYCLE OPERATION	96 479	66 670	1185 780	9×10^{-4} 2×10^{-3}	5.7×10^{-4} 1.8×10^{-3}	5.5×10^{-3} 4.5×10^{-3}	.06 .133	.038 .125	.185 .15	.015	.015	.015
4. BALANCE DISTURBANCE TORQUES	108	126	0	9×10^{-4}	5.7×10^{-4}	0	.06	.038	0	.015	.015	0
5. OFFSET POINTING 100 maneuvers	91	58	0	.23	.15	0	.06	.038	0	3.8	3.8	0
6. SATELLITE TRACKING 100 maneuvers	37	24	0	.09	.06	0	$.2 \times 10^{-3}$	$.13 \times 10^{-3}$	0	.015	.015	0
7. EAST, WEST STATIONKEEPING 8 corrections	2.7	530	2.6	.34	66.3	.32	39.4×10^{-5}	.038	18.4×10^{-5}	873	873	873
8. 90° ROLL FOR N-S STATIONKEEPING 6 maneuvers	96	0	0	4	0	0	.06	0	0	66.7	0	0
9. ATTITUDE CONTROL DURING STATION KEEPING THRUST	37.8	32.4	0	6.3	5.4	0	.021	.018	0	600	600	0
10. ANTENNA PATTERN STUDY MANEUVERS 50 maneuvers	134	85	82	1.34	.85	.82	.06	.038	.185	22.3	22.4	2.2
$I_x = 3198$ $l_x = 4.2$ $I_y = 2424$ $l_y = 5.0$ $I_z = 2115$ $l_z = 4.5$												

Configuration: SK-513-10 (Mesh)

TABLE 6B-2

CONTROL MODE	TOTAL IMPULSE (lb-sec)			IMPULSE P R PULSE (lb-sec)			THRUST SIZE (lb)			PULSE WIDTH (Sec)		
	ROLL	PITCH	YAW	ROLL	PITCH	YAW	ROLL	PITCH	YAW	ROLL	PITCH	YAW
1. INITIAL TUMBLE ARREST	37.3	26.2	35.2	37.3	26.2	35.2	.058	.042	.276	644	625	64
2. ORIENTATION Assume 50 times	390	275	370	3.9	2.75	3.7	.058	.042	.276	67.3	65.5	6.7
3. LIMIT CYCLE OPERATION	92 5600	66.5 13,200	1835 1170	8.7×10^{-4} 6.8×10^{-3}	6.3×10^{-4} 8.7×10^{-3}	8.3×10^{-3} 6.8×10^{-3}	.058 .452	.042 .583	.276 .225	.015	.015	.015
4. BALANCE DISTURBANCE TORQUES	1285	2090	0	8.7×10^{-4}	6.3×10^{-4}	0	.058	.042	0	.015	.015	0
5. OFFSET POINTING 100 maneuvers	89	63	0	.22	.16	0	.058	.042	0	3.8	3.7	0
6. SATELLITE TRACKING 100 maneuvers	36	26	0	.09	.065	0	$.18\times10^{-3}$	$.13\times10^{-3}$	0	.015	.015	0
7. EAST, WEST STATIONKEEPING 8 corrections	2.3	530	3.3	.29	66.1	.41	36.6×10^{-5}	.042	26.2×10^{-5}	788	788	788
8. 90° ROLL FOR N-S STATIONKEEPING 6 maneuvers	93.6	0	0	3.9	0	0	.058	0	0	67.3	0	0
9. ATTITUDE CONTROL DURING STATION-KEEPING THRUST	61.2	61.2	0	10.2	10.2	0	.034	.034	0	600	600	0
10. ANTENNA PATTERN STUDY MANEUVERS 50 maneuvers	130	90	125	1.3	.9	1.25	.058	.042	.276	22.4	21.4	2.3
$I_x = 3945$ $l_x = 5.3$												
$I_y = 2780$ $l_y = 5.3$												
$I_z = 2604$ $l_z = 3.7$												

Configuration: SK-513-11 (Solid)

TABLE 6B-3

CONTROL MODE	TOTAL IMPULSE (sec-lb)			IMPULSE PER PULSE (lb-sec)			THRUST SIZE (lb)			PULSE WIDTH (sec)		
	Roll	Pitch	Yaw	Roll	Pitch	Yaw	Roll	Pitch	Yaw	Roll	Pitch	Yaw
1. INITIAL TUMBLE ARREST	37.4	26.2	35.2	37.3	26.2	35.2	.058	.042	.276	644	625	64
2. ORIENTATION Assume 50 times	390	275	370	3.9	2.75	3.7	.058	.042	.276	67.3	65.5	6.7
3. LIMIT CYCLE OPERATION	92 2700	66.5 5100	1835 1170	8.7×10^{-4} 4.7×10^{-3}	6.3×10^{-4} 5.4×10^{-3}	8.3×10^{-4} 6.8×10^{-3}	.058 .314	.042 .362	.276 .225	.015	.015	.015
4. BALANCE DISTURBANCE TORQUES	494	830	0	8.7×10^{-4}	6.3×10^{-4}	0	.058	.042	0	.015	.015	0
5. OFFSET POINTING 100 maneuvers	89	63	0	.22	.16	0	.058	.042	0	3.8	3.7	0
6. SATELLITE TRACKING 100 maneuvers	36	26	0	.09	.065	0	$.18\times10^{-3}$	$.13\times10^{-3}$	0	.015	.015	0
7. EAST, WEST STATIONKEEPING 8 corrections	2.3	530	3.3	.29	66.1	.41	36.6×10^{-5}	.042	26.2×10^{-4}	788	788	788
8. 90° ROLL FOR N-S STATIONKEEPING 6 maneuvers	93.6	0	0	3.9	0	0	.058	0	0	67.3	0	0
9. ATTITUDE CONTROL DURING STATIONKEEPING THRUST	61.2	61.2	0	10.2	10.2	0	.034	.034	0	600	600	0
10. ANTENNA PATTERN STUDY MANEUVERS 50 maneuvers	130	90	125	1.3	.9	1.25	.058	.042	.276	22.4	21.4	2.3
$I_x = 3945$ $l_x = 5.3$												
$I_y = 2780$ $l_y = 5.3$												
$I_z = 2604$ $l_z = 3.7$												

Configuration: SK-513-11 (Mesh)

TABLE 6B-4

CONTROL MODE	TOTAL IMPULSE (lb-sec)			IMPULSE PER PULSE (lb-sec)			THRUST SIZE (lb)			PULSE WIDTH (sec)		
	Roll	Pitch	Yaw	Roll	Pitch	Yaw	Roll	Pitch	Yaw	Roll	Pitch	Yaw
1. INITIAL TUMBLE ARREST	38.1	24.2	23.5	38.1	24.2	23.5	.06	.038	.185	635	638	635
2. ORIENTATION Assume 50 times	400	255	245	4.0	2.6	2.5	.06	.038	.185	66.7	67.2	6.6
3. LIMIT CYCLE OPERATION	96 450	66 185	1195 780	x 10^{-4} 2.0×10^{-3}	5.7×10^{-4} 9.9×10^{-3}	5.5×10^{-3} 4.5×10^{-3}	.06 .13	.038 .066	.185 .15	.015	.015	.015
4. BALANCE DISTURBANCE TORQUES	55	100	-	x 10^{-4}	5.7×10^{-4}	0	.06	.038	0	.015	.015	0
5. OFFSET POINTING 100 maneuvers	91	58	0	.23	.15	0	.06	.038	0	3.8	3.8	0
6. SATELLITE TRACKING 100 maneuvers	37	24	0	.09	.06	0	$.2\times10^{-3}$	$.13\times10^{-3}$	0	.015	.015	0
7. EAST,WEST STATIONKEEPING 8 corrections	2.7	528	2.6	.34	66.3	.32	39.4×10^{-6}	.038	18.4×10^{-6}	873	873	873
8. 90° ROLL FOR N-S STATIONKEEPING 6 maneuvers	96	0	0	4.0	0	0	.06	0	0	66.7	0	0
9. ATTITUDE CONTROL DURING STATIONKEEPING THRUST	64.2	54.0	0	10.7	9.0	0	.035	.03	0	600	600	0
10. ANTENNA PATTERN STUDY MANEUVERS 50 maneuvers	134	85	82	1.34	.85	.82	.06	.038	.185	22.3	22.4	2.2
$I_x = 3198$ $l_x = 4.2$ $I_y = 2424$ $l_y = 5.0$ $I_z = 2115$ $l_z = 4.5$												

Configuration: SK-513-12 (Solid)

TABLE 6B-5

CONTROL MODE	TOTAL IMPULSE (lb-sec)			IMPULSE PER PULSE (lb-sec)			THRUST SIZE (lb)			PULSE WIDTH (sec)		
	Roll	Pitch	Yaw	Roll	Pitch	Yaw	Roll	Pitch	Yaw	Roll	Pitch	Yaw
1. INITIAL TUMBLE ARREST	38.1	24.2	23.5	38.1	24.2	23.5	.06	.038	.185	635	638	63.5
2. ORIENTATION Assume 50 times	400	255	245	4.0	2.6	2.5	.06	.038	.185	66.7	67.2	6.6
3. LIMIT CYCLE OPERATION	96 131	66 76	1185 780	x 10^{-4} 2.4×10^{-3}	5.7×10^{-4} 6.3×10^{-4}	5.5×10^{-3} 4.5×10^{-3}	.06 .0825	.038 .042	.185 .15	.015	.015	.015
4. BALANCE DISTURBANCE TORQUES	22	26	0	9×10^{-4}	5.7×10^{-4}	0	.06	.038	0	.015	.015	0
5. OFFSET POINTING 100 maneuvers	91	58	0	.23	.15	0	.06	.038	0	3.8	3.8	0
6. SATELLITE TRACKING 100 maneuvers	37	24	0	.09	.06	0	$.2\times10^{-3}$	$.13\times10^{-3}$	0	.015	.015	0
7. EAST, WEST STATIONKEEPING 8 corrections	2.7	528	2.6	.34	66.3	.32	39.4×10^{-5}	.038	8.4×10^{-5}	873	873	873
8. 90 ROLL FOR N-S STATION-KEEPING 6 maneuvers	96	0	0	4.0	0	0	.06	0	0	66.7	0	0
9. ATTITUDE CONTROL DURING STATIONKEEPING THRUST	64.2	54.0	0	10.7	9.0	0	.035	.03	0	600	600	0
10. ANTENNA PATTERN STUDY MANEUVERS 50 maneuvers	134	85	82	1.34	.85	.82	.06	.038	.185	22.3	22.4	22.2
$I_x = 3198$ $l_x = 4.2$												
$I_y = 2424$ $l_y = 5.0$												
$I_z = 2115$ $l_z = 4.5$												

Configuration: SK-513-12 (Mesh)

TABLE 6B-6

CONTROL MODE	TOTAL IMPULSE (lb-sec)			IMPULSE PER PULSE (lb-sec)			THRUST SIZE (lb)			PULSE WIDTH (sec)		
	Roll	Pitch	Yaw	Roll	Pitch	Yaw	Roll	Pitch	Yaw	Roll	Pitch	Yaw
INITIAL TUMBLE ARREST	9.7	5.9	17.6	9.7	5.9	17.6	.015	.0093	.138	635	640	64
2. ORIENTATION Assume 50 times	100	60	185	1.0	.6	1.85	.015	.0093	.138	65.4	64.8	6.7
3. LIMIT CYCLE OPERATION	24.4 6600	14.8 7600	880 585	2.3×10^{-4} 3.8×10^{-3}	1.4×10^{-4} 3.2×10^{-3}	4.1×10^{-3} 3.4×10^{-1}	.015 .254	.0093 .21	.138 .112	.015	.015	.015
4. BALANCE DISTURBANE TORQUES	950	1190	0	2.3×10^{-4}	1.4×10^{-4}	0	.015	.0093	0	.015	.015	0
5. OFFSET POINTING 100 maneuvers	23	14	0	.058	.035	0	.015	.0093	0	3.8	3.8	0
6. SATELLITE TRACKING 100 maneuvers	9.5	.8	0	.024	.0015	0	$.05\times10^{-3}$	$.03\times10^{-3}$	0	.015	.015	.015
7. EAST, WEST STATIONKEEPING 8 corrections	1.4	315	3.5	.17	39.4	.44	8×10^{-5}	.0093	10.3×10^{-5}	2130	2130	2130
8. 90 ROLL FOR N-S STATION-KEEPING 6 maneuvers	24	0	0	1.0	0	0	.015	0	0	65.4	0	0
9. ATTITUDE CONTROL DURING STATIONKEEPING THRUST	15	15	0	2.5	2.5	0	.0084	.0084	0	600	600	0
10. ANTENNA PATTERN STUDY MANEUVERS 50 maneuvers	34	20	62	.34	.2	.62	.015	.0093	.138	21.9	21.6	2.3
$I_x = 1757$ $l_x = 9.0$ $I_y = 1059$ $l_y = 9.0$ $I_z = 1231$ $l_z = 3.5$												

Configuration: SK-512-13- (Solid)

TABLE 6B-7

CONTROL MODE	TOTAL IMPULSE (lb sec)			IMPULSE PER PULSE (lb sec)			THRUST SIZE (lb)			PULSE WIDTH (sec)		
	Roll	Pitch	Yaw	Roll	Pitch	Yaw	Roll	Pitch	Yaw	Roll	Pitch	Yaw
1. INITIAL TUMBLE ARREST	9.7	5.9	17.6	9.7	5.9	17.6	.015	.0093	.138	63[illegible]	640	64
2. ORIENTATION Assume 50 times	100	60	185	1.0	.6	1.85	.015	.0093	.138	65.4	64.8	6.7
3. LIMIT CYCLE OPERATION	1700	2340	585	$.9\times10^{-3}$	1.8×10^{-3}	3.4×10^{-3}	.129	.117	.112	.015	.015	.015
4. BALANCE DISTURBANCE TORQUES	215	365	0	2.3×10^{-4}	1.4×10^{-4}	0	.015	.0093	0	.015	.015	0
5. OFFSET POINTING 100 maneuvers	23	14	0	.[illegible]	.035	0	.015	.0093	0	3.8	3.8	0
6. SATELLITE TRACKING 100 maneuvers	9.5	5.8	0	.02[illegible]	.0015	0	$.05\times10^{-3}$	$.03\times10^{-3}$	0	.015	.015	0
7. EAST,WEST STATIONKEEPING 8 corrections	1.4	315	3.5	.17	39.4	.44	8×10^{-5}	.0093	10.3×10^{-3}	2130	2130	2130
8. 90° ROLL FOR N-S STATIONKEEPING 6 maneuvers	24	0	0	1.0	0	0	.015	0	0	65.4	0	0
9. ATTITUDE CONTROL DURING STATIONKEEPING THRUST	15	15	0	2.5	2.5	0	.0084	.0084	0	600	600	0
10. ANTENNA PATTERN STUDY MANEUVERS 50 maneuvers	34	20	62	.34	.2	.62	.015	.0093	.138	21.9	21.6	2.3
$I_x = 1757$ $l_x = 9.0$												
$I_y = 1059$ $l_y = 9.0$												
$I_z = 1031$ $l_z = 3.5$												

Configuration: SK-513-13 (mesh)

TABLE 6B-8

CONTROL MODE	TOTAL IMPULSE (lb-sec)			IMPULSE PER PULSE (lb-sec)			THRUST SIZE (lb)			PULSE WIDTH (sec)		
	Roll	Pitch	Yaw	Roll	Pitch	Yaw	Roll	Pitch	Yaw	Roll	Pitch	Yaw
1. INITIAL TUMBLE ARREST	22	15.6	23.3	22	15.6	23.3	.035	.025	.183	637	634	63.7
2. ORIENTATION Assume 50 times	232	164	245	2.32	1.64	2.45	.035	.025	.183	67	66.7	6.7
3. LIMIT CYCLE OPERATION	55.5 5700	39.5 9100	1170 770	5.2×10^{-4} 5.2×10^{-3}	3.7×10^{-4} 5.6×10^{-3}	5.5×10^{-3} 1.4×10^{-3}	.035 .349	.025 .373	.183 .047	.015	.015	.015
4. BALANCE DISTURBANCE TORQUES	1460	2280	0	5.2×10^{-4}	3.7×10^{-4}	0	.035	.025	0	.015	.015	0
5. OFFSET POINTING 100 maneuvers	52	37.2	0	.13	.094	0	.035	.025	0	3.7	3.8	0
6. SATELLITE TRACKING 100 maneuvers	21.5	15.4	0	.054	.038	0	$.11\times10^{-3}$	$.08\times10^{-3}$	0	.015	.015	0
7. EAST, WEST STATIONKEEPING 8 corrections	2.5	560	2.5	.31	70.3	.31	21.4×10^{-3}	.025	10.7×10^{-3}	1430	1430	1430
8. 90 ROLL FOR N-S STATIONKEEPING 6 maneuvers	55.5	0	0	2.3	0	0	.035	0	0	66.3	0	0
9. ATTITUDE CONTROL DURING STATION-KEEPING THRUST	27	27	0	4.5	4.5	0	.015	.015	0	600	600	0
10. ANTENNA PATTERN STUDY MANEUVERS 50 maneuvers	77	55	82	.77	.55	.82	.035	.025	.183	22.2	22.4	2.24
$I_x = 2068$ $l_x = 4.7$ $I_y = 1466$ $l_y = 4.7$ $I_z = 2186$ $l_z = 4.7$												

Configuration: SK-513-14 (Solid)

TABLE 6B-9

CONTROL MODE	TOTAL IMPULSE (lb-sec)			IMPULSE PER PULSE (lb-sec)			THRUST SIZE (lb)			PULSE WIDTH (sec)		
	Roll	Pitch	Yaw	Roll	Pitch	Yaw	Roll	Pitch	Yaw	Roll	Pitch	Yaw
1. INITIAL TUMBLE ARREST	22	15.6	23.3	22	15.6	23.3	.035	.025	.183	637	634	63.7
2. ORIENTATION Assume 50 times	232	164	245	2.32	1.64	2.45	.035	.025	.183	67	66.7	6.7
3. LIMIT CYCLE OPERATION	55.5 1940	39.5 3280	1170 770	5.2×10^{-4} 3×10^{-3}	3.7×10^{-4} 3.4×10^{-3}	5.5×10^{-3} 1.4×10^{-3}	.035 .204	.025 .224	.183 .047	.015	.015	.015
4. BALANCE DISTURBANCE TORQUES	495	800	0	5.2×10^{-4}	3.7×10^{-4}	0	.035	.025	0	3.8	3.8	0
5. OFFSET POINTING 100 maneuvers	52	37.2	0	.13	.094	0	.035	.025	0	3.8	3.8	0
6. SATELLITE TRACKING 100 maneuvers	21.5	15.4	0	.054	.038	0	$.11\times10^{-3}$	$.08\times10^{-3}$	0	.015	.015	0
7. EAST, WEST STATIONKEEPING 8 corrections	2.5	560	7.5	.31	70.3	.31	21.4×10^{-3}	.025	10.7×10^{-5}	1430	1430	1430
8. 90 ROLL FOR N-S STATION-KEEPING	55.5	0	0	2.3	0	0	.035	0	0	66.3	0	0
9. ATTITUDE CONTROL DURING STATION-KEEPING THRUST	27	27	0	4.5	4.5	0	.015	.015	0	600	600	0
10. ANTENNA PATTERN STUDY MANEUVERS 50 maneuvers	77	55	82	.77	.55	.82	.035	.025	.183	22.2	22.4	2.24
$I_x = 2068$ $l_x = 4.7$ $I_y = 1466$ $l_y = 4.7$ $I_z = 2186$ $l_z = 4.7$												

Configuration: SK-513-14 (mesh)

TABLE 6B-10

REFERENCES

1. Sutherland, G. S., and Maes, M. E., "A Review of Micro-Rocket Technology: 10^{-6} To 1-Lb Thrust", AIAA Paper No. 65-620, Joint Specialist Conference, Colorado Springs, June 1965.

2. Hardt, A. P., Foley, W. M., and Brandon, R. L., "The Chemistry of Subliming Solids For Micro-Thrust Engines", AIAA Paper No. 65-595, Joint Specialist Conference, Colorado Springs, June 1965.

3. "Design and Evaluation of TSK-2000-1 And TMJ-2000-5 Resistance Jet Thrusters For Station Keeping and Attitude Control Operation", Contract No. NAS 5-9013, September 27, 1965, General Electric Missle And Space Division.

4. Hamilton Standard, Company Brochure Data, Windsor Locks, Conn., 1965.

5. "Hydrazine Thrust Motor Performance and Application Data", Report 0362-945A, Walter Kidde and Company Inc., Belleville, New Jersey.

APPENDIX 6C

PRELIMINARY INERTIA WHEEL CONSIDERATIONS FOR CANDIDATE VEHICLE CONFIGURATIONS

Preliminary Inertia Wheel Considerations

The following discussion presents the rationale, assumptions, and analysis used in the estimation of the required parameters for inertia wheels to be used in the ATS-4 attitude control system.

Use of Inertia Wheels

When inertia wheels are selected as the control moment devices for attitude control of a space vehicle it is generally done for two reasons. One, if the mission life of the spacecraft is long, such as the two year life required for the ATS-4, it is frequently possible to reduce the system weight from that required for a mass expulsion system by the use of inertia wheels. Two, if precise attitude control is required, such as the ±0.1 degree specified for the ATS-4 system, it is necessary to provide the control torque with a finer resolution than is practical with a mass expulsion system.

In the case of the ATS-4 spacecraft the inertia wheels are selected for both of the above reasons, however, the attitude accuracy requirements make it necessary that inertia wheels be considered whether or not their application results in a saving in system weight.

In reviewing the operating modes for ATS-4 it appears that inertia wheels may be used to advantage in the following modes.

- Attitude hold
- Tracking maneuvers
- Offset pointing maneuvers
- Antenna maneuvering study

In the attitude hold mode the attitude control system must maintain the vehicle in a selected orientation relative to the local vertical, orbit plane reference with an accuracy of ±0.1 degrees. Since the spacecraft will be subject to disturbances resulting from solar radiation and other causes some control action will be required to obtain the desired attitude accuracy. In the event mass expulsion reaction jets are used to generate the control torque it will be necessary to have a deadband of the order of ±0.01 degrees. Experience indicates that such a small deadband results in excessive jet operation and fuel consumption because of noise. The use of reaction wheels to generate the control moment will eliminate not only the excessive fuel consumption but also the fuel consumption normally associated with maintaining an undisturbed limit cycle between the limits of the deadband. This is a result of the continuous control moment available from the inertia wheel as contrasted with the one discreet level available from the reaction jets.

The tracking maneuver consists of keeping the vehicle yaw axis pointed at a satellite in a 90 minute orbit as it passes below the ATS-4 spacecraft. It is desired to track with an accuracy of ±0.5 degree. Since the tracking line of sight will have a sinusoidal angular acceleration, the attitude control system must have the capability of producing a smooth angular acceleration of the vehicle in roll and pitch in order to track with suitable accuracy. The torque produced by inertia wheels is continuous within their range and would be compatible with this requirement.

The offset pointing maneuver requires that the vehicle yaw axis be pointed at any point on the earth's desk with an accuracy of ±0.1 degree. Since the inertia wheels are required to obtain suitable accuracy during attitude hold and tracking maneuvers, a relatively small increase in the wheel size makes them suitable for performing the offset maneuver. The end result is saving of jet fuel that would otherwise be consumed.

The antenna maneuvering study consists of the offset pointing maneuver plus a 360 degree rotation about the yaw axis. Since the wheels are to be sized to accommodate the offset pointing maneuver this part of the antenna maneuvering study presents no new conditions on the inertia wheels. However, to allow antenna polarization measurements, a 360 degree rotation in yaw will result in an exchange of angular momentum between the roll and pitch wheels. Therefore, it will be necessary that the roll and pitch wheels be sized to accept the maximum exchange angular momentum. As it turns out this is not a problem since the maximum angular momentum that will be exchanged is less than the maximum capability of the inertia

least the same angular momentum storage in the yaw wheel as provided in the roll wheel for storage of angular momentum due to roll disturbance torque in addition to any storage required for the yaw maneuvers for the antenna study.

Tables 6C-1 and 6C-2 summarize the estimates for the principal parameters of the inertia wheels for the two configurations currently being considered for the ATS-4 vehicle.

Inertia Wheel Angular Momentum and Torque For Solar Disturbance Torque

In order to estimate the size of inertia wheels for attitude control in the presence of disturbance torques resulting from solar radiation it is necessary to establish the angular momentum to be stored by the wheels. For this purpose it will be assumed that the wheels will be sized to store the angular momentum due to disturbance torques for a period of 12 hours. Twelve hours is the half period for the cyclic disturbance torque in the roll and pitch axes, and if the wheels can store the angular momentum for twelve hours, only the angular momentum resulting from unidirectional torques will require unloading. With these assumptions the angular momentum to be stored by the inertia wheel and the peak torque to be exerted by the wheels may be estimated as follows:

The estimates for the vehicle configuration SK-513-10 are,

wheels as dictated by the other modes of operation. However, this maneuver will require a sizeable inertia wheel in the yaw axis in order to produce the 360 degree yaw rotation.

Inertia Wheel Sizing

In estimating the principal parameters of the inertia wheels, it is assumed they will be used in the four operating modes previously discussed.

In sizing the inertia wheels to perform the offset and tracking maneuvers, it is not necessary to provide angular momentum storage for simultaneous execution of these maneuvers. Rather it will be necessary to provide angular momentum storage for whichever one has the greatest requirement.

Although attitude hold will not be performed simultaneously with maneuvers. the disturbance torques that require angular momentum storage during attitude hold are present during maneuvers and therefore, the inertia wheel must be sized to accommodate the simultaneous occurance of the maximum requirements of the disturbance torques and the maneuvers.

Although the disturbance torques about the vehicle yaw axis are essentially zero for sun oriented panels, the yaw axis inertia wheel will exchange angular momentum with the roll inertial wheel as a result of the pitch rate that maintains the yaw axis along the local vertical. It is therefore, necessary to provide at

TABLE 6C-1

System Configuration	Reaction Wheel Angular Momentum lb-ft-sec			Reaction Wheel Torque oz-in			Reaction Wheel Weight lbs		
	Roll	Pitch	Yaw	Roll	Pitch	Yaw	Roll	Pitch	Yaw
SK-513-10	2.0	2.0	8.0	4.0	60	4.0	9.5	12.5	19.2
SK-513-14	3.5	3.5	9.5	4.0	40	4.0	11.2	13.5	21.8

TABLE 6C-2

System Configuration	Reaction Wheel Volume cu.-in.			Reaction Wheel Power Watts					
	Roll	Pitch	Yaw	Roll		Pitch		Yaw	
				Peak	Avg	Peak	Avg	Peak	Avg
SK-513-10	340	450	700	16	1.5	114	1.5	16	1.5
SK-513-14	410	490	790	16	1.5	76	1.5	16	1.5

Roll

Angular Momentum = Avg. torque x time

= $0.72 \times 10^{-5} \times 12 \times 3600$

= 0.31 lb-ft-sec

Peak Torque = 0.80×10^{-5} lb-ft

Pitch

Angular Momentum = Avg. torque x time

= $1.0 \times 10^{-5} \times 12 \times 3600$

= 0.43 lb-ft-sec

Peak Torque = 1.33×10^{-5} lb-ft

The estimates for the vehicle configuration SK-513-14 are:

Roll

Angular Momentum = $3.7 \times 10^{-5} \times 12 \times 3600$

= 1.6 lb-ft-sec

Peak Torque = 5.6×10^{-5} lb-ft

Pitch

Angular Momentum = $6 \times 10^{-5} \times 12 \times 3600$

= 2.58 lb-ft-sec

Peak Torque = 9.3×10^{-5} lb-ft

Effect of Solar Panel Motion on Inertia Wheel Angular Momentum and Torque

If the solar panels are rotated at a constant angular velocity to keep them pointed at the sun, the rate would be essentially earth's rate. It is quite likely that at such a low rate the drive system would operate intermittently rather than at a constant rate. Therefore, it seems advisable to design the drive system so that it positions the solar panels in steps and take advantage of the somewhat simpler mechanization. To this end a drive system that positions the solar panels in steps will be considered. In this case, the steps must be sufficiently small to satisfy the pointing accuracy for the solar panels, ±3 degrees. To insure being within the accuracy limitation the steps will be assumed to be 1.0 degree.

If the drive system moves the solar panels one degree, the vehicle will rotate in the opposite direction an amount proportional to the ratio of the panel and vehicle moments of inertia.

That is

$$\theta_v = (I_p/I_v) \times \theta_p$$

where

θ_v = vehicle rotation

θ_p = solar panel rotation

I_v = vehicle moment of inertia

I_p = solar panel moment of inertia

Therefore, the vehicle rotation for the SK-513-10 and SK-513-14 configuration will be:

SK-513-10

$$\theta_v = \frac{6.72}{2507} \cdot 1.0 \text{ degrees}$$

$$= 0.0027 \text{ degrees}$$

SK-513-14

$$\theta_v = \frac{3.5}{4010} \cdot 1.0 \text{ degrees}$$

$$= 0.0009 \text{ degrees}$$

The inertias for the solar panels used in the above calculations were based on a solar panel weight of 1.0 lb/ft^2.

The small attitude change indicated by the above calculations may well be below the threshold of the attitude control system. In that event, the inertia wheels would not be called on to correct the attitude until the solar panels were repositioned several times.

To obtain an estimate of the attitude control system threshold assume the inertia wheel is driven by an AC motor. Design data for a two phase, 26 volt, 400 cycle motor indicates a starting voltage of 1 volt. Since it is desired to maintain an attitude accuracy of ±0.1 degree, the inertia wheel should develop maximum torque for this error or larger. Therefore, if an error of 0.1 degree causes a voltage of 26 volts at the terminals of the motor, the attitude error that would cause 1 volt at the motor terminals is

$$\frac{0.1}{26} = .0038 \text{ degrees}$$

Therefore, with a system threshold of .0038 degrees the inertia wheels would correct the vehicle attitude after two rotations of the solar panel on the SK-513-10 vehicle and after five on the SK-513-14 vehicle. In other words, the SK-513-10 vehicle would be rotated through .0054 degrees and the SK-513-14 vehicle would be rotated through .0045 degrees. In the interest of simplifying the calculations assume both vehicles are rotated through .006 degrees.

Under these assumptions the vehicle will be accelerated and decelerated as it is rotated 0.006 degrees in pitch. If the acceleration and deceleration are each constant over half the period of the rotation, the angular momentum the wheel must store and the torque the motor must develop may be calculated from:

$$\text{Stored angular momentum} = \frac{2\Theta I}{t}$$

$$\text{Motor torque} = \frac{2\Theta I}{t^2}$$

where

Θ = half angle of rotation in radians

t = time in seconds for rotation Θ

I = vehicle moment of inertia in slug-ft^2

Assuming the period of the rotation is two seconds, then from the above formulas the angular momentum storage and motor torque for the vehicle configurations SK-513-10 and SK-513-14 are:

SK-513-10

$$\text{Angular Momentum} = \frac{2 \times (.003/57.3) \times 2424}{1}$$

$$= .25 \text{ lb-ft-sec}$$

$$\text{Motor Torque} = \frac{2 \times (.003/57.3) \times 2424}{1^2}$$

$$= .25 \text{ lb-ft}$$

SK-513-14

$$\text{Angular Momentum} = \frac{2 \times (.003/57.3) \times 1466}{1}$$

$$= .15 \text{ lb-ft-sec}$$

$$\text{Motor Torque} = \frac{2 \times (.003/57.3) \times 1466}{1^2}$$

$$= .15 \text{ lb-ft}$$

Inertia Wheel Angular Momentum and Torque for the Offset Pointing Maneuver

Since from synchronous altitude the earth's disk only spans 18 degrees, the greatest offset pointing angle required of the ATS-4 vehicle will be ±9 degrees. Assuming 12 minutes is an acceptable period for acquiring the offset pointing orientation and the acceleration and deceleration of the vehicle are each constant over 6 minutes, the angular momentum that must be stored by the wheel and the torque that must be developed by the motor may be calculated with formulas previously used for sizing the wheel for the solar panel motion. That is

$$\text{Angular Momentum} = \frac{2\Theta I}{t}$$

$$\text{Motor Torque} = \frac{2\Theta I}{t^2}$$

Since the offset pointing orientation is not predictable, it will be necessary to provide the capability in both the pitch and roll inertia wheels to perform the maximum offset pointing maneuver. Therefore, the angular momentum storage and motor torque may be calculated as follows:

For vehicle SK-513-10

Roll

$$\text{Angular Momentum} = \frac{2 \times (4.5/57.3) \times 3198}{6 \times 60} = 1.4 \text{ lb-ft-sec}$$

$$\text{Motor Torque} = \frac{2 \times (4.5/57.3) \times 3198}{(6 \times 60)^2} = .0038 \text{ lb-ft}$$

Pitch

$$\text{Angular Momentum} = \frac{2 \times (4.5/57.3) \times 2424}{6 \times 60} = 1.07 \text{ lb-ft-sec}$$

$$\text{Motor Torque} = \frac{2 \times (4.5/57.3) \times 2424}{(6 \times 60)^2} = .0029 \text{ lb-ft}$$

For vehicle SK-515-14

Roll

$$\text{Angular Momentum} = \frac{2 \times (4.5/57.3) \times 2068}{6 \times 60} = 0.91 \text{ lb-ft-sec}$$

$$\text{Motor Torque} = \frac{2 \times (4.5/57.3) \times 2068}{(6 \times 60)^2} = .0025 \text{ lb-ft}$$

Pitch

$$\text{Angular Momentum} = \frac{2 \times (4.5/57.3) \times 1466}{6 \times 60} = 0.65 \text{ lb-ft-sec}$$

$$\text{Motor Torque} = \frac{2 \times (4.5/57.3) \times 1466}{(6 \times 60)^2} = .0018 \text{ lb-ft}$$

Inertia Wheel Angular Momentum and Torque for the Tracking Maneuver

Since the tracking maneuver consists of pointing the vehicle yaw axis at a satellite in a 90 minute orbit as it passes under the observing satellite, the angular velocity of the yaw axis may be expressed as

$$\Omega = \frac{r}{R} \; w \sin w t$$

where

Ω = Angular velocity of LOS in radians per sec

w = Angular velocity of target satellite in its orbit in radians per second

r = Radius of target satellite orbit

R = Radius of observing (synchronous) satellite

Therefore, the angular momentum of the tracking satellite resulting from the tracking maneuver will be

$$\text{angular momentum} = I \; \Omega$$

where I is the vehicle moment of inertia. Substituting for Ω the angular momentum may be expressed as

$$\text{angular momentum} = L = I \left(\frac{r}{R} \right) w \sin w t$$

and the maximum value will occur for $\sin w t = 1$

When $\sin w t = 1$ the ratio $\left(\frac{r}{R}\right)$ has a value of approximately 0.2. Therefore, the maximum value of the angular momentum may be expressed as

$$L_{max} = .2 \cdot \frac{2}{90 \times 60} \cdot (1) \cdot I$$
$$= (2.3 \times 10^{-4}) \; I$$

Since torque is equal to the rate of change angular momentum,

$$\text{torque} = T = I \dot{\Omega}$$

or

$$T = I \frac{r}{R} w^2 \cos w t$$

The maximum value will occur when cos w t = 1 and the ratio $\frac{r}{R}$ has a value of approximately 0.17. Therefore,

$$T_{max} = (.17) \times \left(\frac{2}{90 \times 60}\right)^2 \cdot 1$$

$$= .23 \times 10^{-6} I$$

Since the path of the target vehicle satellite relative to the tracking satellite is not predictable both the roll and pitch wheels must have the capability to perform the tracking maneuver. Therefore, the angular momentum storage and motor torque required in the inertia wheels for this purpose are:

Vehicle configuration SK-513-10

<u>Roll</u>

Angular Momentum	=	$2.3 \times 10^{-4} \times 3198$
	=	0.74 lb-ft-sec
Motor Torque	=	$0.23 \times 10^{-6} \times 3198$
	=	.00074 lb-ft

<u>Pitch</u>

Angular Momentum	=	$2.3 \times 10^{-4} \times 2424$
	=	0.56 lb-ft-sec
	=	$0.23 \times 10^{-6} \times 2424$
	=	.00023 lb-ft

Vehicle Configuration SK-513-14

Roll

Angular Momentum = $2.3 \times 10^{-4} \times 2068$

= 0.48 lb-ft-sec

Motor Torque = $0.23 \times 10^{-6} \times 2068$

= .00048 lb-ft

Pitch

Angular Momentum = $2.3 \times 10^{-4} \times 1466$

= 0.34 lb-ft-sec

Motor Torque = $0.23 \times 10^{-6} \times 1466$

= .00034 lb-ft

Inertia Wheel Angular Momentum and Torque for the Antenna Maneuvering Study

Since, as previously explained, the antenna maneuvering study consists of the offset pointing maneuver plus a rotation of 360 degrees about the yaw axis, the only additional capability the wheels must have to be used for this study is that required for the 360 degree rotation in yaw.

As the vehicle is rotated in yaw there will be a transfer of angular momentum between the pitch and roll inertia wheels. Each 90 degrees of rotation will cause a complete interchange of angular momentum between the wheels. The maximum angular momentum interchange will occur when the roll and pitch wheel are storing the angular momentum accumulated during one half cycle of the disturbance torque. Therefore, in order to perform the antenna maneuver study without unloading the inertia wheels the roll and pitch wheels must be capable of storing the following angular momentum.

SK-513-10

Roll

Angular Momentum = 0.43 lb-ft-sec

Pitch

Angular Momentum = 0.31 lb-ft-sec

SK-513-14

Roll

Angular Momentum = 2.58 lb-ft-sec

Pitch

Angular Momentum = 1.6 lb-ft-sec

Since the 360 degree rotation in yaw is to occur over a period of one hour, the torques require to accomplish this transfer of angular may be estimated as follows.

SK-513-10

Roll Motor Torque = $0.43 \times \frac{2\pi}{3600}$

= .00075 lb-ft

Pitch Motor Torque = $0.31 \times \frac{2\pi}{3600}$

= .0053 lb-ft

SK-57-14

$$\text{Roll Motor Torque} = 2.58 \times \frac{2\pi}{3600}$$

$$= .0045 \text{ lb-ft}$$

$$\text{Pitch Motor Torque} = 1.6 \times \frac{2\pi}{3600}$$

$$= .0027 \text{ lb-ft}$$

Assuming the 360 degree yaw maneuver may be carried out by a constant acceleration during the first half of the period and a constant deceleration during the last half of the period the angular momentum storage and motor torque required in the yaw inertia wheel may be expressed as

$$\text{Angular Momentum} = \frac{2\theta I}{t}$$

$$\text{Motor Torque} = \frac{2\theta I}{t^2}$$

where the symbols have been previously defined.

Therefore, the angular momentum storage required for the two vehicle configurations under consideration are

SK-51-14

$$\text{Angular Momentum} = \frac{2 \times (180/57.3) \times 2115}{1800}$$

$$= 7.4 \text{ lb-ft-sec}$$

$$\text{Motor Torque} = \frac{2 \times (180/57.3) \times 2115}{(1800)^2}$$

$$= .0041 \text{ lb-ft}$$

SK-513-14

$$\text{Angular Momentum} = \frac{2 \times (180/57.3) \times 2168}{1800}$$

$$= 7.6 \text{ lb-ft-sec}$$

$$\text{Motor Torque} = \frac{2 \times (180/57.3) \times 2168}{(1800)^2}$$

$$= .0042 \text{ lb-ft}$$

Summary of Inertia Wheel Angular Moment and Torque Estimates

Table 6C-3 summarizes the estimates of angular momentum storage and the motor torque required in inertia wheels for the indicated modes of operation. As previously discussed it is not necessary to provide inertia wheels with a capability equal to the sum of the requirements indicated in the table. The maneuvers are not performed simultaneously, however, the disturbances are ever present. Therefore, it is only necessary to size the wheels to provide capability for attitude control and solar panel operation plus whichever of the three maneuvers imposes the most stringent requirement. The last entry in the table "Required Inertia Wheel Capability" is this summation rounded off to provide a flight safety factor.

Estimation of Inertia Wheel Weight and Volume

The estimation of the inertia wheel weight and volume is based on design data published by Eclipse-Pioneer Division of the Bendix Corporation in

[illegible]ating [illegible]	Angular Momentum Storage lb-[illegible] sec						Motor Torque [illegible]					
	[illegible]			[illegible]-14			[illegible]-10			K-[illegible]-14		
	[illegible]	Pitch	Yaw	Roll	Pitch	Yaw	Roll	Pitch	Yaw	Roll	Pitch	Yaw
Attitude Hold	[illegible]	[illegible]	[illegible]	1.6	2.58	1.6	.0015	.0025	.0014	[illegible]	[illegible]	[illegible]
[illegible] Panel Opr		0.25			0.15			18.0			26.8	
[illegible]king	0.74	[illegible]		0.[illegible]8	0.34		.34	.044		.092	.005	
Offset Pointing	[illegible]	[illegible].07		0.91	0.65		[illegible]	.56		.48	.35	
[illegible]na Study	0.42	[illegible]	[illegible]	2.58	1.6	7.6	.14	.10	.79	.86	.52	.81
Required Inertia Wheel Capability	2.0	2.0	[illegible]	3.5	3.5	9.5	4	60	4	4	40	4

TABLE 6C-3

publication No. 6311-5. From this information, the weight of an inertia wheel unit may be approximated by the formula

$$\text{Weight (lbs)} = 6.3 + 170 \text{ inertia (slug-ft}^2\text{)}$$

if the motor is required to have a stall torque greater than approximately 8 oz-in. If the motor must develop a torque greater than 8 oz-in the weight obtained from the above formula must be increased.

The inertia to be used in the weight formula may be calculated from

$$\text{Inertia (slug-ft}^2\text{)} = \frac{\text{Max Momentum (lb-ft-sec)}}{\text{Unload Speed (RPM)} \times 2\pi/60}$$

For these calculations the unload speed has been assumed to be 1000 RPM Therefore, the weight for the inertia wheels is estimated as indicated in Table 6C-4.

The volume of the inertia wheels is estimated on the basis of the average density of wheels built by Bendix Corporation. Inertia wheels of approximately the same capability as those required for the ATS-4 vehicle have a volume to weight ratio of approximately 36 cu.in/lb. Using this information and the weights from Table 6C-4 the volume was calculated as indicated in Table 6C-5.

Estimation of Average and Peak Power

To obtain an estimate of the average power consumed by the inertia wheels it is assumed the motor has an average speed of 500 RPM, a friction load of

[illegible] ratio				[illegible]		Additional Motor Weight lbs			Total [illegible] Weight [illegible]		
			Roll	Pitch	Yaw	Roll	Pitch	Yaw	Roll	Pitch	Yaw
[illegible] 10	[illegible]	[illegible]	[illegible].5	[illegible]	19.2	0	[illegible].0	0	[illegible].5	[illegible]2.5	19.[illegible]
[illegible]4	[illegible]	.0[illegible]	[illegible]	[illegible]2	21.8	0	2.[illegible]	0	11.2	13.5	21.[illegible]

TABLE 60-[illegible]

Vehicle Configuration	Inertia Wheel Volume cu.in.		
	Roll	Pitch	Yaw
SK-513-10	340	450	700
SK-513-14	410	490	790

TABLE 6C-5

2 oz-in and an efficiency of 50%. With these assumptions the input power will be

$$\text{Input power (watts)} = 7.4 \times 10^{-4} \times \text{torque (oz-in)} \times \text{speed (RPM)} \times \frac{1}{\text{eff}}$$

$$= (7.4 \times 10^{-4}) \times (2) \times (500) \times \frac{1}{.5}$$

$$= 1.48 \text{ watts}$$

The estimation of peak power for the inertia wheels is based on the stall power listed for similar wheels in the Bendix Corporation publication No. 6311-5. It was estimated that the pitch wheels for vehicle configurations SK-513-10 and SK-513-14 should have stall torque of 60 ox-in and 40 oz-in, respectively. From the data available on wheels of this approximate capability the power to stall torque ratio was determined to be about 1.9 watts/oz-in. Therefore, the peak power for the pitch wheels will be:

SK-513-10

$$\text{Peak Power} = (60 \text{ oz-in}) \times (1.9 \text{ watts/oz-in})$$

$$= 114 \text{ watts}$$

SK-513-14

$$\text{Peak Power} = (40 \text{ oz-in}) \times (1.9 \text{ watts/oz-in})$$

$$= 76 \text{ watts}$$

It was estimated that the roll and yaw wheels for both the SK-513-10 and SK-513-14 vehicle configurations should have a stall torque of approximately 4 oz-in to insure having the peak required torque of about 1 oz-in available

at all motor speeds up to the unload speed. Wheels of this approximate stall torque indicate a power to stall torque ratio of approximately 4 watts/oz-in. Therefore, the peak power for the roll and pitch wheels is estimated as:

$$\text{Peak Power} = 4 \text{ (oz-in)} \times 4 \frac{\text{watts}}{\text{oz-in}}$$

$$= 16 \text{ Watts}$$

Conclusions

The principal conclusions to be drawn from the information derived during the study of inertia wheels for the ATS-4 vehicle are:

- Of the two vehicle configurations being considered the SK-513-10 configuration places the lesser requirements on the reaction wheels.
- The yaw maneuver in the antenna maneuver study is the greatest single factor in the weight and volume of the wheels.
- The disturbance resulting from the solar panel positioning is the greatest single factor in the power consumption of the inertia wheels.

APPENDIX 6D

PRELIMINARY COMBINED WHEEL/JET SYSTEM CONSIDERATIONS

INERTIA WHEEL/PURE JET WEIGHT COMPARISON

This discussion presents the basis for estimating the weight of jet fuel and tankage eliminated through the use of inertia wheels.

The inertia wheel weight estimate was presented in Appendix 6c. In these estimates the wheels were sized so as to complete the tracking offset pointing or antenna study maneuver without unloading the wheels. Therefore the fuel and tankage chargeable to these maneuvers will be eliminated.

Also the wheels were sized to store the angular momentum of a half cycle of the pitch disturbance torque without unloading, and so the fuel and tankage assigned to the control of the pitch disturbance torque and limit cycle will be eliminated. Since the roll disturbance torque is unidirectional the angular momentum resulting from this source must be unloaded from the wheels periodically and no jet fuel will be eliminated in this case. However, any fuel chargeable to the maintenance of the roll limit cycle will be eliminated.

There is essentially no disturbance torque about the yaw axis of the vehicle, assuming oriented solar panels, and therefore no jet fuel is consumed for this purpose. However, the jet fuel that would be used in maintaining the yaw limit cycle would be eliminated.

Appendix 6B shows the total impulse required by a mass expulsion system to perform the various attitude control modes or functions. Using this information and information on the weight for a monopropellant hydrazine system the jet fuel and tankage eliminated by the inertia wheels was estimated and is listed in Table 6D-1 for vehicle configurations SK-513-10 and SK-513-14.

In order to make a comparison between the weight added to the vehicle by the inertia wheels and the weight of the jet fuel and tankage eliminated by their use, Table 6D-2, was compiled. Table 6D-2 tabulates the inertia wheel weight and an estimate of the weight that must be added to the vehicle in the way of solar panels, batteries, and power conditioning equipment to supply power for the operation of the wheels. Although the average power to operate the inertia wheels is estimated to be only 4.5 watts, it is estimated that the pitch inertia wheels will have peak loads of 20 to 25 times this amount for periods of the order of 5 seconds. Therefore in order to handle the peak load it is assumed the power supply will carry a 500% overload for this short period and the continous rating of the supply will be 1/5 of the peak power required by the pitch wheels.

Referring to previous estimates of vehicle weight per watt of converted sine wave power in the 400 cps range the estimates have ranged from one pound to 3.5 pounds per watt. Therefore, it was assumed that the power supply would be in about the middle of this range of 2.25 lbs/watt.

TABLE 6D-1
WEIGHT OF JET FUEL AND TANKAGE ELIMINATED BY INERTIA WHEELS

	VEHICLE CONFIGURATION SK-513-10	VEHICLE CONFIGURATION SK-513-14
Limit Cycle Impulse (lb-sec)	1347	1265
Disturbance Torq. Impulse (lb-sec)	126	800
Offset Pointing Impulse (lb-sec)	149	89.2
Tracking Impulse (lb-sec)	61	36.9
Antenna Study Impulse (lb-sec)	301	214
Total Impulse (lb-sec)	1984	2405.1
Fuel Tankage Weight (lbs)	44.8	50.5
Fuel Tankage Weight with safety Factor of 2 (lbs)	89.6	101

TABLE 6D-2

VEHICLE WEIGHT FOR INERTIA WHEELS

	VEHICLE CONFIGURATION SK-513-10	VEHICLE CONFIGURATION SK-513-14
Weight of Inertia Wheels (lbs)	41.2	46.5
Weight of Power Supply for Inertia Wheels (lbs)	52.0	33.0
Total Weight of Inertia Wheel System (lbs)	93.2	79.5

Since the pitch wheel for the SK-513-10 vehicle configuration has a peak power of 114 watts, with the above assumptions a power supply with a continuous rating of 23 watts and a weight of approximately 52 pounds will be required. The pitch wheel for the SK-513-14 vehicle configuration has a peak power requirement of 76 watts and therefore will require a power supply with a continuous rating of about 15 watts and a weight of approximately 33 pounds.

Table 6D-3 summarizes the results presented in the previous two tables and permits the desired comparison between the weight of the inertia wheel system and the jet fuel and tankage eliminated by the use of inertia wheels. From this comparison it is apparent that there is no weight advantage in using inertia wheels for vehicle configuration SK-513-10 of approximately 21 pounds if wheels are used for vehicle configuration SK-513-14.

It should be pointed out that much of the weight in the inertia wheel system is the result of the high torque requirement estimated for the pitch wheels. If this torque requirement can be reduced, the inertia wheels should show a greater weight advantage. This will be the subject of further study.

Trade-off Comparison of Configuration SK-513-17 and -18 (FIXED SOLAR PADDLES)

From previous study results on inertia wheels and reaction jet it was determined that it was advantageous to use reaction jet for the following modes of control.

TABLE 6D-3

COMPARISON OF JET FUEL & INERTIA WHEEL WEIGHT

	VEHICLE CONFIGURATION SK-513-10	VEHICLE CONFIGURATION SK-513-14
Total Weight of Inertia Wheel System (lbs)	93.2	79.5
Weight of Jet Fuel & Tankage Eliminated (lbs)	89.6	101

a) Tumbling arrest

b) Acquisition

c) Unload wheels (as result of average disturbance torques)

d) Manuevers required for ΔV corrections

e) Hold attitude is presence of ΔV misalignments

f) Antenna pattern maneuvers (if high rates are required)

The values of parameters used in determining impulse and thrust levels are:

Tumble rates

Roll	-1°/sec	-17.4×10^{-3} rad/sec
Pitch	-0.5°/sec	-8.7×10^{-3} rad/sec
Yaw	- 1°/sec	-17.4×10^{-3} rad/sec

Search Rates

Roll	- 0.2°/sec	$- 3.49 \times 10^{-3}$ rad/sec
Pitch	- 0.2°/sec	$- 3.49 \times 10^{-3}$ rad/sec
Yaw	- 0.05°/sec	$- 0.87 \times 10^{-3}$ rad/sec

Antenna maneuver rate

Roll	- 0.1°/sec	$- 1.74 \times 10^{-3}$ rad/sec
Pitch	- 0.1°/sec	-1.74×10^{-3} rad/sec

Field-of-view

Horizon Sensor	- ±10°	- °0.175 rad
Star Tracker	- ±1°	- ±0.0175 rad

Configuration SK-513-17

I_y - 1226 slug-ft^2

I_z - 1677 slug-ft^2

Jet Moment Arm - 2.5 ft.

ΔV engine - 1 lb_f (NS engine on y axis, EW engine on x-axis)

ΔV engine - CG variance - 0.6 inch

Total ΔV impulse - 15,000 lb. sec.

Configuration SK-513-18

I_x - 2068 slug-ft^2

I_y - 1466 slug-ft^2

I_z - 2186 slug-ft^2

Jet Moment arm - 2.5 ft

ΔV engine - 1 lb_f (1 engine on z axis)

ΔV engine - CG variance - 0.6 inch

Total ΔV impulse - 15,000 lb. sec

ΔV Maneuver rates - 0.2 degrees/sec

Considerations in Determination of Thrust Levels

Several considerations must be satisfied in selecting the thrust levels.

1. The thrust must be large enough to balance the misalignment torques resulting from the firing of the ΔV engines.
2. The thrust must be large enough to acquire the references within the field-of-view of the sensors with the required search rates. The search rates are dictated by the time allowed for acquisition.
3. The thrust should be small enough to allow wheels to maintain control of attitude during unloading periods.

The misalignment torque due to the ΔV engines in .05 ft. lb. for both configurations. Assuming a 70% duty cycle for the attitude control reaction jets the jet torque must be .715 ft-lb to hold attitude. The required roll and pitch thrust is .0286 lb. and the required yaw thrust is .0143 lb.

The thrust required for acquisition or orientation is shown in Table 6D-4, for various search rates.

Table 6D-4 Thrust Levels for Acquisition

Axis & Configuration	Thrust levels-pounds					
	Search Rate (°/sec)					
	.3°/sec	.25°/s	.2°/sec	.15°/sec	.1°/sec	.05°/sec
Configuration 17						
Roll	.067	.046	.029	-	-	-
Pitch	.038	.026	.017	-	-	-
Yaw	-	-	-	.065	.029	.007
Configuration 18						
Roll	.064	.045	.028	-	-	-
Pitch	.045	.031	.020	-	-	-
Yaw	-	-	-	.085	.038	.01

The times to complete the initial acquisition maneuver for various search rates are tabulated in Table 6D-5. The times listed allow for acceleration and deceleration times.

Table 6D-5 Acquisition Time

Time in seconds

	Search Rates				
Pitch	.3°/sec	.25°/s	.2°/s	.2°/s	.15°/sec
Roll	.3°/sec	.25°/s	.2°/s	.2°/s	.15°/sec
Yaw	.15°/sec	.1°/s	.1°/s	.05°/s	.05°/s
90° pitch	435	533	656	656	870
360° roll	1335	1613	2006	2006	2670
32° yaw	156	234	234	468	468
Total	1926	2380	2896	3130	4008

Since one hour is considered as the required time for acquisition, the chosen rates of maneuvering for acquisition are 0.2°/s in pitch and roll and 0.05°/sec in yaw. This allows use of a jet thrust which is compatible with that required for balancing the misalignment torques. The maximum jet torque will be .075 ft-lbs (0.3 lbs with 2.5 ft moment arm) or 14.4 oz-in.

If the inertia wheel has a stall torque capability of 10 oz-in, this jet size is low enough to permit wheel control of the vehicle during the unloading period. The wheel reversal torque should be 15 to 18 oz-in at the unload point. Unloading can still be done on a timed pulse basis which will allow the wheel to maintain control of the attitude with the required accuracy.

Reaction Jet Momentum Storage

1. Arrest Tumbling -

Configuration SK-513-17

Roll = 2150 x 17.4 x 10^{-3} = 38 ft-lb-sec
Pitch = 1226 x 8.7 x 10^{-3} = 11 ft-lb-sec
Yaw = 1677 x 17.4 x 10^{-3} = 29 ft-lb-sec

Configuration SK-513-18

Roll = 2068 x 17.4 x 10^{-3} = 36 ft-lb-sec
Pitch = 1466 x 8.7 x 10^{-3} = 13 ft-lb-sec
Yaw = 2186 x 17.4 x 10^{-3} = 38 ft-lb-sec

2. Acquisition

Acquisition of the sun from random orientation requires rotation about the pitch and yaw axis; acquisition of earth required rotation about the roll axis and acquisition of the star a rotation about the yaw axis. The assumed number of acquisitions is 25. Each rotation consists of a start and stop.

Configuration SK-513-17

Roll = $(25)(2)(2150)(3.49 \times 10^{-3})$ = 376 ft-lb-sec
Pitch = $(25)(2)(1226)(3.49 \times 10^{-3})$ = 214 ft-lb-sec
Yaw = $(25)(2)(1677)(3.49 \times 10^{-3})$ = 293 ft-lb-sec
$(25)(2)(1677)(0.87 \times 10^{-3})$ = 73 ft-lb-sec

Configuration SK-513-18

Roll = $(25)(2)(2068)(3.49 \times 10^{-3})$ = 362 ft-lb-sec
Pitch = $(25)(2)(1466)(3.49 \times 10^{-3})$ = 256 ft-lb-sec
Yaw = $(25)(2)(2186)(3.49 \times 10^{-3})$ = 382 ft-lb-sec
$(25)(2)(2186)(0.87 \times 10^{-3})$ = 95 ft-lb-sec

3. Disturbance Torques

The momentum required to unload the wheels due to steady state torques is due to unbalance of solar radiation pressure and gravity gradient at offset points. Momentum due to gravity gradient was found by assuming a 0.1 radian offset in pitch and roll for a total of one year. The values are:

Configuration SK-513-17

Roll - 30 ft-lb-sec

Pitch - 24 ft-lb-sec

Configuration SK-513-18

Roll - 48 ft-lb-sec

Pitch - 6 ft-lb-sec

For solar radiation pressure the average value for roll was determined. These values are:

Configuration SK-513-17 - 2620 ft-lb-sec

Configuration SK-513-18 - 2320 ft-lb-sec

For pitch and yaw, it was assumed that an average value of 10% of peak disturbance torque existed. The following assumptions were made with fixed panels.

Panel area - 40 sq-ft-each

Moment arm - 15 feet

Radiation pressure - 1×10^{-7} lb/ft^2

For a two year period this is 378 ft-lb-sec.

4. Maneuvers for ΔV correction

No maneuvers are required for configuration SK-513-17. A total of 16 pitch and 4 roll maneuvers were used for configuration SK-513-18. Each maneuver consists of a start-stop at 90° and start-stop back to zero. The momentum requirements are:

Configuration SK-513-18

Roll = $(4)(4)(2068)(3.49 \times 10^{-3})$ = 115 ft-lb-sec

Pitch = $(16)(4)(1466)(3.49 \times 10^{-3})$ = 327 ft-lb-sec

5. Misalignment torque due to ΔV engine

A total impulse of 15,000lb-sec is assumed for ΔV corrections. For configuration SK-513-17 it is assumed that 1/2 the total impulse is in each of the engines. Also the EW engine causes torques about the y and z axes and the NS engine causes torques about the x and z axes. The CG variance is 0.6 inch. For configuration 18 the engine causes a torque about the x and y axis.

Configuration SK-513-17

Roll = (1/2)(15,000) (.6/12)(1) = 375 ft-lb-sec

Pitch = (1/2)(15,000) (.6/12)(1) = 375 ft-lb-sec

Yaw = (1)(15,000)(.6/12)(1) = 750 ft-lb-sec

Configuration SK-513-18

Roll = (15,000)(.6/12)(1) = 750 ft-lb-sec

Yaw = (15,000)(.6/12)(1) = 750 ft-lb-sec

6. Antenna Pattern Maneuver

The antenna maneuver consists of a start and stop at +30°, start and stop at -30° and start and stop to 0°. Ten maneuvers are assumed for roll and pitch.

Configuration SK-513-17

Roll = (10)(6)(2150)(1.74 x 10^{-3}) = 225 ft-lb-sec

Pitch = (10)(6)(1226)(1.74 x 10^{-3}) = 128 ft-lb-sec

Configuration SK-513-18

Roll = (10)(6)(1466)(1.74 x 10^{-3}) = 216 ft-lb-sec

Pitch = (10)(6)(1466)(1.74 x 10^{-3}) = 153 ft-lb-sec

The total momentum storage required of the reaction jet system is shown in Table 6D-6.

Table 6D-6 Momentum Storage Requirements

Mode	Ft-lb-sec					
	Configuration SK-513-17			Configuration SK-513-18		
	Roll	Pitch	Yaw	Roll	Pitch	Yaw
1. Arrest Tumbling	38	11	29	36	13	38
2. Acquisition	376	214	293	362	256	382
3. Disturbance Torque	30 2620	24 378	- 378	48 2320	6 378	- 378
4. Maneuvers for ΔV	-	-	-	115	327	-
5. Misalignment Torque	375	375	750	750	-	750
6. Antenna Maneuvers	225	128	-	216	156	-
Totals	3664	1130	1423	3847	1133	1643

The total impulse is as follows:

Configuration 17 = $\frac{3664 + 1130 + 1423}{2.5}$ = 2490 lb-sec

Configuration 18 = $\frac{3847 + 1133 + 1643}{2.5}$ = 2550 lb-sec

With a 100% contingency 5000 lb-sec of impulse can be considered adequate for either configuration.

Using the above information, the basic inertia wheel characteristics for vehicle configurations SK-513-17 and SK-513-18 was determined. This information is shown in Tables 6D-7 through 6D-10.

SYSTEM CONFIGURATION	MOMENT OF INERTIA SLUG-FT^2			WEIGHT LBS.	DISTURBANCE TORQUES lb-ft x 10^{-5}					
					ROLL		PITCH		YAW	
	I_x	I_y	I_z		Peak	Avg.	Peak	Avg.	Peak	Avg.
SK-513-17	2150	1226	1677		8.4	4.7	7.9	0	6.9	0
SK-513-18	2068	1466	2186		10.1	5.3	8.5	0	6.9	0

Table 6D-7

OPERATING MODE	ANGULAR MOMENTUM STORAGE lb-ft-sec						MOTOR TORQUE					
	SK-513-17			SK-513-18			SK-513-17			SK-513-18		
	Roll	Pitch	Yaw	Roll	Pitch	Yaw	Roll	Pitch	Yaw	Roll	Pitch	Yaw
Attitude Hold	2.03	2.2	2.0	2.3	2.4	2.3	.028	.016	.042	.032	.017	.049
Tracking	0.49	0.29		0.48	0.34		.095	.054		.092	.065	
Offset Pointing	0.95	0.54		0.91	0.65		0.5	0.29		0.48	0.35	
Unloading							10	10	10	10	10	10
Required Inertia Wheel Capability	3.0	3.0	2.0	3.5	3.4	2.3	10	10	10	10	10	10

TABLE 6D-8

SYSTEM CONFIGURATION	INERTIA WHEEL ANGULAR MOMENTUM lb-ft-sec			INERTIA WHEEL MOMENT OF INERTIA SLUG-FT²			INERTIA WHEEL STALL TORQUE OZ-IN			INERTIA WHEEL WEIGHT lbs.		
	Roll	Pitch	Yaw	Roll	Pitch	Yaw	Roll	Pitch	Yaw	Roll	Pitch	Yaw
-5 17	3.0	3.0	2.0	.029	.029	.019	10	10	10	11.3	11.3	9.6
SK-51 18	3.5	3.4	2.3	.034	.033	.022	10	10	10	12.1	11.9	10.1

TABLE 6D-9

SYSTEM CONFIGURATION	INERTIA WHEEL POWER, WATTS						POWER SUPPLY WEIGHT LBS	CONTROL ELECTRONIC WEIGHT LBS	TOTAL WEIGHT OF INERTIA WHEEL SYSTEM LBS	ESTIMATED O.D. EACH WHEEL IN.	ESTIMATED HEIGHT EACH WHEEL IN.
	Roll		Pitch		Yaw						
	Peak	Avg.	Peak	Avg.	Peak	Avg.					
SK-513-17	60	1.5	60	1.5	60	1.5	9.3	9.0	50.5	10	4.5
SK-513-18	60	1.5	60	1.5	60	1.5	9.3	9.0	52.4	10	4.5

TABLE 6D-10

APPENDIX 6E

PRELIMINARY TRANSFER ORBIT CONTROL MODE ANALYSIS

Preliminary Transfer Orbit Control Mode Analysis

There are two alternate approaches to accomplishing the transfer orbit and synchronous injection. If the Burner II injection stage is used, the vehicle would be actively stabilized throughout the transfer orbit and injection phase using the Burner II control system. In this case the spacecraft control system would begin functioning at separation of the Burner II stage. For performance and cost comparison, a second approach is considered in which a 9000 lb thiokol engine is used for injection and the vehicle is spin stabilized from Centaur separation until after burnout of the injection engine. This preliminary analysis is directed toward determining the spin rates, the pointing accuracy (precession and neutation), and the spin-up and despin system requirements of the spin stabilized approach.

Thrust Misalignment

The largest disturbance requiring a means of control will be the angular and offset misalignment of the 9000 pound apogee injection engine. An angular misalignment of ±0.25 degree (3 σ) will produce a component of 39.7 lb_f of thrust normal to the body and at a moment arm of 3.5 feet for configuration SK-513-17 and 4.4 feet for configuration SK-513-18. This results in a disturbing torque of

$$(39.7\ lb_f)(3.5\ \text{feet}) = 139.0\ \text{ft-lbs}\ (\text{SK-513-17})$$

$$(39.7\ lb_f)(4.4\ \text{feet}) = 174.7\ \text{ft-lbs}\ (\text{SK-513-18})$$

This results in the following spin rates:

$$w_z = \left[\frac{\frac{2(450)}{1140}}{\left(\frac{303}{1140}\right)\left(1 - \frac{303}{1140}\right)(.017)}\right]^{1/2} = 15.4 \text{ rad/sec} = 147 \text{ RPM (SK-513-17)}$$

$$w_z = \left[\frac{\frac{2(450)}{2962}}{\left(\frac{529}{2962}\right)\left(1 - \frac{529}{2962}\right)(.017)}\right]^{1/2} = 11.0 \text{ rad/sec} = 105 \text{ RPM (SK-513-18)}$$

Therefore, the spin rate during apogee thrusting must be greater than the RSS of the two required rates to assure a coning angle of less than one degree. This is given as follows:

$$w_z = \left[(82)^2 + (147)^2\right]^{1/2} = 168 \text{ RPM (SK-513-17)}$$

$$w_z = \left[(69)^2 + (105)^2\right]^{1/2} = 124 \text{ RPM (SK-513-18)}$$

Centaur Separation Rates

The pitch rate at separation of the Centaur stage is given as 1.8 deg/sec. The spin rate required to maintain less than a one degree cone in this case is given as follows:

$$\tan \lambda = \frac{I_y w_y}{I_z w_z}$$

$$w_z = \frac{I_y w_y}{I_z \tan\lambda}$$

$$w_z = \frac{(2962)(.0315)}{(529)(.017)} = 10.4 \text{ rad/sec} = 99 \text{ RPM (SK-513-17)}$$

$$w_z = \frac{(1140)(.0315)}{(303)(.017)} = 7.0 \text{ rad/sec} = 67 \text{ RPM (SK-513-18)}$$

producing a neutation or coning angle. The spin rate required to assure that this torque will not produce a coning angle greater than λ is given by the following equation:

$$w_z^2 = \frac{\frac{2M}{I_y}}{\frac{I_x}{I_y}\left(1 - \frac{I_x}{I_y}\right)\lambda}$$

The data for the two configurations is as follows:

	SK-513-17	SK-513-18	Units
I_y:	1140	2962	Slugs-ft^2
I_z:	303	529	Slugs-ft^2
M :	139.0	174.7	ft-lb$_f$
λ :	1.0	1.0	deg.

This results in a spin rate of:

$$w_z = \left[\frac{\frac{2(139)}{1140}}{\left(\frac{303}{1140}\right)\left(1 - \frac{303}{1140}\right)(.017)}\right]^{1/2} = 8.6 \text{ rad/sec} = 82 \text{ RPM (SK-513-17)}$$

$$w_z = \left[\frac{\frac{2(174)}{2962}}{\left(\frac{529}{2962}\right)\left(1 - \frac{529}{2962}\right)(.017)}\right]^{1/2} = 7.2 \text{ rad/sec} = 69 \text{ RPM (SK-513-18)}$$

Also considering a c.g. offset of ±0.6 inches, a second disturbing torque is obtained.

$$M = \frac{(9000)(0.6)}{12} = 450 \text{ ft-lb}$$

Spin-up Mode

Generating the required spin rate would be accomplished by two spin-up jets mounted on either side of the spin axis (z) at 2.5 feet moment arms. To obtain a given spin rate, the total impulse (I_t) required is determined as follows:

$$I_t = \frac{W_z I_z}{I}$$

for configuration SK-513-17,

$$I_t = \frac{(168)(529)}{(2.5)} \qquad \frac{360}{(60)(57.3)} = 3722 \text{ lb-sec}$$

for configuration SK-513-18,

$$I_t = \frac{(124)(303)}{(2.5)} \qquad \frac{360}{(60)(57.3)} = 1574 \text{ lb-sec}$$

Ascent Coast Phase

During the 15.75 hour coast to the third nodal crossing, the disturbance torques are considered. Solar pressure, which will provide a disturbance, will be on the order of 1×10^{-7} lb/ft^2 acting on a calculated surface area of 200 ft^2 and at a pressure moment arm of 5 feet. This results in a torque of 1×10^{-4} foot-pounds which is well below the thrust misalignment disturbance torque. Also, gravity gradient torques will be as high as 2.8×10^{-3} foot-pounds, while aerodynamic torques near perigee could be as high as 0.5×10^{-3} foot-pounds. In view of these disturbances, a spin rate of 60 RPM is sufficient to maintain spin axis orientation within one degree of its initial orientation.

Observation

From the foregoing calculations, it is evident that spin rates in excess of the structual limit of the stowed antenna (60 RPM) would be required if pure spin stabilization were employed. In addition, these larger spin rates would require significant spin-up impulse and despin yo-yo mass.

A more feasible approach is to use a much lower spin rate coupled with an active lateral rate damping system. This system would employ the existing spacecraft gyro unit for rate measurement, and a single on-off reaction jet mounted near the injection engine nozzle. The exact size of this jet and the required spin rate cannot be determined from closed form solutions. Therefore, an analog computer solution of the differential equation-of-motion will be required.

If a spin rate of 60 RPM is selected, the spin-up jets must provide the following total impulse:

For configuration SK-513-17,

$$I_t = \frac{(60)(529)}{(2.5)} \qquad \frac{(360)}{(60)(57.3)} = 1320 \text{ lb-sec}$$

For configuration SK-513-18,

$$I_t = \frac{(60)(303)}{(2.5)} \qquad \frac{(360)}{(60)(57.3)} = 763 \text{ lb-sec}$$

As an example, this would require two 25 pound engines 15 to 25 seconds to accomplish. The system would weight from 8 to 13 pounds using an I_{sp} of 200 seconds.

The yo-yo despin system for configuration SK-513-17, sized for a 60 RPM spin rate, and sufficient to reduce the spin rate to less than 5 degrees per second will weigh 14.7 pounds with the yo-yo wires wrapped twice around the vehicle. This produces a 400 pound tension on each wire. For configuration SK-513-18, the yo-yo system will weigh 8.5 pounds with a wire tension of 225 pounds. Alternately despin jets equivalent to the spin-up jets could be used with no significant weight change.

This control system would consist of two spin-up jets, one reaction jet for lateral axis rate control (possibly 2 level thrust), switching electronics, and a yo-yo despin system. Rate measurements could be made with the existing spacecraft gyro system.